SYSTEMATIC DISSECTION OF ROLES FOR CHROMATIN REGULATORS IN DYNAMICS OF TRANSCRIPTIONAL RESPONSE TO STRESS IN YEAST

A Dissertation Presented

By

Hsiuyi Chen

Submitted to the Faculty of the

University of Massachusetts Graduate School of Biomedical Sciences, Worcester

in partial fulfillment of the requirements for the degree of

DOCTOR OF PHILOSOPHY

December 17, 2015

INTERDISCIPLINARY GRADUATE PROGRAM

A Dissertation Presented By

HSIUYI CHEN

The signatures of the Dissertation Defense Committee signify completion and approval as to style and content of the Dissertation

Oliver Rando M.D. Ph.D., Thesis Advisor

Thomas Fazzio Ph.D., Member of Committee

Paul Kaufman Ph.D., Member of Committee

Nick Rhind Ph.D., Member of Committee

Kevin Struhl Ph.D., Member of Committee

The signature of the Chair of the Committee signifies that the written dissertation meets the requirements of the Dissertation Committee

Craig Peterson Ph.D., Chair of Committee

The signature of the Dean of the Graduate School of Biomedical Sciences signifies that the student has met all graduation requirements of the school.

Anthony Carruthers, Ph.D., Dean of the Graduate School of Biomedical Sciences

Program in Basic Biomedical Sciences

December 17, 2015

Dedication

I would like to dedicate my work to my mom and my husband. My mom has always inspired me different ways of exploring the world and she stands by me every time I fall. Only after being a mom myself, I start to realize how much she sacrifices for me. My husband is truly my best friend both in life and in science. I enjoy discussing and arguing science with him. I cannot imagine a life without him.

Acknowledgements

This work would not be possible without the contributions from my mentor and collaborators. First of all, my mentor, Oliver Rando, provides me insightful guidance that is fundamental to this work. Members in Rando Laboratory support me in both science and life. Amanda Hughes and Marta Radman-Livaja teach me how to work with yeast. Jeremy Shea and Ben Carone challenge me scientifically in every possible way. I also need to thank John Holic, Upasna Sharma, Lina Song, and Caitlin Connelly for their technical assistance and helpful discussion. I must thank Assaf Weiner and Nir Friedman for their numerous contributions to this work. Thanks go to Luis Soares and Stephen Buratowski for helping analyzing the intron effect on ribosomal protein genes. I want to thank Mohanram Gudipati and Jeffrey Pleiss for running gene expression microarrays for Set1 deletion mutant in diamide stress. Finally, I need to thank my TRAC members and DEC members who play crucial roles in this work.

Abstract

The following work demonstrates that chromatin regulators play far more pronounced roles in dynamic gene expression than they do in steady-state. Histone modifications have been associated with transcription activity. However, previous analyses of gene expression in mutants affecting histone modifications show limited alteration. I systematically dissected the effects of 83 histone mutants and 119 gene deletion mutants on gene induction/repression in response to diamide stress in yeast. Importantly, I observed far more changes in gene induction/repression than changes in steady-state gene expression. The extensive dynamic gene expression profile of histone mutants and gene deletion mutants also allowed me to identify specific interactions between histone modifications and chromatin modifiers. Furthermore, by combining these functional results with genome-wide mapping of several histone modifications in the same time course, I was able to investigate the correspondence between histone modification occurrence and function. One such observation was the role of Set1-dependent H3K4 methylation in the repression of ribosomal protein genes (RPGs) during multiple stresses. I found that proper repression of RPGs in stress required the presence, but not the specific sequence, of an intron, an element which is almost unique to this gene class in *Saccharomyces cerevisiae*. This repression may be related to Set1's role in antisense RNA-mediated gene silencing. Finally, I found a potential role for Set1 in producing or maintaining uncapped mRNAs in cells through a mechanism that does not involved nuclear

exoribonucleases. Thus, deletion of Set1 in *xrn1*Δ suppresses the accumulation of uncapped transcripts observed in *xrn1*Δ. These findings reveal that Set1, along with other chromatin regulators, plays important roles in dynamic gene expression through diverse mechanisms and thus provides a coherent means of responding to environmental cues.

Table of Contents

List of Tables[a]

[a] Since the majority of tables derived from genomics analysis are extremely large, they have mostly been excluded from the printed version of this thesis. Tables from Chapter I can be found at http://journals.plos.org/plosbiology/article?id=10.1371/journal.pbio.1001369. Tables from other chapters are available upon request.

List of Figures

List of Symbols, Abbreviations or Nomenclature

Acronym	Term
RNA Pol II	RNA Polymerase II
HAT	Histone acetyltransferases
HDAC	Histone deacetylases
WT	Wild-type
RPG	Ribosomal protein gene
RiBi	Genes involved in rRNA maturation
S.cerevisiae	*Saccharomyces cerevisiae*
S.pombe	*Schizosaccharomyces pombe*
ts	Temperature-sensitive

Preface

Chapter I is reprinted from the following co-authored work:

Systematic dissection of roles for chromatin regulators in a yeast stress response

Assaf Weiner*, Hsiuyi V. Chen*, Chih Long Liu, Ayelet Rahat, Avital Klien, Luis Soares, Mohanram Gudipati, Jenna Pfeffner, Aviv Regev, Stephen Buratowski, Jeffrey A. Pleiss, Nir Friedman, Oliver J. Rando

PLoS Biol. 2012 10(7): e1001369.

*****Contributions are listed at the beginning of Chapter I in its own preface.

Chapter II contains unpublished data produced by myself

H3K4 methylation is required for ribosomal protein genes to be adequately repressed in response to a stress.

Chapter III is a manuscript in preparation with myself as the first author:

Set1 and Xrn1 antagonistically regulate total mRNA levels in *S. cerevisiae*.

Hsiuyi V. Chen, Oliver J. Rando

INTRODUCTION

The eukaryotic genome is packaged into chromatin, which affects virtually every process occurring on DNA. The basic building block of chromatin is the nucleosome, which comprises 147 base pairs (bp) of DNA wrapped around a core histone octamer containing two copies of 4 highly conserved histone proteins H2A, H2B, H3, and H4 (Luger et al., 1997). While the packaging of DNA into nucleosomes overcomes the topological problem of storing a long stretch of DNA into the nucleus, nucleosomes also serve as barriers to many cellular processes by restricting access to DNA. To deal with this problem, eukaryotic cells have developed several approaches to relieve this constraint. Those approaches include: replacement of canonical histones with different histone variants, post-transcriptional histone modifications, and moving or removing nucleosomes.

Histone variants

Histone variants have been implicated in playing distinct roles from canonical histones and helping to create specific chromatin domains for different cellular pathways. A nucleosome consists of two histone H3-H4 and H2A-H2B dimers. H2A has one highly conserved variant, H2A.Z/HTZ1 in *Saccharomyces cerevisiae*. H2A.Z shares higher sequence similarity with H2A.Z from other species than to the canonical H2A within the same organism, suggesting H2A.Z plays a conserved role distinct from H2A (Talbert and Henikoff, 2010). In higher

eukaryotes, there are many more H2A variants such as H2A.X, H2A.Bbd, and macroH2A. Histone H3.3 and CENP-A have been identified as H3 variants. H3.3 differs from the canonical H3 (H3.1 in metazoans) only by 5 amino acids. While H3.1 is incorporated into chromatin during replication, the variant H3.3 incorporation can be replication-independent (Ahmad and Henikoff, 2002). Another example reinforces the idea that histone variants play different roles from canonical histones.

H2A.Z was identified in mouse leukemia cells in 1980 by gel separation of acid extracted proteins from nuclei (West and Bonner, 1980). While H2A.Z protein is a highly conserved protein from yeast to human (Malik and Henikoff, 2003), it is only essential in certain organisms (*Drosophila*, *Tetrahymena*, and mouse) (van Daal and Elgin, 1992; Faast et al., 2001; Liu et al., 1996). In *Saccharomyces cerevisiae*, H2A.Z/HTZ1 is not essential but deletion of *HTZ1* results in slow growth (Jackson and Gorovsky, 2000), chromosome instability (Carr et al., 1994; Krogan et al., 2004), and gene silencing defects (Meneghini et al., 2003). Notably, loss of H2A cannot be complemented by H2A.Z in *Saccharomyces cerevisiae* and *Tetrahymena thermophila,* suggesting H2A.Z plays a different role from H2A (Liu et al., 1996). Unlike H2A, H2A.Z is constitutively expressed and incorporated into chromatin by chromatin remodeling complexes SWR1 and INO80 (Luk et al., 2010; Papamichos-Chronakis et al., 2011). Interestingly, genome-wide studies showed that H2A.Z primarily localizes to promoters in

Saccharomyces cerevisiae and nucleosome-depleted region (NDR) in mammals (Albert et al., 2007; Nekrasov et al., 2012; Raisner et al., 2005). The crystal structure of a nucleosome containing H2A.Z revealed subtle destabilization of the interaction between the H2A.Z-H2B dimer and H3-H4 tetramer (Suto et al., 2000). Taken together, it is believed that the incorporation of H2A.Z helps maintain chromatin in an " open" state, which facilitates the binding of transcription factors or the recruitment of DNA repair machinery.

Histone modifications

Histone modifications affect many DNA-dependent cellular processes, such as transcription, chromatin assembly, DNA repair…etc (Kouzarides, 2007). The N-terminal tails of the histones extend outside the nucleosome core and are subject to a variety of posttranslational modifications, including methylation, acetylation, phosphorylation, ubiquitylation, sumoylation, proline isomerization, ADP-ribosylation, carbonylation, biotinylation, citrullination, β-N-glycosylation, crotonylation, N-formylation, propinylation, and butyrylation (Sadakierska-Chudy and Filip, 2014). Amino acid residues that tend to be modified are lysine (K), arginine (R), serine (S), tyrosine (Y), threonine (T), glutamate (E), and proline (P). While the N-terminal tails of histones are easily accessible, recent reports reveal that the C-terminal and globular domains of histones can also be targeted for posttranslational modifications (Tessarz and Kouzarides, 2014; Xu et al., 2005; Ye et al., 2005). To date, 130 different residues on histone proteins have

been found to subject to at least 15 types of post-translational modifications (Sadakierska-Chudy and Filip, 2014). The list of histone modifications is ever increasing, as mass spectrometry advances.

Histone modifications are reversible and dynamic. While histone acetylation and phosphorylation have been known to be reversible, histone methylation was thought to be irreversible until 2004, when the first histone demethylase was identified by the Shi laboratory and shattered the myth. The first histone demethylase, LSD1, was discovered unexpectedly. In an effort to detect polyamine oxidase activity for a metabolic enzyme homolog named nPAO (nuclear polyamine oxidase), they found nPAO demethylates histone H3 that was dimethylated at H3K4 after switching substrates from polyamine to methylated histone H3 (Shi et al., 2004). More than 20 histone demethylases have been identified since 2004 and catalyze the demethylation of almost all known histone lysine methylation sites (Shi and Tsukada, 2013).

Interestingly, histone methylation has much longer half-life comparing to histone acetylation and histone phosphorylation. The turnover rates measured by isotopic pulse labeling demonstrated that: acetylation has a short half-life ranging from 3-40 minutes, phosphorylation can last for few hours, while methylation turns over in a few days (Chestier and Yaniv, 1979; Jackson et al., 1975; Zee et al., 2010). The different turnover rates for different histone modifications are

believed to be critical for their biological roles. It is suggested that the high turnover of acetylation, rather than the presence of acetylation, facilitates transcription activation (Barth and Imhof, 2010). On the other hand, the long half-life of histone methylation makes it a potential information carrier for passing down information to the next generation.

Histone modifications exist in various combinations under different circumstances. Single residues can be modified with different modifications or different degrees of a specific modification, such as histone H3 lysine 4 (H3K4) being mono-, di-, trimethylated or acetylated (Guillemette et al., 2011; Pokholok et al., 2005). Furthermore, analysis by mass spectrometry reveals co-occurrence of various histone modifications on a single histone tail. The genome-wide distribution and colocalization of histone modifications based on ChIP-chip or ChIP-seq results confirms the complex combinations of histone marks (Liu et al., 2005). The complexity of histone modifications is so striking that many efforts have been made to understand their biological roles. A well-known hypothesis, the “histone code”, proposed that “distinct histone modifications, on one or more tails, act sequentially or in combination to form a histone code that is read by other proteins to bring about distinct downstream events.” (Strahl and Allis, 2000) Nevertheless, the existence of the histone code has been heavily debated ever since.

Crosstalk between histone modifications

Emerging evidence suggests the existence of "crosstalk" between histone modifications, where the existence of one modification influences that of the other histone modification (Lee et al., 2010). The simplest example would be the mutual exclusion of different modifications that occur on the same residue. For example, methylated H3K4 prevents the same residue from being acetylated. More complex scenarios arise when histone modifying enzymes and proteins that recognize specific modifications are involved. In the case of H3K9 methylation and H3S10 phosphorylation, phosphorylation of H3S10 disrupts the interaction between H3K9 methylation and heterochromation protein HP1 (Fischle et al., 2005). Other scenarios show trans-histone effects, where modifications on one histone affect the modifications of a different histone. In *S. cerevisiae*, H2B ubiquitylation (H2Bub) by Rad6/Bre1 proteins is required to trigger H3K4 and H3K79 methylation by recruiting a subunit of COMPASS methyltransferase complex and stimulating the catalytic activity of Dot1 methyltransferase (Weake and Workman, 2008). Subsequently, ubiquitylation of H2B by Ubp8p allows Ctk1 kinase to associate with DNA and permits Ctk1p to phosphorylate serine 2 in C-terminal domain of RNA Polymerase II (RNA Pol II) (Wyce et al., 2007). Set2 methyltransferase then associates with RNA Pol II CTD and methylates H3K36 during transcription elongation (Kizer et al., 2005). Histone crosstalk describes diverse interactions between histone modifications

and confounds our ability to decipher the contribution of each individual modification leading to a biological consequence.

Histone modifications and transcription regulation

Transcription is one of the fundamental cellular processes affected by chromatin. The discovery that packaging of DNA into nucleosomes inhibits transcription both in vitro and in vivo suggests that the contacts between nucleosomes or DNA-nucleosomes need to be disrupted for transcription to occur, which could be accomplished by histone modifications (Han and Grunstein, 1988; Lorch et al., 1987). Over 40 years ago, Allfrey and colleagues made the observation that histone acetylation and methylation may regulate RNA synthesis (Allfrey et al., 1964). However, even for well-known histone modifications, such as H3K4 trimethylation, the strongest evidence supporting this idea is the correlation between histone modifications and transcription rate. As a consequence, how histone modifications regulate transcription remains to be comprehensively elucidated.

Histone acetylation plays an important role in transcription activation. Histone lysine acetylation is highly dynamic. Two enzyme families regulate the level of acetylation: histone acetyltransferases (HATs) and histone deacetylases (HDACs). HATs catalyze the transfer of an acetyl group to the ε-amino group of lysine side chain by using acetyl-CoA as coenzyme. HDACs do the opposite to

remove the acetyl group from lysine. Most of the acetylation sites fall within the N-terminal tails of histone proteins. For example, lysine 5, 8, 12, 16 and 20 of histone H4, lysine 9, 14, 18, and 23 of histone H3 are dominant acetylation sites. However, lysine residues on the global domain can also be acetylated, such as H3K56. HATs and HDACs are usually fairly nonspecific and modify more than one lysine.

Genome-wide mapping of histone acetylation shows strong correlation between histone acetylation and transcription activity (Pokholok et al., 2005). Although strong correlation is established, the mechanism of how acetylation might promote transcription activation is less clear. It was proposed earlier that acetylation causes chromatin relaxation by removing the positive charges of lysine and thus affecting its interaction with negatively charged DNA (Allfrey, 1966). Supporting the hypothesis, histone acetylation has been shown to facilitate the access of transcription factor to nucleosomal DNA (Lee et al., 1993; Nightingale et al., 1998; Vettese-Dadey et al., 1996). Nevertheless, direct evidence is required to validate the hypothesis. While acetylation of some sites is functionally redundant, acetylation of other sites has specific impact on gene expression. For example, mutants of H4K5, K8, K12 have nonspecific, cumulative effect on gene expression. On the other hand, H4K16 mutant specifically affects genes involved in the regulation of the silent mating type in budding yeast (Dion et al., 2005).

Histone phosphorylation is usually associated with mitosis, meiosis, and DNA repair. However, growing evidence indicates they may also play a role in transcription. Histone phosphorylation can occur on serine (S), threonine (T), and tyrosine (Y). So far, phosphorylation of residues on all four core histones have been identified: H3S10, S28, T3, T11, T32, H4S1, H2AS1, H2A.XS129, and H2BS14. Among them, H3S10 phosphorylation is one the most heavily studied phosphorylation. H3S10 phosphorylation has been linked to transcription activation of many genes (Hartzog and Tamkun, 2007). Importantly, phosphorylation is also highly dynamic and responds to environmental changes. For example, Crosio et al. found a light pulse induced H3S10 phosphorylation in the suprachiasmatic nucleus of rat, accompanying with the activation of c-fos and c-jun genes (Crosio et al., 2000).

Histone lysine methylation is involved in both transcription activation and repression. Of all the histone-modifying enzymes, histone lysine methyltransferases appear to be the most specific. Consequently, lysine methylation is one of the best-characterized modifications. Lysine methylation has been associated with transcription activation or repression depending on the methylation sites. In budding yeast, three methylation sites are linked to active transcription: H3K4, H3K36, and H3K79. H3K4 trimethylation, catalyzed by COMPASS or Set1C, is enriched in the 5' end of active-transcribing genes (Pokholok et al., 2005). Highly abundant genes tend to have high level of H3K4

trimethylation. The H3K4 methyltransferase, Set1, interacts with RNA Pol II (Dehé et al., 2006; Ng et al., 2003). However, direct evidence that demonstrates that H3K4 trimethylation plays a role in active transcription is still missing. On the other hand, Set2 associates with elongating RNA Pol II and catalyzes H3K36 methylation in the coding region of active genes. Subsequently, H3K36 trimethylation in the gene body is bound by Eaf3 which recruits deacetylase complex, Rpd3S. Rpd3S deacetylates the histones in the coding region and suppresses spurious transcription within the gene body (Carrozza et al., 2005; Joshi and Struhl, 2005; Keogh et al., 2005). Ninety percent of the yeast genome is actively transcribed and bears H3K79 methylation catalyzed by Dot1 (van Leeuwen et al., 2002). This observation was extended to mammalian cells, in which it was demonstrated that the level of H3K79 methylation correlates with expression level (Steger et al., 2008). Thus, H3K79 methylation also serves as a mark for active transcription, perhaps due to its effect on heterochromatin formation by inhibiting heterochromatin protein Sir3 binding to H3K79 methylated nucleosome (Katan-Khaykovich and Struhl, 2005; Welsem et al., 2008). While *S.cerevisiae* has no repressive histone mark, methylation of H3K9, K27 and H4K20 in higher eukaryotes is associated with transcription repression and heterochromatin formation.

Set1, H3K4 methyltransferase

The SET domain is a 130 to 140 amino acid long domain found in, and named for, the *Drosophila melanogaster* genes *Su(Var)*3-9, *Enhancer of zeste*, and *trithorax* (Stassen et al., 1995; Tschiersch et al., 1994). *SET1* was discovered in 1997 as the *Saccharomyces cerevisiae* gene with the greatest similarity to SET domain (Nislow et al., 1997). *SET1* encodes a 1080 amino acid protein with a C-terminal SET domain. Much like other proteins bearing SET domains, Set1 possesses histone lysine methyltransferase activity. In fact, it is the first identified histone H3 lysine 4 (H3K4) methyltransferase (Roguev, 2001). In *S. cerevisiae*, Set1 is the only H3K4 methyltransferase that catalyzes mono-, di-, and trimethylation of H3K4 (Boa et al., 2003; Briggs et al., 2001; Nagy et al., 2002). Therefore, deletion of *SET1* results in complete loss of H3K4 methylation in vivo (Briggs et al., 2001; Krogan et al., 2002). Unsurprisingly, the H3 methyltransferase activity of Set1 is dependent on an intact SET domain (Santos-Rosa et al., 2002).

In addition to the C-terminal SET domain, Set1 bears two RRM (RNA recognition motif) domains (Roguev, 2001; Trésaugues et al., 2006). Both domains are highly conserved from yeast to human. RRM domains are characterized by a typical anti-parallel $\beta\alpha\beta\beta\alpha\beta$ motif that presents 2 conserved sequence motifs, RNP1 and RNP2 (Nagai et al., 1995) that are often involved in RNA recognition. Initially, only one RRM domain (RRM1) was identified in Set1 (Roguev, 2001).

Mutation or deletion of Set1 RRM1 resulted in a global decrease in H3K4 trimethylation, but not dimethylation (Fingerman et al., 2005; Schlichter and Cairns, 2005). It was hypothesized at the time that Set1 bound to RNAs and the binding was required for H3K4 trimethylation. However, the 3-D structure of Set1 RRM1 showed this RRM1 could not bind to RNA by itself despite having a canonical βαββαβ fold (Trésaugues et al., 2006). Interestingly, when Tresaugues *et al.* further analyzed the *SET1* sequence, they revealed a second RRM domain (RRM2) just downstream of RRM1. A protein construct containing both RRM1 and RRM2 was able to bind RNA in vitro, suggesting that Set1 may indeed bind RNA in vivo (Trésaugues et al., 2006). However, they also found that mutations affecting Set1's RNA-binding activity in vitro did not perturb H3K4 methylation and vice versa, suggesting that these two activities of Set1 are independent. Furthermore, only SET1 mRNAs have been found to co-purify with TAP-tagged Shg1 protein, a subunit in the Set1 complex, confirming that Set1 does not bind non-Set1 RNAs to promote H3K4 methylation (Halbach et al., 2009).

Set1 belongs to a multi-subunit complex called COMPASS (Complex Proteins Associated with Set1) or Set1C (Miller et al., 2001; Roguev, 2001). The complex consists of Set1, Swd1, Swd2, Swd3, Bre2, Sdc1, Spp1, and Shg1. Each subunit specifically affects complex integrity, Set1 stability, and global H3K4 methylation. Set1's methyltransferase activity is only active in the context of COMPASS (Schneider et al., 2005). Set1 and the 2 WD40 repeat proteins Swd1 and Swd3

form the core of the complex. In the absence of the Swd1-Swd3 heterodimer, the amount of Set1 is greatly decreased and yeast cells lose H3K4 mono-, di-, trimethylation (Dehé et al., 2006). The association of a Bre2-Sdc1 heterodimer with the complex requires the SET domain. Loss of Bre2 or Sdc1 does not affect complex integrity but decreases trimethylation at the 5'end of active genes (Dehé et al., 2006; Schneider et al., 2005). Loss of Spp1, which is required for proper H3K4 trimethylation, reduces the amount of Set1 (Dehé et al., 2006). Among them, only Swd2 is essential, because it is also a subunit of the cleavage and polyadenylation factor (Cheng et al., 2004; Dichtl et al., 2004). Interestingly, in the absence of Bre2 or Spp1, when H3K4 trimethylation is lost, the recruitment of COMPASS to chromatin is not affected. Consequently, it was proposed that removal of Bre2 or Spp1 leads to conformational changes in the complex and/or shifts in the active site of Set1, which results in loss of H3K4 trimethylation (Schneider et al., 2005).

Although the *set1* null mutant is viable, the mutant is defective in many aspects: *set1*Δ cells vary more in size than wild-type (WT) cells, frequently contain several buds and large protrusions, have thinner cell walls, and are compromised in their ability to recover from stationary phase. However, there is no difference in doubling time between *set1*Δ and WT cells when grown to log phase in liquid cultures (Nislow et al., 1997).

The *set1* null mutant also has severe developmental defects. *set1*Δ homozygous diploids are incapable of sporulation, suggesting that meiosis is impaired (Nislow et al., 1997). During meiosis, one of the early events is programmed DNA double-strand breaks (DSBs) that initiate meiotic homologous recombination. Interestingly, the regions flanking DSBs have high levels of H3K4 trimethylation and DSB formation at recombination hot spots is greatly reduced in *set1* null mutant (Borde et al., 2009). This finding revealed a role for Set1 in meiosis. Deletion of *Spp1* or *Swd3* which lead to reduction or loss of H3K4 di- and trimethylation, respectively, have similar DSB phenotypes to *set1*Δ. Spp1 was found to specifically associate with meiotic DSB sites in meiosis and interact with Mer2, an axis-associated protein required for meiotic DSB formation (Sommermeyer et al., 2013). Thus it was proposed that the PHD finger of Spp1 reads H3K4 trimethylation at recombination hot spots and promotes DSB formation by interacting with Mer2 and activating cleavage by DSB proteins.

Set1 is the sole enzyme that catalyzes H3K4 mono-, di-, trimethylation in *Saccharomyces cerevisiae*. Interestingly, mono-, di-, and trimethylation exhibit distinct localized patterns in the genome. While H3K4 monomethylation is enriched at the 3' end of the gene, dimethylation spreads throughout the coding region. Unlike mono- or dimethylation, H3K4 trimethylation marks the 5' end of the gene (Li et al., 2007; Santos-Rosa et al., 2002). Interestingly, trimethylation is found to specifically present at the 5' end of transcriptionally active genes (Boa et

al., 2003; Santos-Rosa et al., 2002). The pattern of trimethylation also correlates with Set1 occupancy (Ng et al., 2003). Additionally, Set1 was shown to interact with serine 5 phosphorylated, but not serine 2 phosphorylated, RNA Pol II (Ng et al., 2003). All evidence lead to the obvious hypothesis: H3K4 trimethylation is required for active transcription. The hypothesis was supported by early studies where *set1*Δ was shown to decrease RNA abundance in single gene and some genome-wide studies (Boa et al., 2003; Santos-Rosa et al., 2002). Paradoxically, later genome-wide analysis found that the *set1*Δ mutant had very limited effect on RNA abundance for whole genome. Only a few hundred of genes involved in meiosis and s porulation were derepressed in *set1*Δ. Furthermore, another conflicting study found that Set1 interacts with both serine 5- and serine 2-phosphorylated forms of RNA Pol II (Dehé et al., 2006). Therefore, the role, if any, that H3K4 trimethylation plays in active transcription remains an interesting, open question.

In contrast to a r ole in transcription activation, Set1 is also involved in transcription repression. A reporter assay to monitor the normally silenced HML locus or telomeres showed that silencing was disrupted in *set1*Δ. Importantly, the silencing defect in set1 mutant can be rescued by expressing the conserved SET domain of Set1 (Nislow et al., 1997). Chromatin immunoprecipitation assays show that Set1-dependent H3K4 methylation is present at the rDNA locus. Loss of H3K4 methylation impairs the Set1-dependent repression of RNA Pol II

transcription within rDNA repeats (Briggs et al., 2001; Bryk et al., 2002; Fingerman et al., 2005).

Set1 participates in the regulation of non-coding RNAs. An antisense *Ty1* cryptic unstable transcript (CUT) was found to silence the transcription of the *Ty1* retrotransposon and repress *Ty1* mobility (Berretta et al., 2008). *Ty1* antisense RNA is destabilized by 5'-3' exoribonuclease Xrn1. Interestingly, deletion of *SET1* in an *xrn1*Δ background restores the level of *Ty1* sense RNA and slightly decreases *Ty1* antisense RNA. It was concluded that *Ty1* antisense RNA-mediated *Ty1* silencing requires Set1 (Berretta et al., 2008). Loss of Set1 was also found to result in a decrease of another antisense RNA, *PHO84*, which silences transcription of its own gene both in *cis* and in *trans* (Camblong et al., 2007). This resulted in defective *PHO84* trans-silencing (Camblong et al., 2009). Set1 has also been implicated in regulation of a new class of non-coding RNAs that were identified in *xrn1*Δ mutants and are called XUTs (Xrn1-sensitive unstable transcripts). Silencing of antisense XUT-containing genes requires Set1 (van Dijk et al., 2011). Additionally, Set1 plays a role in transcriptional termination of snoRNAs and CUTs (Terzi et al., 2011) which are terminated via Nrd1-Nab3-Sen1 pathway. Importantly, Nrd1 recruitment is decreased in *set1*Δ, suggesting Set1 regulates early termination of snoRNAs and CUTs by elevating Nrd1 recruitment. Set1 appears to play many roles in the regulation of non-coding RNAs via different mechanisms.

It is not uncommon for SET-containing proteins to have targets other than histone tails, In fact Set1 has a non-histone substrate – Dam1. Zhang et al. found that deletion of *SET1* suppresses temperature sensitivity and chromosome loss in a mutant of Ipl1 Aurora Kinase, which is important for chromosome segregation during mitosis. Surprisingly, the suppression is not linked to H3K4 methylation. In search of the potential substrates, Dam1, a kinetochore protein, was identified to be methylated by Set1. Dam1 methylation and phosphorylation level turns out to be critical for normal chromosome segregation (Zhang et al., 2005). Hence, Set1 plays an important role in mitosis, which is independent of H3K4 methylation. Therefore Set1 affects many cellular activities via many different pathways, which may or may not be associated with its H3K4 methyltransferase activity.

Dynamic gene expression vs. stready-state gene expression

Genome-wide mapping of histone modifications links modification patterns to gene structure and gene activity (Liu et al., 2005; Pokholok et al., 2005). Lenstra et al. found specific mutant effect on mRNA expression in each of the 165 deletion mutants of chromatin regulators (Lenstra et al., 2011). Many chromatin complexes have been characterized using proteomic approaches or systematic genetic interactions (Collins et al., 2007; Krogan et al., 2006). Importantly, most studies focus on changes at steady state, a situation in which many compensatory and homeostatic pathways occur.

On the other hand, single-gene studies on chromatin-regulating proteins have revealed their roles in regulating dynamic gene expression, which were previously masked in steady state experiments. For instance, in a time course during phosphate starvation, the induction of *PHO5* was significantly delayed in a gcn5Δ mutant, however the final induction level of *PHO5* remained unaffected (Barbaric, 2001). A similar observation was made in an *asf1* mutant. The delay was due to a decrease in the rate of histone eviction (Korber et al., 2006). To survive, cells need to response to environmental changes promptly and properly. Genes need to be induced/repressed in a timely manner after sensing an environmental cue. Regulation of gene induction/repression kinetic is equally, if not more, important as the level of final induction/repression. Studies will need to monitor gene expression dynamics in order to accurately characterize the effect on gene expression.

RNA Pol II–mediated transcription is a highly coordinated process, which requires the control of the magnitude, timing, and accuracy of the transcripts. Histone modifications may regulate transcription through a variety of mechanisms. They may help anchor chromatin remodeling complex to the promoters, thus control the accessibility of DNA to transcription factors (Hassan et al., 2002). Additionally, histone modifications may disrupt the contacts between nucleosomes to assist transcription (Shogren-Knaak et al., 2006). Furthermore, crosstalk between different modifications may suppress spurious

transcription arising in the gene body during transcription (Carrozza et al., 2005). Hence, in order to dissect the role of individual histone modification in the regulation of gene expression, it is crucial to develop a method that can monitor gene expression dynamics and allow for a global identification of histone crosstalk relationships. In the following chapters, I utilize a unique approach to globally identify interactions between histone modifications and chromatin regulators, based on their effects on dynamic gene expression. The results provide a comprehensive view of regulatory roles of histone modifications in gene expression and open up avenues for novel discoveries in chromatin pathways.

CHAPTER I

PREFACE

Chapter I is reprinted from the following co-authored work:

Systematic dissection of roles for chromatin regulators in a yeast stress response

Assaf Weiner*, Hsiuyi V. Chen*, Chih Long Liu, Ayelet Rahat, Avital Klien, Luis Soares, Mohanram Gudipati, Jenna Pfeffner, Aviv Regev, Stephen Buratowski, Jeffrey A. Pleiss, Nir Friedman, Oliver J. Rando

PLoS Biol. 2012 10(7): e1001369.

Contributions

The author(s) have made the following declarations about their contributions: Conceived and designed the experiments: Oliver J. Rando, Nir Friedman, Assaf Weiner, Hsiuyi V. Chen, Jeffrey A. Pleiss, Stephen Buratowski, and Aviv Regev. Performed the experiments: Hsiuyi V. Chen, Assaf Weiner, Chih Long Liu, Luis Soares, and Mohanram Gudipati. Analyzed the data: Assaf Weiner, Oliver J. Rando, Hsiuyi V. Chen, and Nir Friedman. Contributed reagents/materials/ analysis tools: Jeffrey A. Pleiss, Aviv Regev, Avital Klien, and Ayelet Rahat. Wrote the paper: Hsiuyi V. Chen, Assaf Weiner, Nir Friedman, and Oliver J. Rando.

CHAPTER I

Systematic dissection of roles for chromatin regulators in a yeast stress response

Abstract

Packaging of eukaryotic genomes into chromatin has wide-ranging effects on gene transcription. Curiously, it is commonly observed that deletion of a global chromatin regulator affects expression of only a limited subset of genes bound to or modified by the regulator in question. However, in many single-gene studies it has become clear that chromatin regulators often do not affect steady-state transcription, but instead are required for normal transcriptional reprogramming by environmental cues. We therefore have systematically investigated the effects of 83 histone mutants, and 119 gene deletion mutants, on induction/repression dynamics of 170 transcripts in response to diamide stress in yeast. Importantly, we find that chromatin regulators play far more pronounced roles during gene induction/repression than they do in steady-state expression. Furthermore, by jointly analyzing the substrates (histone mutants) and enzymes (chromatin modifier deletions) we identify specific interactions between histone modifications and their regulators. Combining these functional results with genome-wide mapping of several histone marks in the same time course, we systematically investigated the correspondence between histone modification occurrence and

function. We followed up on one pathway, finding that Set1-dependent H3K4 methylation primarily acts as a gene repressor during multiple stresses, specifically at genes involved in ribosome biosynthesis. Set1-dependent repression of ribosomal genes occurs via distinct pathways for ribosomal protein genes and ribosomal biogenesis genes, which can be separated based on genetic requirements for repression and based on chromatin changes during gene repression. Together, our dynamic studies provide a rich resource for investigating chromatin regulation, and identify a significant role for the ‘‘activating’’ mark H3K4me3 in gene repression.

Introduction

Packaging of eukaryotic genomes into chromatin has wide-ranging effects on gene transcription in eukaryotes (Kornberg and Lorch, 1999). There are two major ways in which cells modulate nucleosomal influences on gene expression. ATP-dependent chromatin remodeling machines utilize the energy of ATP hydrolysis to disrupt histone-DNA contacts, often resulting in nucleosome eviction and changed nucleosomal location or subunit composition (Clapier and Cairns, 2009). In addition, the highly conserved histone proteins are subject to multiple types of covalent modification, including acetylation, methylation, phosphorylation, ubiquitination, SUMOylation, and ADP-ribosylation. These covalent histone modifications often occur during the process of transcription, and in turn have many effects on transcription. Moderately well-understood

effects of histone modifications include epigenetic gene silencing, control of transcript structure via repression of ‘‘cryptic’’ internal promoters, control of splicing, and transcriptional activation (Kouzarides, 2007; Margueron and Reinberg, 2010; Rando and Chang, 2009; Rusche et al., 2003; Strahl and Allis, 2000). Altogether, there are myriad interactions and feedback loops between chromatin state and transcription. At present, the effect of most modifications on transcription is unclear, even for reasonably well- characterized ones.

A large number of systematic genome-wide analyses have been carried out to characterize the complex interplay between chromatin regulation and gene transcription. Genome-wide mapping studies (Liu et al., 2005; Pokholok et al., 2005) show that modification patterns are correlated with gene structure and gene activity levels. Genome-wide mRNA profiling has been used for over a decade to identify transcriptional defects in chromatin mutants (Bernstein and Schreiber, 2002). A recent tour de force from the Holstege lab examined the effects on gene expression of deleting each of 174 different chromatin regulators (Lenstra et al., 2011). Proteomic studies characterize many of the protein complexes that play a role in chromatin regulation (Gavin et al., 2006; Krogan et al., 2006). Systematic genetic interaction profiling (using growth rate as a phenotype) has been used to identify chromatin complexes, and to delineate interactions between chromatin pathways (Collins et al., 2007; Dixon et al., 2009; Keogh et al., 2005). Importantly, most of these genomic screens have been

carried out in steady-state conditions, typically in yeast actively growing in rich media.

In contrast, single gene studies suggest that chromatin regulators have important roles in dynamic processes that are masked at steady-state. For instance, deletions of the histone acetylase Gcn5 or the histone chaperone Asf1 have little effect on the eventual induction of *PHO5* by phosphate starvation, but both of these deletions cause significant delays in *PHO5* induction kinetics (Barbaric, 2001; Korber et al., 2006). Similarly, mutation of H3K56, whose acetylation plays a role in histone replacement, delays *PHO5* induction by slowing nucleosome eviction upon gene activation (Williams et al., 2008). Similar results hold for other classic model genes, such as the galactose-inducible GAL genes (Bryant et al., 2008). Because steady-state gene expression in mutants is subject to widespread compensatory or homeostatic mechanisms, we reasoned that analysis of mutant responses to a stressful stimulus would help reveal direct functions of transcriptional regulators. Thus, the dynamics of response to stimuli should uncover the transcriptional roles of histone-modifying enzymes and other chromatin regulators. We chose diamide stress in yeast as a model system, as it has been shown to involve a rapid, dramatic reorganization of the yeast transcriptome with 602 genes induced more than 2-fold and 593 genes repressed (Gasch et al., 2000).

Here, we carried out a time course of diamide stress in 202 yeast mutants and characterized gene expression changes at 170 selected transcripts (Figure I.S1A–C). Importantly, analysis of thousands of genome-wide mRNA profiling studies shows that genes typically are co-regulated in coherent clusters (Eisen et al., 1998; Ihmels et al., 2004; Wapinski et al., 2007), meaning that the behavior of the majority of co-regulated clusters can be captured by analyzing 100–200 transcripts. For example, analyzing mutant effects on six ribosomal protein genes suffices to capture the majority of mutant effects on all 250 of these genes. We find that the majority of chromatin regulators have greater effects on gene induction/repression kinetics than they do on steady-state mRNA levels, confirming that dynamic studies can identify unanticipated functions for chromatin regulators. We show that grouping deletion mutants with similar gene expression defects identifies known complexes, and that joint analysis of histone mutants and deletion mutants associates many histone-modifying enzymes with their target sites. In addition to known relationships between chromatin regulators, we identify a number of novel connections, including a previously unknown connection between H3K4 and H3S10 modifications. We further carried out genome-wide mapping of five relevant histone modifications during the same stress time course (Figure I.S1D–E). By combining functional data with genome-wide mapping data, we identify a key role for Set1-dependent H3K4 methylation in repression of ribosomal biogenesis genes. H3K4 methylation and H3S10 phosphorylation are both required for full repression of ribosomal protein genes

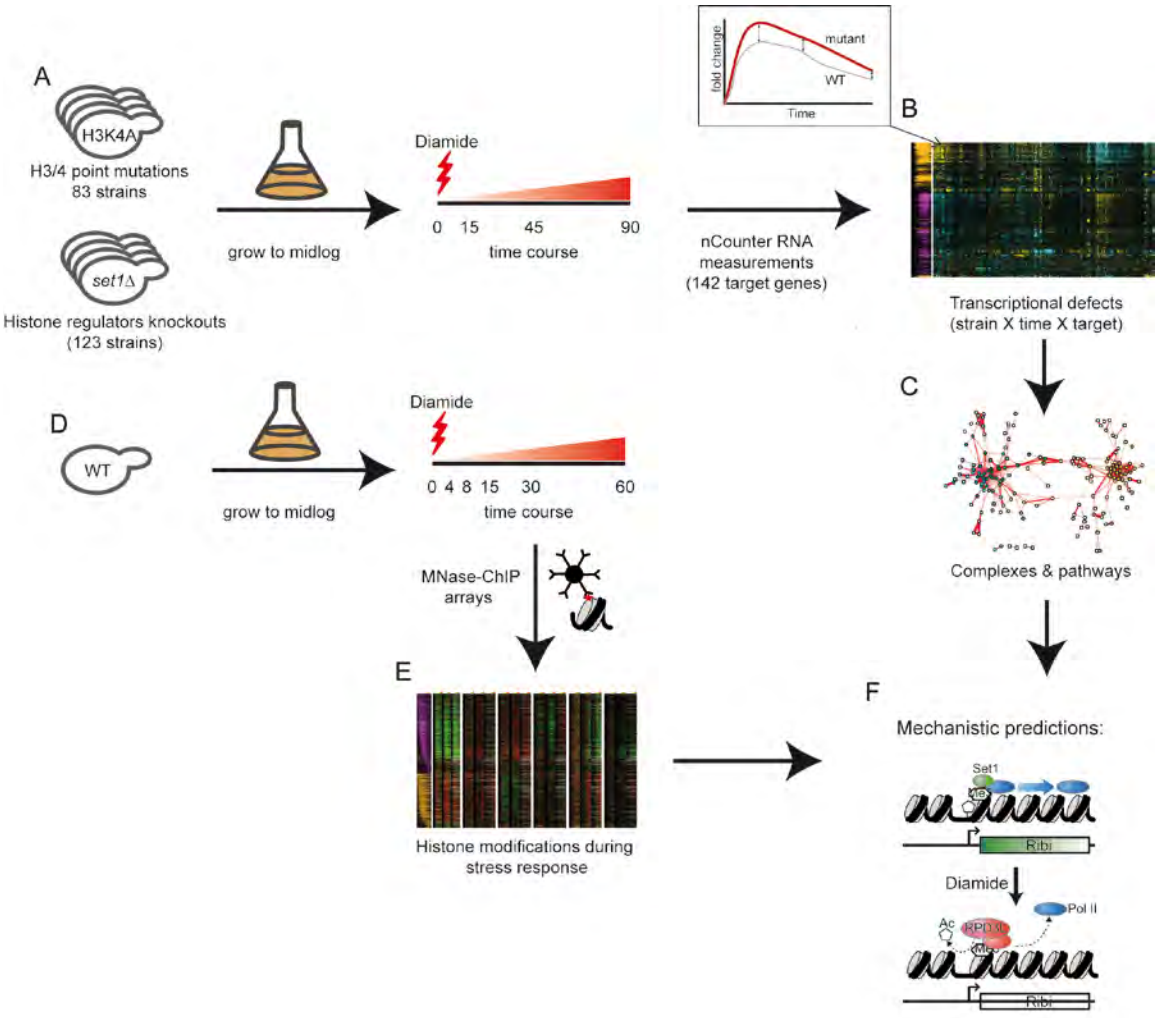
A
H3K4A
H3/4 point mutations
83 strains
set1Δ
Histone regulators knockouts
(123 strains)
grow to midlog
Diamide
0 15 45 90
time course
fold change
mutant
WT
Time
nCounter RNA
measurements
(142 target genes)
B
Transcriptional defects
(strain X time X target)
C
Complexes & pathways
D
WT
grow to midlog
Diamide
0 4 8 15 30 60
time course
MNase-ChIP
arrays
E
Histone modifications during
stress response
F
Mechanistic predictions:
Set1
Me
Ribi
Diamide
Pol II
Ac
RPD3L
Me
Ribi

Figure I.S1

Overview of experimental and analytical approach

(**A**) For each of 202 mutants analyzed, mutant was grown to midlog, then treated with diamide to induce a transcriptional stress response.

(**B**) Expression of 200 transcripts was analyzed by nCounter analysis, and for each mutant gene expression defects relative to wild-type were calculated.

(**C**) Mutants with similar gene expression profiles were clustered, identifying chromatin regulatory complexes and connections between chromatin regulators and specific histone residues.

(**D**) In parallel, wild-type yeast was treated with diamide for a time course and 5 histone modifications were mapped genome-wide using tiling microarrays.

(**E**) Diamide-regulated genes were clustered to identify patterns of histone modifications over specific subsets of induced or repressed genes.

(**F**) Combining functional data with localization data lead to a number of mechanistic hypotheses, one of which we investigated in greater detail.

(RPG) and of genes involved in rRNA maturation (RiBi), but repression of RPGs and RiBi genes operate via two distinct pathways downstream of these histone marks. Thus, the classic ‘‘activating’’ mark H3K4me3 in fact serves primarily to facilitate repression in budding yeast under multiple stress conditions. Together, these data provide a rich multi-modal view on the role of chromatin regulators in gene induction and repression dynamics, and suggest that understanding the myriad roles of chromatin structure in gene regulation on a genome-wide scale will require extending mutant analyses to kinetic studies.

Results

Time Course Analysis of Stress Response in Chromatin Mutants

We used nCounter technology (Geiss et al., 2008) to carry out genome-scale gene expression profiling. Briefly, this technology utilizes hybridization of labeled oligonucleotides in a flow cell to directly count individual RNA molecules, without any enzymatic steps, for several hundred RNAs in yeast extracts. For this experiment, we focused on gene expression during a stress response time course (using the sulfhydryl oxidizing agent diamide). We used whole genome mRNA abundance and Pol2 localization data from prior diamide exposure time courses (Gasch et al., 2000; Kim et al., 2010), along with a compendium of prior whole genome mRNA analyses and transcript structure analyses in various mutants (Ihmels et al., 2004; Wapinski et al., 2007), to select 200 probes reporting on 170 transcripts (142 genes, of which 30 had two sense probes, as

well as another 28 antisense transcription units) that capture the majority of the different patterns of gene expression behavior in this stress. Using this probeset, we measured transcript abundances over a 90-min time course of diamide exposure (Figure I.1). Experimental replicates are highly reproducible (Table I.S1), and these data provide a detailed kinetic perspective on gene expression dynamics during the diamide stress response (Figure I.1A–D).

We carried out identical time course experiments for 119 deletion strains for chromatin regulatory genes and for 83 mutants in histones H3 and H4 (Dai et al., 2008), covering the majority of individual KRR, KRQ, KRA, RRK, and SRA mutants, and several H3 and H4 N-terminal tail deletions. For most mutants, we analyzed mRNA abundance at four time points (t = 0, 15, 45, and 90 min) as these time points capture the major phases of the diamide stress response. Figure I.1A–D show example data for wild-type yeast and three mutants in the HDA1/2/3 complex. The entire dataset, comprising ~1,000 experiments carried out for 202 mutant strains, is shown in Figure I.1F–G, with mutant time courses clustered according to the similarity between their effects on gene expression across all four time points (see also Table I.S1).

Most Chromatin Mutants Have Greater Effects on Gene Induction/Repression Than on Steady-State Expression

Close inspection of the cluster in Figure I.1G (Table I.S1) revealed that many of

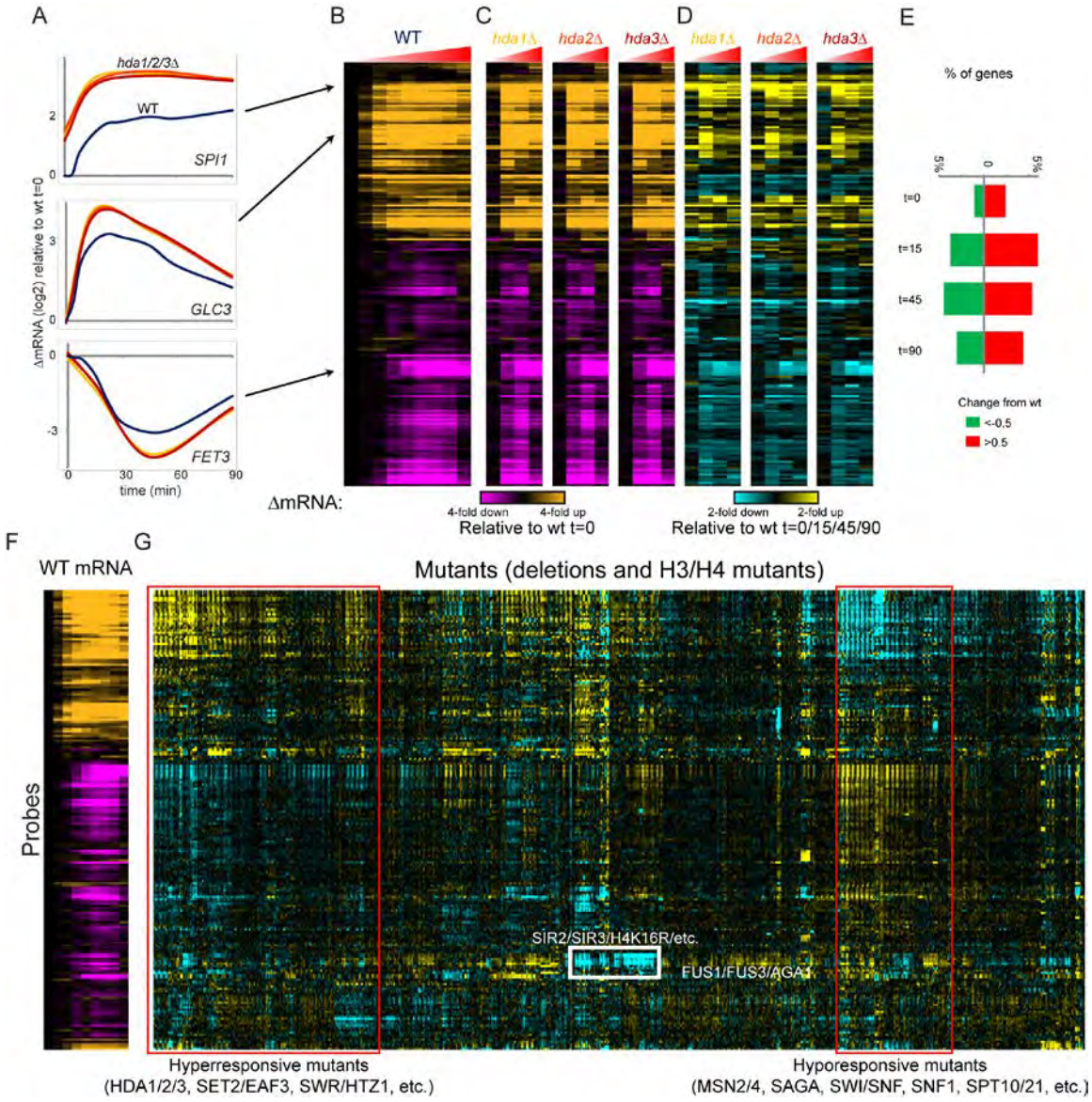
A
B
C
D
E
hda1/2/3Δ
WT
SPI1
GLC3
FET3
ΔmRNA (log2) relative to wt t=0
time (min)
WT
hda1Δ
hda2Δ
hda3Δ
ΔmRNA:
4-fold down
4-fold up
Relative to wt t=0
2-fold down
2-fold up
Relative to wt t=0/15/45/90
% of genes
5%
0
5%
t=0
t=15
t=45
t=90
Change from wt
<-0.5
>0.5
F
G
WT mRNA
Mutants (deletions and H3/H4 mutants)
Probes
SIR2/SIR3/H4K16R/etc.
FUS1/FUS3/AGA1
Hyperresponsive mutants
(HDA1/2/3, SET2/EAF3, SWR/HTZ1, etc.)
Hyporesponsive mutants
(MSN2/4, SAGA, SWI/SNF, SNF1, SPT10/21, etc.)

Figure I.1

Chromatin mutant effects on mRNA expression dynamics during stress.

(A) Time course data for three genes in wild type and three mutant (*hda1*Δ, *hda2*Δ, and *hda3*Δ) yeast. For each time course, data are normalized to wild type t = 0. Wild type time course includes nine time points after diamide addition (0, 4, 8, 15, 22.5, 30, 45, 60, and 90 min after diamide addition), while mutant time courses cover four time points (t = 0, 15, 45, 90).

(B) Wild type stress response. Data for all 200 probes are shown as log2 fold change relative to t = 0, with probes ordered by hierarchical clustering (Eisen et al., 1998).

(C) As in (B), but for the three indicated mutants. As in (B), data are normalized to wild type t = 0.

(D) ''Difference map'' for three mutants. Here, data for the three mutants are normalized relative to the equivalent wild type time point. *hda1*Δ t = 15 is compared to wt t = 15, etc. Note that many more dramatic effects on gene expression are observed during diamide stress than are observed at t = 0.

(E) Chromatin mutants have more widespread effects on gene expression during the stress response than during steady-state growth in YPD. Plotted are the fractions of (mutantxprobe) effects with increased, or decreased, expression of the probe in question. This number represents the fraction of all entries in the 200 probex202 mutant matrix (for each time point) with an absolute log2 change in RNA abundance of greater than 0.5.

(F–G) Entire dataset for diamide stress.

(F) shows wild type data as in (B).

(G) shows data for 202 indicated mutants, normalized relative to equivalent wild type time points as in (D). All four time points for each mutant are contiguous, resulting in a ''striped'' appearance for groups of mutants that specifically affect a subset of time points during diamide stress. Red boxes indicate large groups of mutants that exhibit a widespread decrease (''hyporesponsive'') or increase (''hyperresponsive'') in the amplitude of the overall diamide stress response. White box indicates an example of a subcluster expected from prior knowledge. Mutants in the Sir heterochromatin complex express pheromone response genes at low levels due to the ''pseudodiploid'' state caused by derepression of the silent mating loci in these mutants. Data are also provided in Table I.S1.

the gene expression defects observed in these mutants were only observed during the stress response, but not before stress. This is apparent in Figure I.1A and I.1D, where many more genes exhibit different levels between wild-type and *hda* mutants at 15 and 45 min of the stress response than at t = 0 (midlog growth). These differences include both kinetic delays in gene induction/ repression and defects in the extent of gene regulation (see below). To determine the generality of this phenomenon, we determined the distribution of mutant effects on RNA abundance at each of the four time points in the stress response. Many more significant gene expression changes relative to wild-type occur at 15 and 45 min (,10% of probe/mutant pairwise interactions) after diamide addition than at t = 0 (,3.5% of pairwise interactions, Figure I.1E). As the yeast acclimate to the stress environment (e.g., at t = 90), the transcriptome reaches a new steady-state where we see fewer large mutant effects, although there are still more changes than at t=0. Thus, consistent with observations from classical model genes such as *PHO5*, we find that chromatin mutants have much more extensive effects during changes in transcription than during steady-state conditions.

Overall Stress Responsiveness Correlates with Nucleosome Occupancy

We sought to identify major classes of gene expression defect in various chromatin mutants, as a first step in eventually linking chromatin transitions to the genetic requirements for different chromatin regulators. Immediately apparent in

Figure I.1G (red boxes) are two large groups of mutants with opposing behaviors with respect to the stress response—mutants that appear to be transcriptionally ‘‘hyper-responsive’’ to diamide stress and ‘‘hypo-responsive’’ mutants that exhibit blunted stress responses. These two major classes of mutants are also captured by principal component analysis (PCA) of our dataset. Here, the first principal component, which explains 30% of the variance in the dataset, corresponds to hyper- and hypo-responsive mutants (Figure I.S2A–B). Interestingly, not all genes induced or repressed during diamide stress were affected by hyper- or hypo-responsive mutants. Genes whose induction was most affected by hyper-responsive mutants, for example, tended to be those with highly nucleosome-occupied promoters in YPD (Figure I.S2C) (Field et al., 2008; Tirosh and Barkai, 2008; Weiner et al., 2010).

Hypo-responsive mutants to diamide stress included a number of expected mutants, including deletion mutants lacking the general stress transcription factors Msn2 and Msn4, or with compromised coactivator complexes such as Swi/Snf or SAGA. Hyper-responsive mutants, conversely, included a number of histone deacetylases such as Hda1/2/3. Beyond acetylation/deacetylation, hyper-responsive and hypo-responsive mutants included a variety of deletions known to affect histone turnover and/or occupancy. Several of these factors have previously been shown to affect bulk H3 turnover (Rtt109, Cac2/Rtt106, Htz1, Hat1, Rsc1, and Nhp10;

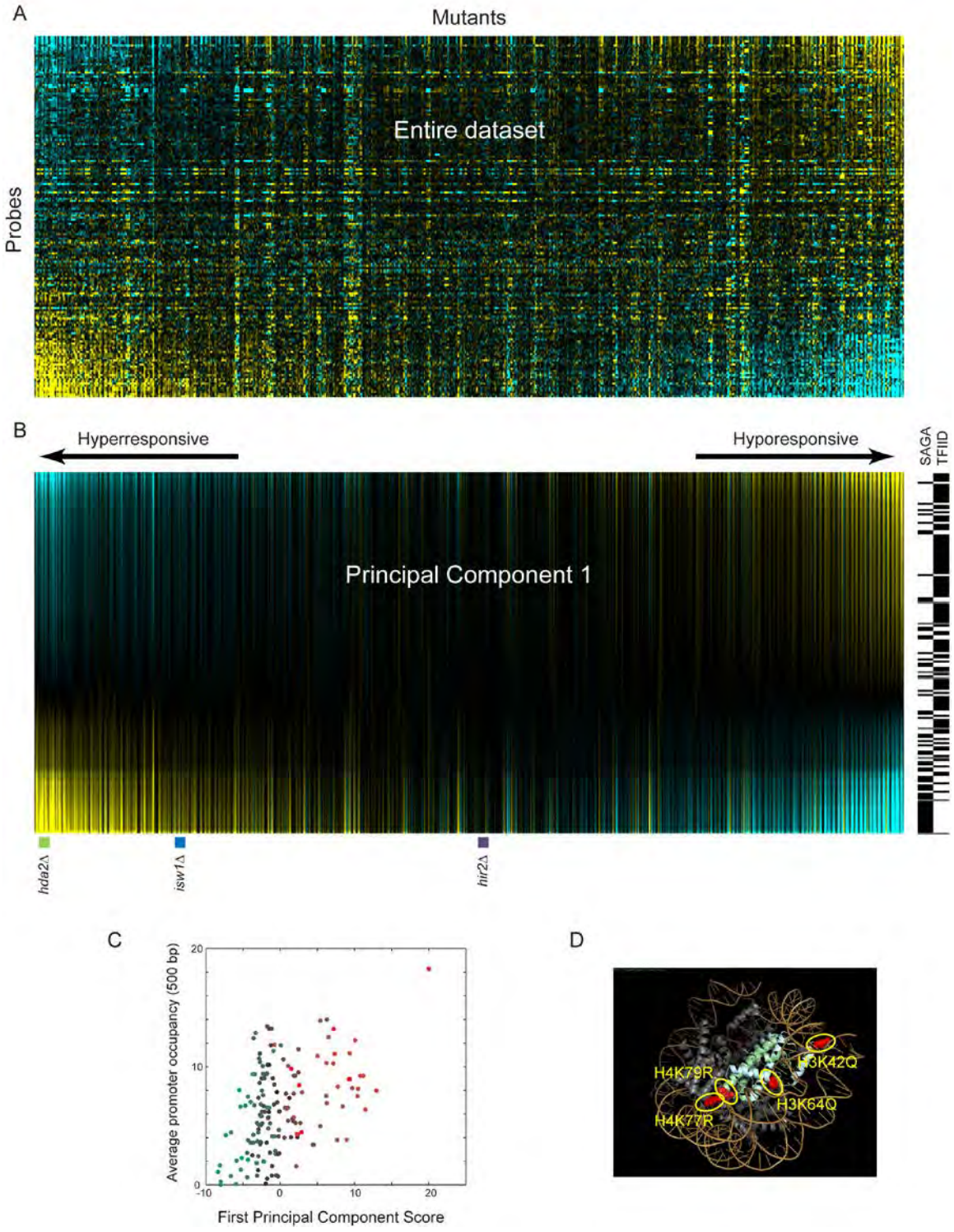
A
Mutants
Entire dataset
Probes
B
Hyperresponsive
Hyporesponsive
Principal Component 1
SAGA
TFIID
hda2Δ
isw1Δ
hir2Δ
C
Average promoter occupancy (500 bp)
First Principal Component Score
D
H4K79R
H3K42Q
H3K64Q
H4K77R

Figure I.S2

Hypo- and hyper-responsive mutants

(**A**) Data from **Figure 1** sorted by the effect of each mutant on transcriptional induction/repression. Mutants to the right represent “hyporesponsive” mutants exhibiting a blunted diamide stress response.

(**B**) Representation of the first principal component of the nCounter dataset. The relative contribution of the first principal component is shown here in blue-yellow heatmap, with mutants and genes ordered as in (**A**). Right panel shows whether genes are regulated primarily by TFIID or by SAGA (Huisinga and Pugh, 2004).

(**C**) Responsiveness to chromatin mutants correlates with promoter nucleosome occupancy. X axis shows the effects of hyper/hyporesponsive mutants on diamide regulation of each probe in our dataset, y axis shows average nucleosome occupancy (Weiner et al., 2010) for 500 bp upstream. Genes are colored red-green based on their induction/repression in wild-type.

(**D**) Hyporesponsive histone point mutants occur at histone-DNA contact areas. Mutations exhibiting diminished amplitude of the diamide stress response are mapped on to the nucleosome crystal structure, and are shown as sphere models in red. All mutants in the globular domains of H3 and H4 occur at histone-DNA contact regions.

(Dion et al., 2007; Imbeault et al., 2008; Kaplan et al., 2008; Lopes da Rosa et al., 2011; Radman-Livaja et al., 2011; Rufiange et al., 2007; Verzijlbergen et al., 2011)) or histone levels/occupancy (Rtt109, Yta7, Rtt106, Cac2, Spt21, H3K42Q; (Fillingham et al., 2008; Hyland et al., 2011; Lombardi et al., 2011)). Interestingly, we noticed that among those histone mutants that decreased the stress response program, the subset of those mutations that are located in the globular domains of H3/H4 (as opposed to the N-terminal tails) are all situated at histone-DNA interfaces (Figure I.S2D), which we speculate could affect nucleosomal stability and/or replacement dynamics. Taken together, these results support a model in which many chromatin regulators have roles on global transcriptional responsiveness resulting from their overall effects on nucleosome stability.

Single Cell Analysis of Chromatin Regulation of Gene Expression

Our RNA abundance measurements provide a population-averaged view of chromatin effects on gene expression, but hide a great deal of stochastic behavior that can be revealed by single-cell approaches. For example, RNA data on hyper-responsive mutants come from many thousands of cells, meaning the mechanistic basis for stress hyper-responsiveness is unknown. Do hyper-responsive mutants have a greater fraction of cells exhibiting diamide-driven gene induction (as might be observed if gene induction depends on cell cycle stage and mutants exhibit cell cycle delays), or do all individual cells exhibit greater amplitude responses?

We therefore extended our studies to include single cell analysis of protein expression using high throughput microscopy of GFP- tagged proteins in several key mutants. As protein stability significantly confounds measures of gene repression, we focused on four diamide-induced genes, and examined each reporter in wild type and in nine deletion mutants. We conducted time-lapse microscopy of yeast cells during the diamide response (Figure I.2A, Methods). After detecting cells (average n=120 for each of 40 strains, two biological replicates), we quantified the temporal profile of GFP intensity for each cell. Figure I.2B shows the median intensity as a function of time for one reporter in wild-type and several mutants. Importantly, we found excellent agreement between defects in protein induction in various hypo- and hyper-responsive mutants and the corresponding nCounter RNA measurements (Figure I.2C).

In general, we noted that GFP induction in individual cells followed a sigmoid-like curve consistent with a window of stress-increased protein production followed by a gradual return to baseline production levels. This behavior is consistent with a simple model in which there is a time window of diamide-induced gene transcription, followed by gradual mRNA decay. We implemented a simple mathematical model with cells transitioning from low expression to high expression and back, with a constant rate of mRNA production during the open window (Materials and Methods). This model is clearly oversimplified — each parameter covers multiple processes — but provides very good fit to the

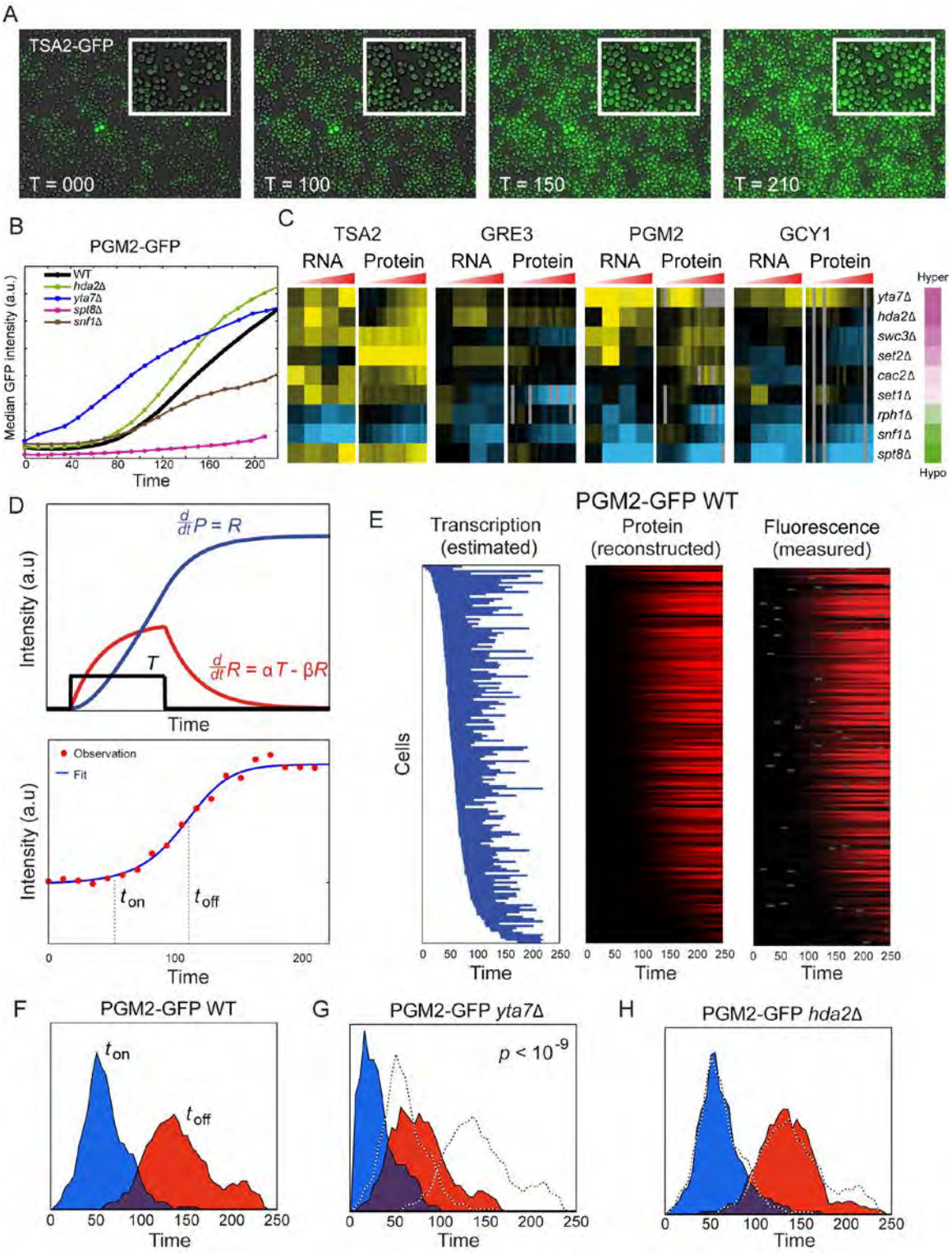
A
TSA2-GFP
T = 000
T = 100
T = 150
T = 210
B
PGM2-GFP
WT
hda2Δ
yta7Δ
spt8Δ
snf1Δ
Median GFP intensity (a.u.)
Time
C
TSA2
GRE3
PGM2
GCY1
RNA
Protein
Hyper
yta7Δ
hda2Δ
swc3Δ
set2Δ
cac2Δ
set1Δ
rph1Δ
snf1Δ
spt8Δ
Hypo
D
Intensity (a.u)
Time
Observation
Fit
E
PGM2-GFP WT
Transcription (estimated)
Protein (reconstructed)
Fluorescence (measured)
Cells
F
PGM2-GFP WT
G
PGM2-GFP yta7Δ
p < 10-9
H
PGM2-GFP hda2Δ

Figure I.2

Single cell analysis of mutant effects on gene induction

(**A**) Sample images from a time-lapse microscope analysis of a Tsa2-GFP fusion reporter at the indicated times after diamide treatment. Midlog yeast cells were grown in a mono-cell layer on glass bottom plate coated with Concavalin-A. The cells are attached to the glass and thus remain at the same location in successive images. Shown is GFP image overlaid on transmitted light image (both at 40X magnification).

(**B**) Time course fluorescence data for Pgm2-GFP for wild-type and the four indicated mutants. Each curve represents median fluorescence versus time for responding cells of a specific strain (n ~250 +/- 100).

(**C**) Protein expression recapitulates mutant effects on RNA abundance. Data are shown for four GFP fusions, each analyzed in 9 deletion mutants. Left panel shows hyper/hypo responsiveness score for the mutant in question (Figure I.S2). For each of the four promoters, left panel shows RNA data as in Figure I.1G, while right panel shows the log-ratio between median GFP expression in wild-type and in a given mutant.

(**D**) Analytical model to extract promoter "open" time and expression rate. A simple model in which cells transition from a low expression state to a high expression state was fit for each cell, resulting in three parameters – t_{on} (time from diamide treatment to beginning of high expression), t_{off} (time of return to low expression), and production rate during high expression. Figure shows data (red dots) and fit (blue curve) for a single cell expressing Pgm2-GFP.

(**E**) Model accurately captures GFP expression with few parameters. Left panel shows the duration of the high expression state for Pgm2-GFP (wild-type) as a blue bar, with cells ordered by t_{on}. Middle panel shows model predictions of protein levels. Right panel shows data for each cell.

(**F-H**) Two hyperresponsive mutants differ in the mechanism for enhanced PGM2-GFP production. Histograms of single cell distributions for t_{on} (blue) and t_{off} (red) are shown for wild-type (**F**), *yta7*Δ (**G**), and *hda2*Δ (**H**).

measured intensity profiles (Figure I.2D). Fitting the model for each cell, we can estimate the transcriptional time windows for individual cells as well as the rate of protein production during this time and examine the variability in the timing and speed of transcriptional response in a genetically homogenous population of cells (Figure I.2E).

We then used the extracted parameters for individual cells to determine whether hyper- or hypo-responsiveness corresponded to a change in the responsive fraction of cells, a population-wide change in promoter open time, and so forth. In general, we found that most mutants did not affect the fraction of cells responding to diamide. The fraction of cells exhibiting diamide induction of GFP was 87±3% across all 40 strains, and no strain differed from wild-type by even 10% of cells responding. Notably, we found that different hyper-responsive mutants could act at different stages in gene expression. For example, deletion of YTA7, which is involved in histone gene transcription and affects nucleosome occupancy (Fillingham et al., 2009; Lombardi et al., 2011), leads to accelerated promoter opening during diamide stress, whereas deletion of *HDA2* predominantly affects GFP production rate rather than promoter opening (Figure I.2F,G). Together, these results independently validate our RNA measurements, confirm that RNA changes are reflected in protein abundance, and show that, for the nine mutants analyzed, mutant effects on transcriptional response occur in the majority of cells rather than reflecting changes in the fraction of diamide-

responsive cells.

Similarity Between Mutant Profiles Identifies Complexes and Pathways

Beyond the major groups of mutants that affect overall stress responsiveness and likely report on global histone occupancy/dynamics, we observed a wide variety of gene expression effects that were specific to smaller sets of mutants. For example, the white box in Figure I.1G highlights the well-understood gene expression changes that occur in mutants related to the Sir heterochromatin complex—repression of mating-related genes secondary to the pseudodiploid state of these mutants (Rusche et al., 2003). To systematically group mutants according to their gene expression phenotypes, we calculated the correlations between the changes (relative to wild-type) in stress response in each mutant and clustered mutants according to these correlations (Figure I.3A, Table I.S2, Materials and Methods). We kept histone mutants and deletion mutants separate to allow more intuitive interpretation of clusters.

Grouping deletion mutants by this method recovers a great deal of known chromatin biology, validating our approach. In general, mutants in different subunits of known chromatin complexes exhibit similar defects in gene expression, indicating shared function. Most white boxes in Figure I.3A highlight a subset of clear examples, including the grouping of subunits of the Sir complex, the HDA1/2/3 complex, COMPASS, Cac2/Rtt106, Set3C, and the Ino80 complex.

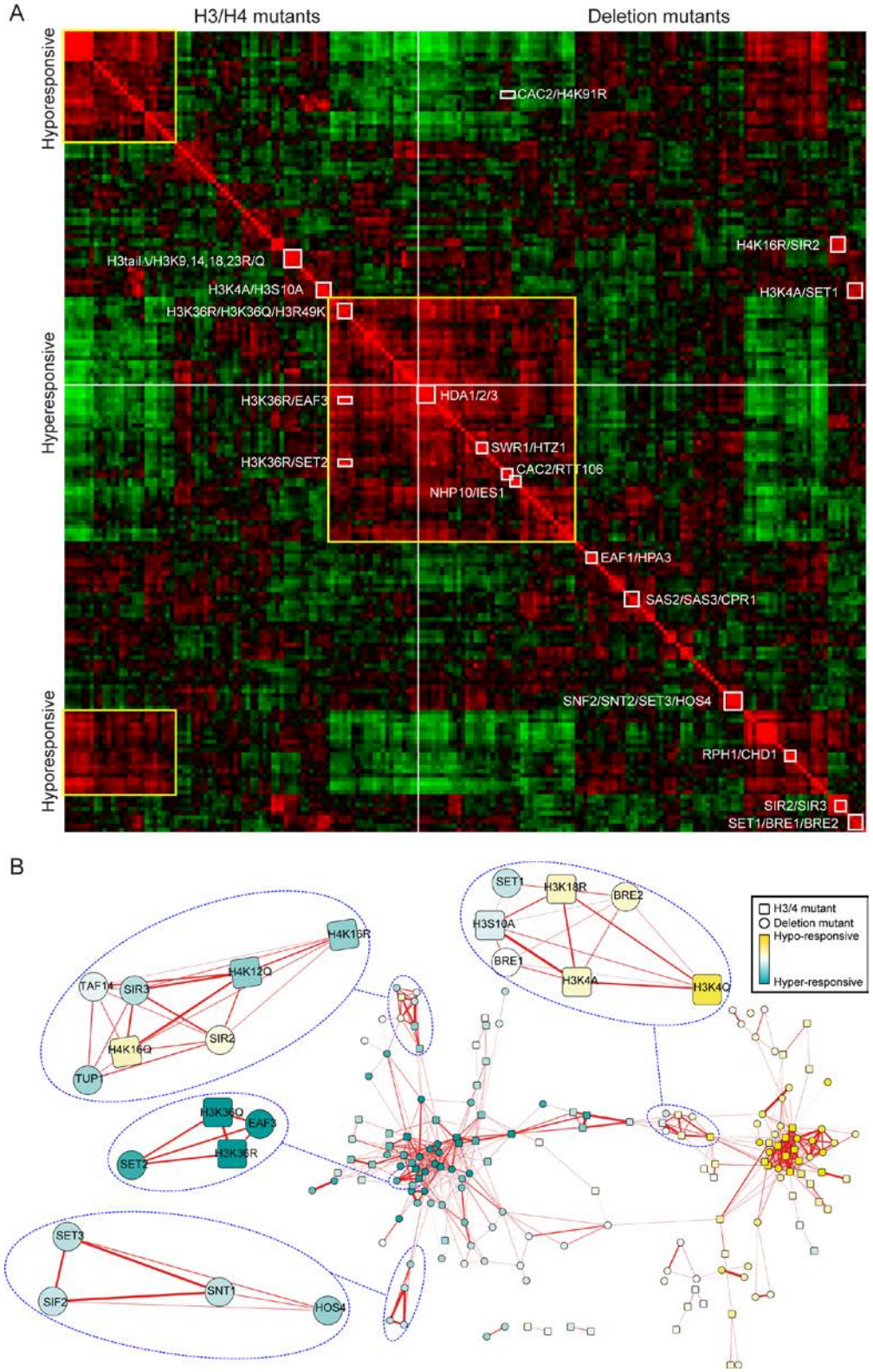
A
H3/H4 mutants
Deletion mutants
Hyporesponsive
Hyperesponsive
Hyporesponsive
CAC2/H4K91R
H4K16R/SIR2
H3tail\/H3K9,14,18,23R/Q
H3K4A/H3S10A
H3K4A/SET1
H3K36R/H3K36Q/H3R49K
H3K36R/EAF3
HDA1/2/3
SWR1/HTZ1
H3K36R/SET2
CAC2/RTT106
NHP10/IES1
EAF1/HPA3
SAS2/SAS3/CPR1
SNF2/SNT2/SET3/HOS4
RPH1/CHD1
SIR2/SIR3
SET1/BRE1/BRE2
B
H3/4 mutant
Deletion mutant
Hypo-responsive
Hyper-responsive
SET1
H3K18R
BRE2
H3S10A
BRE1
H3K4A
H3K4Q
H4K16R
TAF14
SIR3
H4K12Q
SIR2
H4K16Q
TUP1
H3K36Q
EAF3
SET2
H3K36R
SET3
SIF2
SNT1
HOS4

Figure I.3

Correlation matrix identifies complex membership and enzyme-substrate relationships

(A) Correlation matrix for all 202 mutants. Correlation between each mutant's effects on diamide stress response was calculated across the entire time course, and mutants were clustered by correlation coefficient. Rows and columns are ordered identically. Note that histone mutants and gene del etion mutants are kept separate, as indicated. Boxes indicate highly-correlated groups of mutants corresponding to known co-membership in protein complexes (eg SIR2/SIR3), known pathways (eg SWR1/HTZ1), novel predicted pathways (eg RPH1/CHD1), and expected or novel relationships between histone residues and chromatin regulators (eg H3K36/SET2/EAF3).

(B) Network wiring of chromatin regulators. Genes were grouped according to correlations (thresholded at 0.45), and r elated genes are clustered using the spring embedded algorithm. Subnetworks corresponding to several complexes are emphasized as indicated.

Furthermore, several pathways were recovered. The histone variant H2A.Z (encoded by *HTZ1*) was linked to components of the Swr1 complex responsible for H2A.Z incorporation (Kobor et al., 2004; Krogan et al., 2003; Mizuguchi et al., 2004), the H3K4 methylase Set1 was linked to the H2B ubiquitin ligase Bre1 whose activity is required for K4 methylation (Hwang et al., 2003), and the H3K36 methylase Set2 was linked to Eaf3, the binding partner for H3K36me3 (Carrozza et al., 2005; Joshi and Struhl, 2005; Keogh et al., 2005).

In addition to known chromatin regulatory complexes and pathways, our results also suggest a number of hypotheses for novel chromatin pathways. For example, we find strong correlations between gene expression defects in mutants lacking the H4K16 acetylase Sas2 and those lacking the proline cis/trans isomerase Cpr1. Similarly, our results link the H3K36 demethylase Rph1 with ATP-dependent remodeler Chd1, suggesting the possibility that H3K36 methylation regulates Chd1 in budding yeast, an idea that finds support in prior studies showing that H3K36 mutants and chd1 mutants have similar genetic interactions in vivo (Quan and Hartzog, 2010).

Analysis of histone mutations revealed similar structure. We observe two larger clusters that correspond to hyper- and hypo- responsive mutations (Figure I.3A, yellow boxes), as well as many smaller groups. Many of these groups are comprised of several mutations in the same residue (e.g., all three mutations in

H3K36 are tightly clustered together) or in the same tail (e.g., H3 tail delete and simultaneous K-.Q/R mutations in H3 tail lysines 4, 9, 14, 18, and 23). Many other groups of histone mutants were unanticipated and may identify functionally relevant nucleosomal surfaces (Dai et al., 2008) or novel examples of histone crosstalk (Suganuma and Workman, 2008). Below, we explore the relevance of one such novel connection, between H3K4A and H3S10A mutants.

Many of the connections between chromatin regulatory genes observed here also can be ob served in systematic genetic interaction profiles, or in gene expression studies carried out in midlog growth conditions (Collins et al., 2007; Lenstra et al., 2011). A unique aspect of our study is the joint analysis of gene deletion mutants with histone point mutants. Many of the strongest correlations between deletion and histone mutants correspond to known enzyme-substrate and modification-binding partner relationships. For example, gene expression defects resulting from deletion of the H3K36 methylase Set2 were most strongly correlated with the defects in H3K36R and H3K36Q mutants, and w ith the H3K36me3-binding protein Eaf3 (Figure I.3A).

Analysis of multiple different mutations of the same lysine residue can provide insight into the biochemical function of modifications at this residue. While both KRR and K RQ mutants disrupt modification-specific binding by proteins (e.g., bromo- and chromo domain proteins), they differ in their charge. Indeed, lysine

mutants for which KRR and KRQ mutants exhibited similar gene expression defects tend to occur at lysines with well-characterized modification-specific binding partners (e.g., Eaf3, Sir3). In contrast, lysines for which KRR and KRQ mutants had opposing effects on gene expression often were known acetylation substrates, although we counterintuitively observe that for these lysines the KRR mutations were generally correlated with deletions in histone deacetylases (Figure I.S3).

To systematically identify relationships between chromatin factors, we identified significant correlations between mutants (Materials and Methods), recovering for example the Set2 -> H3K36R -> Eaf3 pathway (Figure I.S4A–B, Table I.S3). Data for all correlations above a threshold significance are visualized in a network view in Figure I.3B to show not only connections within strongly connected pathways but also connections between pathways. Other known relationships recovered this way included the association between Set1 and H3K4, and the association between the Sir complex and H4K16 (Figure I.S4).

Furthermore, we found that Cac2, a CAF-1 subunit, and Rtt106, histone chaperones that were strongly correlated with one another, exhibited transcriptional effects most related to the H3K91R mutant (Figure I.3A). H4K91 acetylation is a little-studied modification reported to occur on newly synthesized histones (Ye et al., 2005), and in systematic genetic interaction studies, H4K91R

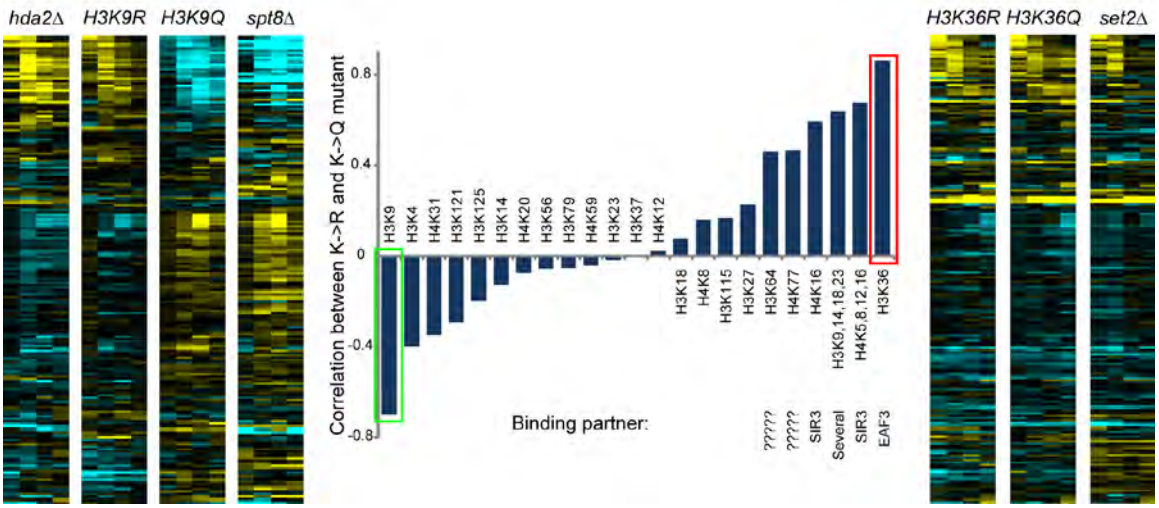

Figure I.S3

Comparison of K->R and K->Q mutations

Correlation between K->R and K->Q mutations for 23 H3/H4 lysines. Residues exhibiting high correlation between such several lysines whose modified state has a well-understood binding partner (eg H3K36me3-Eaf3, H4K16ac-Sir3). Conversely, residues for which R and Q mutations had anticorrelated effects on gene expression were generally known acetylation sites, and c ould plausibly report on charge-dependent chromatin transactions.

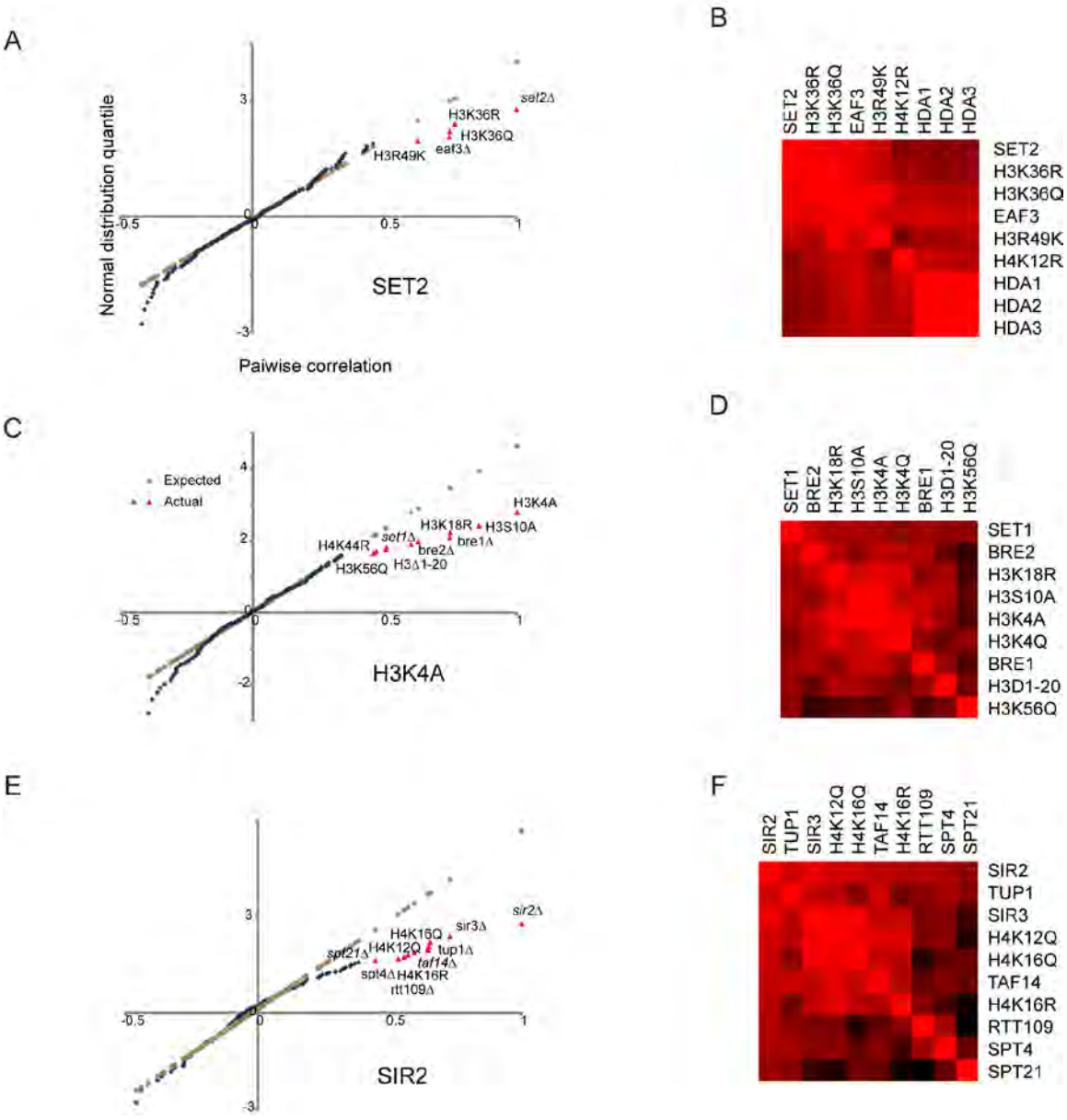
A
Normal distribution quantile
Paiwise correlation
set2Δ
H3K36R
H3K36Q
eaf3Δ
H3R49K
SET2
B
SET2
H3K36R
H3K36Q
EAF3
H3R49K
H4K12R
HDA1
HDA2
HDA3
C
Expected
Actual
H3K4A
H3K18R
H3S10A
sef1Δ
bre1Δ
H4K44R
bre2Δ
H3K56Q
H3Δ1-20
H3K4A
D
SET1
BRE2
H3K18R
H3S10A
H3K4A
H3K4Q
BRE1
H3D1-20
H3K56Q
E
sir2Δ
H4K16Q
sir3Δ
spt21Δ
H4K12Q
tup1Δ
taf14Δ
spt4Δ
H4K16R
rtt109Δ
SIR2
F
SIR2
TUP1
SIR3
H4K12Q
H4K16Q
TAF14
H4K16R
RTT109
SPT4
SPT21

Figure I.S4

Identification of chromatin pathways from correlation matrix

(A) Identification of significant associations between mutants. QQ plot shows, for each mutant, the correlation with the test mutant (here, *set2*Δ) on the x axis, with the theoretical distribution of correlations expected from a normal distribution on the y axis. Points distant from the x=y line are significant correlations.

(B) Local cluster of mutants significantly correlated with *set2*Δ. Data from Figure 3A, re-clustered using only highly-correlated mutants with *set2*Δ.

(C-D) As in (A-B), but for H3K4A.

(E-F) As in (A-B), for *sir2*Δ.

and -related lysine the H3K56 exhibited similar genetic
interactions (Dai et al., 2008). We therefore hypothesize that H4K91 acetylation
might affect chromatin assembly by CAF-1 or Rtt106. 0 ther conne
no obvious literature precedent—the HMG protei
nucleosome
et al., 2010), was correlated I.S2) and H3K
represent
either
on one such observation, the surprising linkage
mutants and the H3S10A histone mutant.

Our data show that joint analysis of histone mutants with related gene deletion mutants can systematically link histone-modifying enzymes with their substrates, as well as modification-specific binding proteins to the relevant modified histone residue (Tables I.S2 and I.S3).

Genome-Wide Histone Modification Dynamics

We next sought to understand why only particular genes were affected by mutants in various chromatin regulators. One of the central questions in chromatin regulation is why broadly localized histone marks appear to have extremely localized effects on gene expression? In other words, given that H3K4me3 occurs at nearly all +1 nucleosomes, why do *set1*Δ mutants exhibit

relatively minor (Guillemette et al., 2011; Lenstra et al., 2011) gene expression changes? Our functional results suggest that many transcriptional effects of chromatin mutants are masked at steady-state by feedback mechanisms, but can be uncovered during dynamic changes in gene e xpression. To address the relationship between histone mark occurrence and function in a dynamic context, we therefore extended our studies by carrying out genome-wide mapping of several histone modifications (Tables I.S4 and I.S5) during a six time point diamide stress time course (t = 0, 4, 8, 15, 30, and 60 min). We focused these experiments on two relatively well-characterized modifications: H3K36me3 and H3K4me3, and related marks H3K14ac, H3S10P, and H3R2me2a. Our mapping data for unstressed yeast are concordant with known aspects of modification localization patterns from either prior genome-wide mapping efforts (Liu et al., 2005; Pokholok et al., 2005) or related studies (Figure I.4A, Figure I.S5).

Given the surprising correlation between H3K4A and H3S10A mutants (Figure I.3A, Figure I.S4), we focused on how the histone modifications H3K4me3 and H3S10P change genome-wide during diamide stress. As noted above, H3K4me3 occurs at the 5' ends of transcribed genes, and genes induced during the stress response gained H3K4me3 over time, as expected (Figure I.4C, Figure I.S5B). H3S10P, which had not been mapped genome-wide in yeast, is most strikingly localized to, 20 kb surrounding yeast centromeres (Figure I.S5G), consistent with its pericentric localization by immunofluorescence in mammalian cells

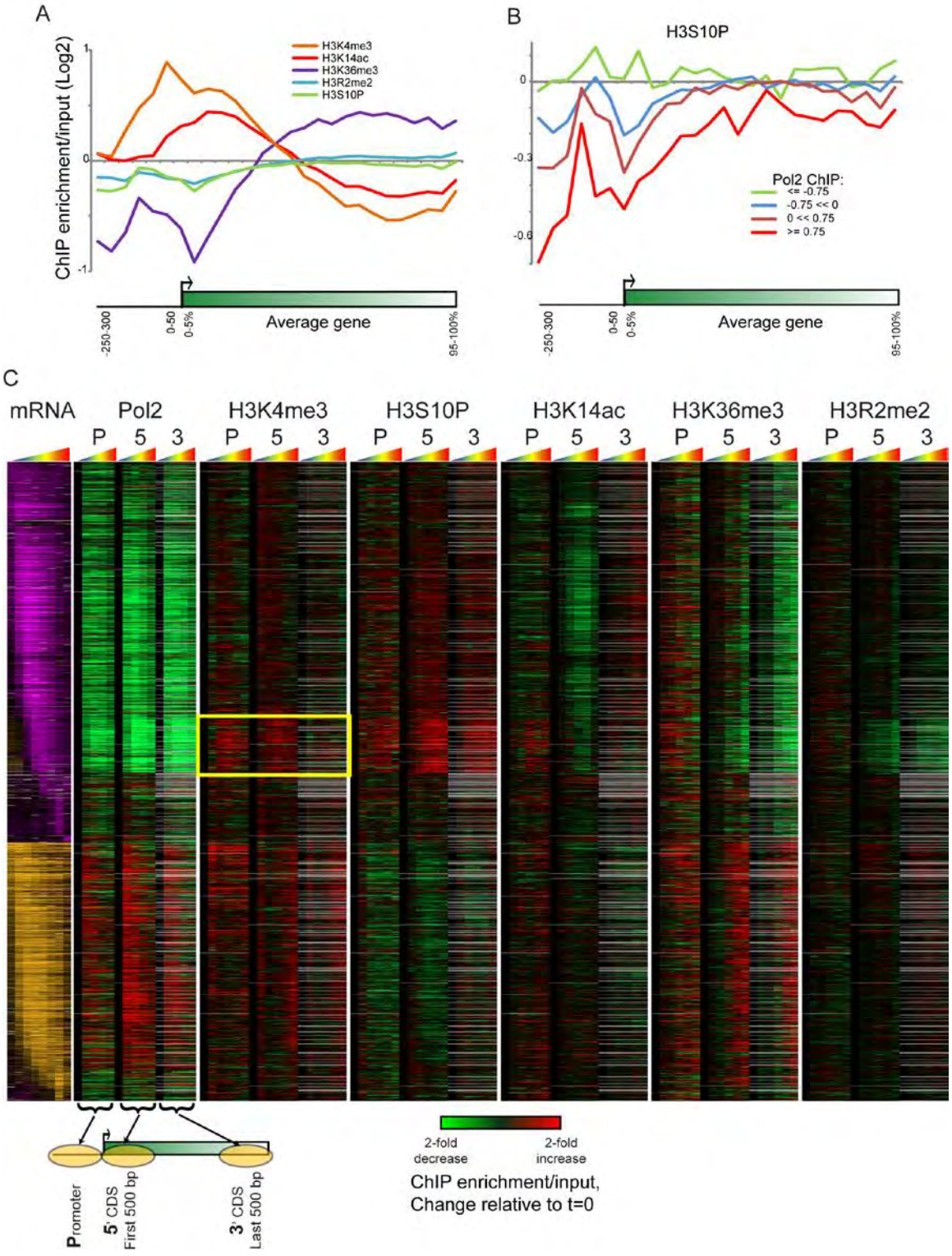
A
ChIP enrichment/input (Log2)
H3K4me3
H3K14ac
H3K36me3
H3R2me2
H3S10P
Average gene
-250-300
0-50
0-5%
95-100%
B
H3S10P
Pol2 ChIP:
<= -0.75
-0.75 << 0
0 << 0.75
>= 0.75
Average gene
C
mRNA
Pol2
H3K4me3
H3S10P
H3K14ac
H3K36me3
H3R2me2
P 5 3
2-fold decrease
2-fold increase
ChIP enrichment/input,
Change relative to t=0
Promoter
5' CDS First 500 bp
3' CDS Last 500 bp

Figure I.4

Genome-wide histone modification changes during diamide stress

(A) Metagene analysis of the 5 histone marks analyzed here. The indicated modifications were mapped genome-wide by ChIP-chip using ~250 bp resolution tiling microarrays, normalized to nucleosome occupancy. All genes are length-normalized, and ChIP enrichments for the 5 marks at t=0 (eg midlog growth) are shown averaged for all genes.

(B) Metagene analysis for genes grouped according to transcription rate as measured in Kim et al.(Kim et al., 2010), with H3S10P mapping data averaged for each set of genes.

(C) Chromatin changes at all diamide-regulated genes. Genes up- or down-regulated by over 1.8-fold (Gasch et al., 2000) are shown, with mRNA changes represented in orange/purple. Genes are ordered by time of change in gene expression (Chechik et al., 2008). Tiling microarray probes for Pol2 (Kim et al., 2010) and for 5 histone marks were associated with gene promoters, 5' ends, or 3' ends as shown in schematic underneath Pol2 panel (Dion et al., 2007). Data for each time course are shown as changes relative to t=0, thus representing the change in the modification over the time course of diamide stress. Pol2 data are for t=0, 15, 30, 60, and 120 minutes after diamide stress, whereas histone modification data were collected at t=0, 4, 8, 15, 30, and 60 minutes after diamide stress. Grey entries represent missing data (generally due to an absence of any microarray probes at the relevant genomic location). Yellow box highlights "paradoxical" gain of H3K4me3 at the 5' ends of a large group of diamide-repressed genes.

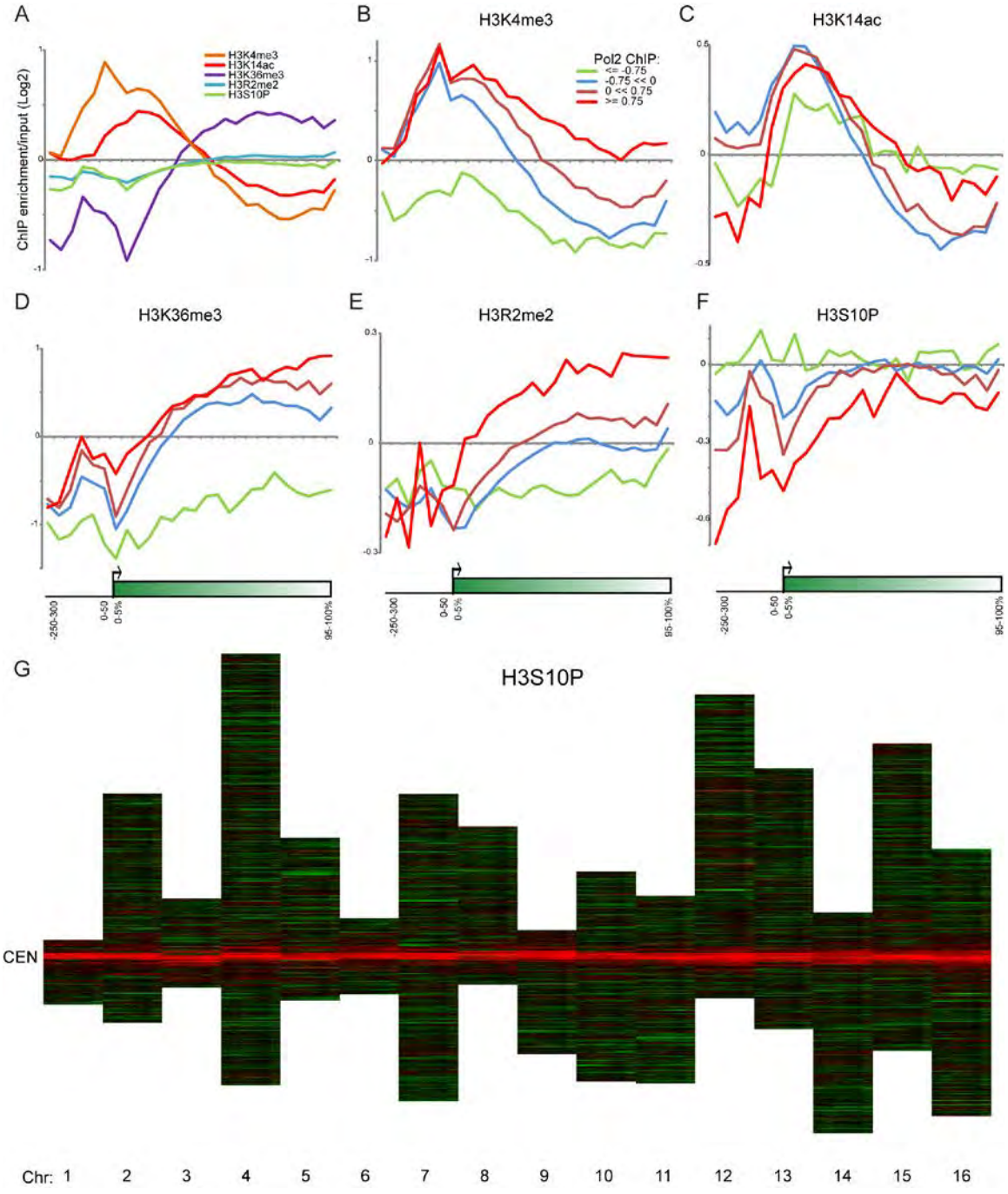
A
B
H3K4me3
C
H3K14ac
ChIP enrichment/input (Log2)
H3K4me3
H3K14ac
H3K36me3
H3R2me2
H3S10P
Pol2 ChIP:
<= -0.75
-0.75 << 0
0 << 0.75
>= 0.75
D
H3K36me3
E
H3R2me2
F
H3S10P
-250-300
0-50
0-5%
95-100%
G
H3S10P
CEN
Chr: 1 2 3 4 5 6 7 8 9 10 11 12 13 14 15 16

Figure I.S5

Genome-wide histone modification mapping

(A) Genome-wide mononucleosome-resolution mapping of H3K4me3, H3K36me3, H3S10P, H3K14ac, and H3R2me2 was carried out by ChIP-chip (relative to mononucleosomal input to control for histone occupancy). All open reading frames are converted to a “metagene” with 6 bins reporting on 50 bp increments from 0 to 300 bp upstream of the TSS, and 20 bins reporting on 5% intervals covering the ORF.

(B-F) Genes are broken into 4 classes according to Pol2 levels (Kim et al., 2010), and data for the indicated modifications is presented as in (A).

(G) H3S10P localization to pericentric regions. All chromosomes are aligned by their centromere, and H3S10P mapping data is shown in red-green heatmap.

(Crosio et al., 2002). However, we also noted that H3S10P on chromosome arms was heterogeneous, and localized to coding regions with a pattern opposite to that of H3/H4 turnover (Dion et al., 2007; Rufiange et al., 2007). H3S10P is depleted from the 5' ends of genes, and over coding regions anticorrelates with transcription rate (Figure I.4B). Furthermore, during the stress response H3S10P levels increase over repressed coding regions, and decrease over induced genes, indicating that the anticorrelation between H3S10P and transcription is dynamic (Figure I.4C).

Overall, many of the chromatin changes over stress-activated or repressed genes fit expectations. At stress-activated genes, promoter H3K4me3 levels increased while H3K36me3 increased over gene bodies. However, we also observed several unexpected dynamic behaviors (e.g., increasing H3K36me3 over the promoters of many stress-responsive genes). Furthermore, H3K14, whose acetylation scales with transcription rate during midlog growth (Liu et al., 2005; Pokholok et al., 2005), was only deacetylated at a small subset of repressed genes during diamide stress, with most repressed genes exhibiting surprising minimal changes in H3K14ac (see below).

Most curiously, we found that H3K4me3 levels increase at the 5' ends of a substantial number of diamide-repressed genes during their repression (Figure I.4C, yellow box). Not only do these genes gain H3K4me3, they also gain

H3S10P, and as noted above H3K4 mutants and H3S10 mutants exhibit similar gene expression defects (Figure I.3A, Figure I.S4). Thus these marks are linked both functionally and in terms of dynamic localization changes. Curiously, the H3K4methylase Set1 and one of the H3S10 kinases, Ipl1, also share the nonhistone substrate Dam1 (Zhang et al., 2005), indicating a more general connection between H3K4 and H3S10 based on shared nonhistone substrates for their modifying enzymes. It is unlikely that the gene expression defects observed here stem from nonhistone substrates of these enzymes as the gene expression changes are observed in histone point mutants as well as modifying enzyme deletions, but the connection is curious nonetheless.

Below, we attempt to connect the changes in H3K4me3 and H3S10P localization with the functional effects of relevant mutants. Are the genes that are misregulated in K4 and S10 mutants the same genes that exhibit dynamic changes in these marks during stress?

Set1-Dependent H3K4 Methylation Primarily Serves in Gene Repression Rather Than Activation

Set1 methylates H3K4 to create a gradient over coding regions from K4me3 at the 5' end to K4me1 at the 3' end, and this methylation pattern correlates with transcription rate during midlog growth ((Liu et al., 2005; Pokholok et al., 2005), Figure I.S5B). The correlation between H3K4me3 and transcription rate leads to

this mark being referred to as an ‘‘activating mark,’’ yet *set1*Δ mutants exhibit few gene expression defects in midlog growth, and in fact increasing evidence points to a primarily repressive role for K4 methylation in yeast. *set1*Δ mutants exhibit increased basal expression of repressed genes such as *PHO5* (Carvin and Kladde, 2004; Wang et al., 2011), and moreover exhibit widespread defects in repression of sense transcription by antisense transcripts (Berretta et al., 2008; Camblong et al., 2009; van Dijk et al., 2011; Kim and Buratowski, 2009). We noted in our initial gene expression dataset that *set1*Δ and related mutants showed defects in repression of ribosomal protein (‘‘RPG’’) and ribosomal biogenesis (‘‘Ribi’’) genes (Table I.S1). We therefore extended these results to whole genome mRNA profiling, finding that the major gene expression defect in *set1*Δ mutants during diamide stress is a failure to adequately repress RPG and Ribi genes (Figure I.5A). This result is interesting in light of prior observations that Set1 is required for full repression of the rRNA repeats (Briggs et al., 2001; Bryk et al., 2002) during steady-state growth (when a subset of rDNA repeats are silenced), and shows that Set1 plays a general role in repression of all aspects of ribosomal biogenesis. Notably, although some snoRNA genes are found in RPG introns, we observed Set1 effects on the majority of ribosomal protein genes, most of which do not carry snoRNAs in their introns, indicating that the observed effect is not a consequence of Set1’s known effects on termination at snoRNA genes (Terzi et al., 2011).

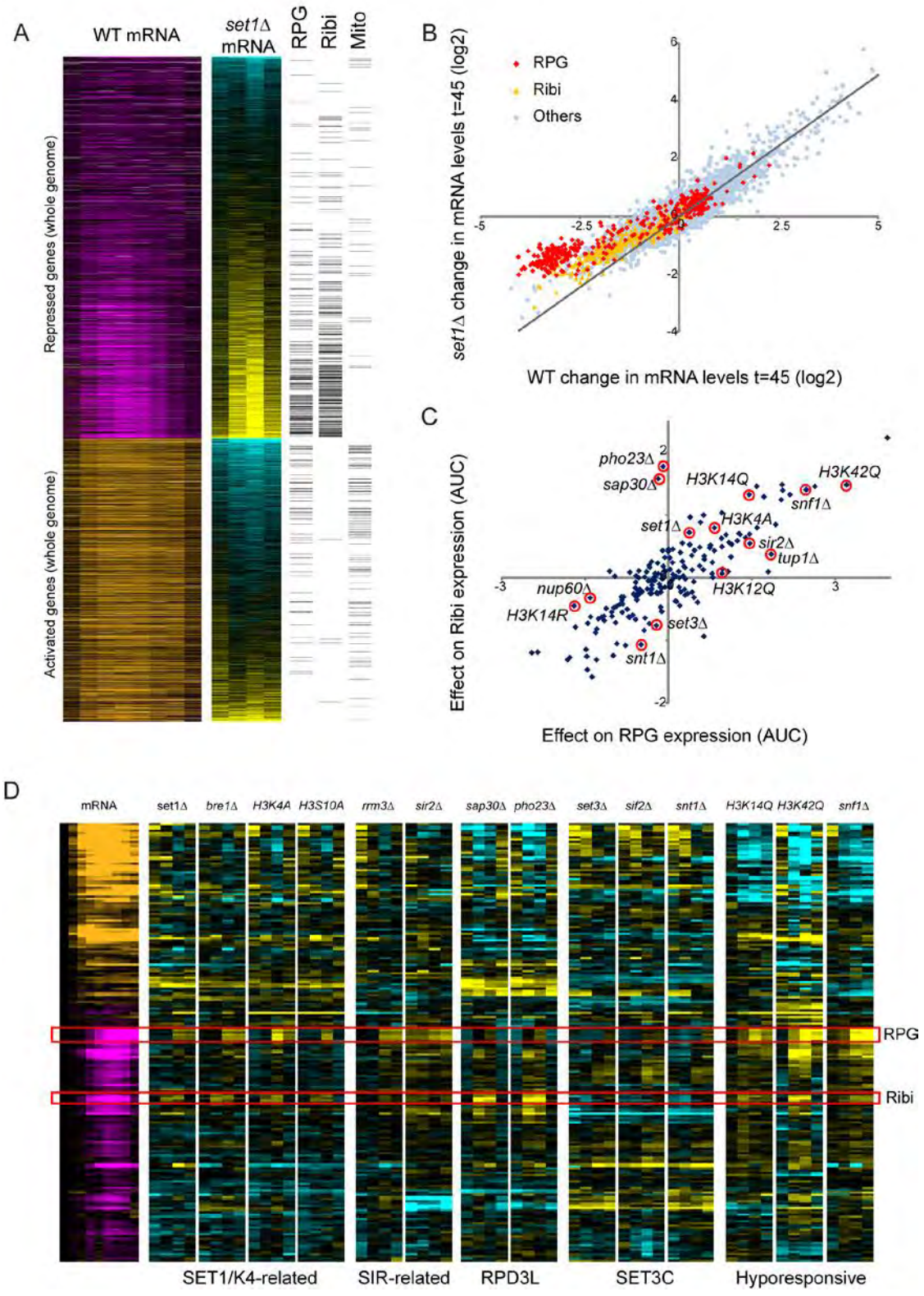
A
WT mRNA
set1Δ mRNA
RPG
Ribi
Mito
Repressed genes (whole genome)
Activated genes (whole genome)
B
RPG
Ribi
Others
set1Δ change in mRNA levels t=45 (log2)
WT change in mRNA levels t=45 (log2)
C
pho23Δ
sap30Δ
H3K14Q
H3K42Q
snf1Δ
set1Δ
H3K4A
sir2Δ
tup1Δ
nup60Δ
H3K12Q
H3K14R
set3Δ
snt1Δ
Effect on Ribi expression (AUC)
Effect on RPG expression (AUC)
D
mRNA
set1Δ
bre1Δ
H3K4A
H3S10A
rrm3Δ
sir2Δ
sap30Δ
pho23Δ
set3Δ
sif2Δ
snt1Δ
H3K14Q
H3K42Q
snf1Δ
RPG
Ribi
SET1/K4-related
SIR-related
RPD3L
SET3C
Hyporesponsive

Figure I.5

Set1 is predominantly a repressor

(A) Whole genome analysis of *set1*Δ effects on diamide stress response. Left panel: gene expression data from Gasch et al (Gasch et al., 2000) for all genes induced or repressed at least 1.8 fold. Middle panel: Effect of *set1*Δ on diamide stress, for t=0, 15, 45, or 90 minutes, using whole-genome microarray data. Genes are grouped by repressed/activated, then subsequently sorted by the average *set1*Δ effect on gene expression. Right panel: ribosomal protein (RPG) or ribosomal biogenesis (Ribi) GO annotations for individual genes are indicated as black bars. The majority of genes that repress poorly in *set1*Δ mutants are involved in ribosome biosynthesis.

(B) Set1 functions primarily as a repressor. Scatterplot of change in mRNA abundance in wild-type (x axis) or *set1*Δ (y axis) yeast at diamide t=45 minutes. There is overall excellent correlation between the two datasets except for blunted repression of ribosomal protein genes and ribosomal biogenesis genes, as indicated.

(C) In silico analysis of mutant effects on RPG and Ribi gene expression. nCounter data were averaged for RPG or Ribi genes, and for each mutant the difference between mutant and wild-type expression is scatterplotted for the two gene classes – specific mutants of interest are indicated with red circles. In general mutants have highly correlated effects on expression of these genes during diamide stress, with “hyporesponsive” mutants such as H3K42Q exhibiting diminished repression of both gene classes. However, a subset of mutants separate RPG from Ribi gene expression – most notably, mutants in the RPD3L complex (*sap30*Δ□and *pho23*Δ) have no effect on RPG repression, but dramatically affect Ribi repression.

(D) nCounter data for selected mutants with variable effects on RPG/Ribi gene repression. Data are shown as in Figures I.1B, D. Mutants from several complexes of interest are highlighted here.

Overall, deletion of SET1 resulted predominantly in diminished repression of ribosome-related genes, with very few large effects on diamide-activated genes (Figure I.5B, Figure I.S6A–C). Importantly, loss of Set1 had a distinct effect on ribosomal gene repression from that observed in ‘‘hypo-responsive’’ mutants. Comparison of a given mutant’s effects on overall gene repression to its effects on ribosomal gene repression identifies Set1-related and Sir2-related mutants as having specific defects in ribosomal gene repression (Figure I.S6D, see also below). We next asked whether Set1’s role in ribosomal repression was specific to diamide stress. We therefore assayed gene expression of our 200 probes in wild type and *set1*Δ yeast responding to another stress response, heat shock, or responding to nutrient deprivation signals induced by the small molecule rapamycin (Hardwick et al., 1999; Humphrey et al., 2004). Each of these stress responses exhibited different repression kinetics of the RPG genes, yet in all three stresses *set1*Δ strains suffered defects in RPG repression (Figure I.5C). Thus, Set1 appears to act fairly generally as a repressor of ribosomal biogenesis under suboptimal growth conditions.

H3K4 Methylation and H3S10 Phosphorylation Jointly Contribute to Ribosomal Protein Gene Repression

Comparing *set1*Δ effects on mRNA abundance with modification mapping data, we noted that many genes repressed in a Set1-dependent manner were often associated with stress-induced gains in H3K4me3 and H3S10P at their 5’ ends

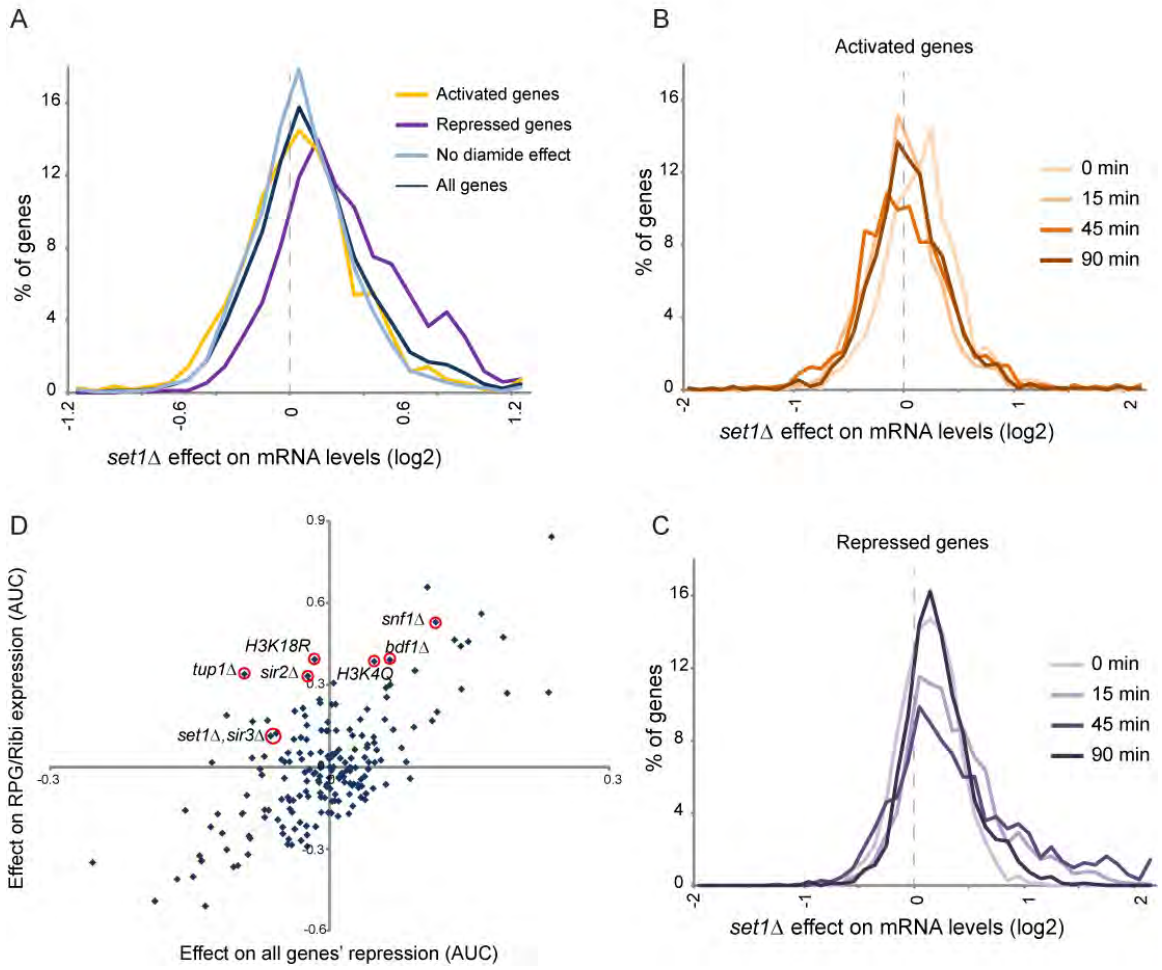
A
Activated genes
Repressed genes
No diamide effect
All genes
% of genes
set1Δ effect on mRNA levels (log2)
B
Activated genes
0 min
15 min
45 min
90 min
% of genes
set1Δ effect on mRNA levels (log2)
D
snf1Δ
bdf1Δ
H3K18R
tup1Δ
sir2Δ
H3K4Q
set1Δ,sir3Δ
Effect on RPG/Ribi expression (AUC)
Effect on all genes' repression (AUC)
C
Repressed genes
0 min
15 min
45 min
90 min
% of genes
set1Δ effect on mRNA levels (log2)

Figure I.S6

Set1 is a ribosomal repressor during stress.

(A) Histograms of *set1*Δ effects on genome-wide diamide-induced gene expression. Histograms are shown for all genes, for genes unaffected by diamide (<1.8-fold change in expression) or up- or down-regulated >1.8-fold by diamide, as indicated. Note that only repressed genes show substantially different behavior than the bulk behavior of all genes, with very few activated genes showing Set1 dependence.

(B–C) As in (A), but for each individual time point of diamide treatment. Genes are broken into activated (B) and repressed (C) based on their maximal fold change during the time course.

(D) Set1 is not a general hyporesponsive mutant. For all mutants analyzed by nCounter, the average effect on repressed genes (*x*-axis) is plotted against the effect specifically on RPG repression (*y*-axis). Overall effect on repression is calculated as the area under the curve (AUC) across the entire time course. General hyporesponsive mutants are found in the upper right quadrant, while mutants related to H3K4 methylation or the Sir complex are located above the diagonal, indicating specific defects in ribosomal gene repression.

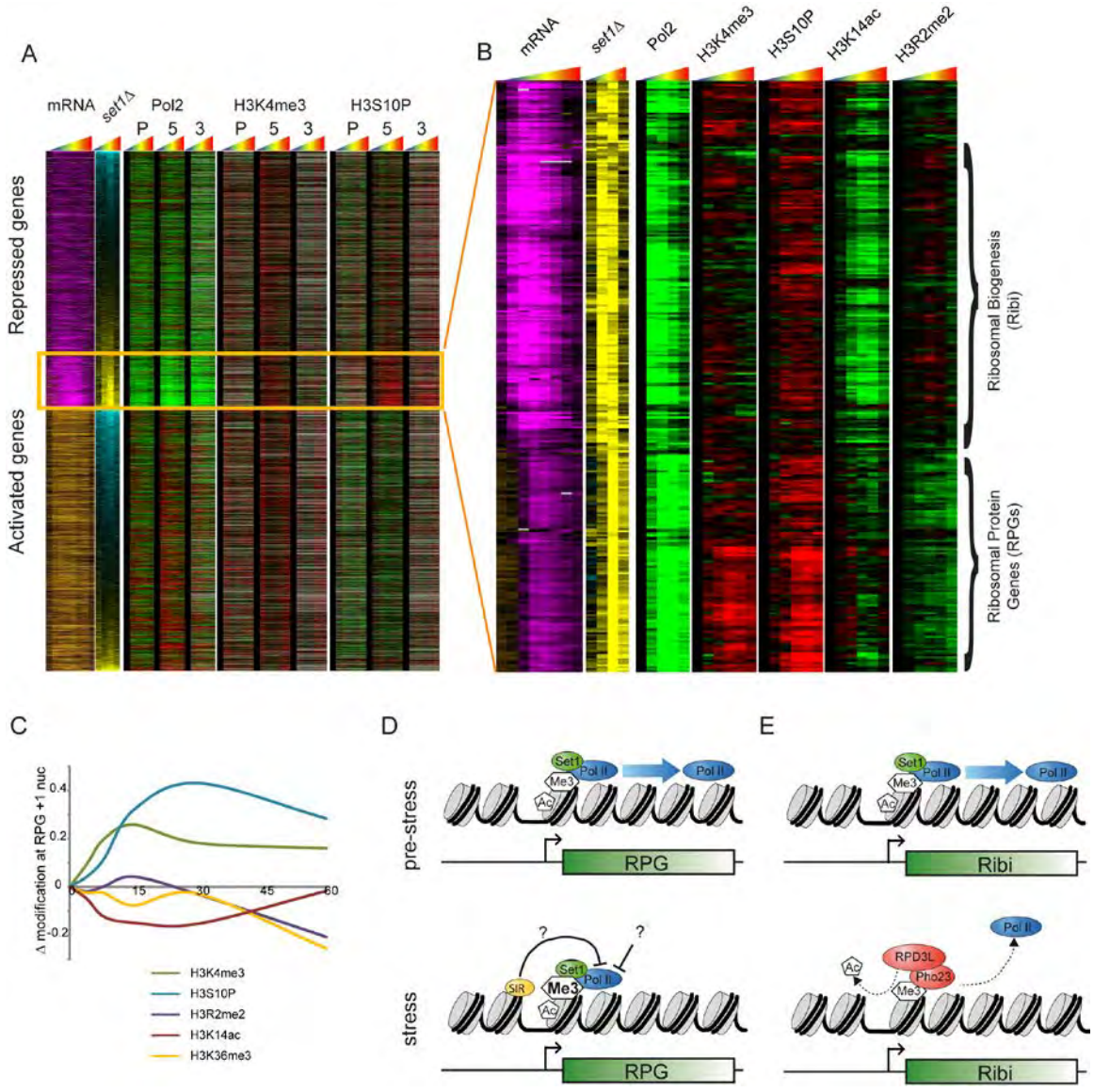
A
mRNA
set1Δ
Pol2
H3K4me3
H3S10P
P 5 3
Repressed genes
Activated genes
B
mRNA
set1Δ
Pol2
H3K4me3
H3S10P
H3K14ac
H3R2me2
Ribosomal Biogenesis (Ribi)
Ribosomal Protein Genes (RPGs)
C
Δ modification at RPG +1 nuc
0.4
0.2
0
-0.2
0
15
30
45
60
H3K4me3
H3S10P
H3R2me2
H3K14ac
H3K36me3
D
pre-stress
stress
Set1
Pol II
Me3
Ac
RPG
SIR
?
E
Ribi
RPD3L
Pho23

Figure I.6

Specific chromatin changes occur at RPG and Ribi genes during repression

(A) Whole genome mRNA (Gasch et al., 2000), *set1*Δ effects on mRNA (this study), Pol2 mapping (Kim et al., 2010) and tiling microarray data for H3K4me3 and H3S10P (this study) are shown for all genes sorted as in Figure 5A.

(B) RPG and Ribi genes exhibit distinct chromatin changes during diamide stress. Diamide-repressed genes whose repression is diminished in *set1*Δ mutants were clustered according to their associated changes in chromatin marks. Tiling microarray data are shown only for 5'CDS probes for each mark. A clear separation can be observed between predominantly RPG genes, which exhibit increased 5' H3K4me3, and decreased 5' H3R2me2, and predominantly Ribi genes, which exhibit decreased 5' H3K14ac.

(C) Specificity of H3K4me3 gain at RPG 5' ends. Probes corresponding to the +1 nucleosome at RPGs were analyzed specifically, and time course data for all five modifications is shown as indicated.

(D-E) Model for Set1-dependent RPG (D) and Ribi (E) repression. See main text.

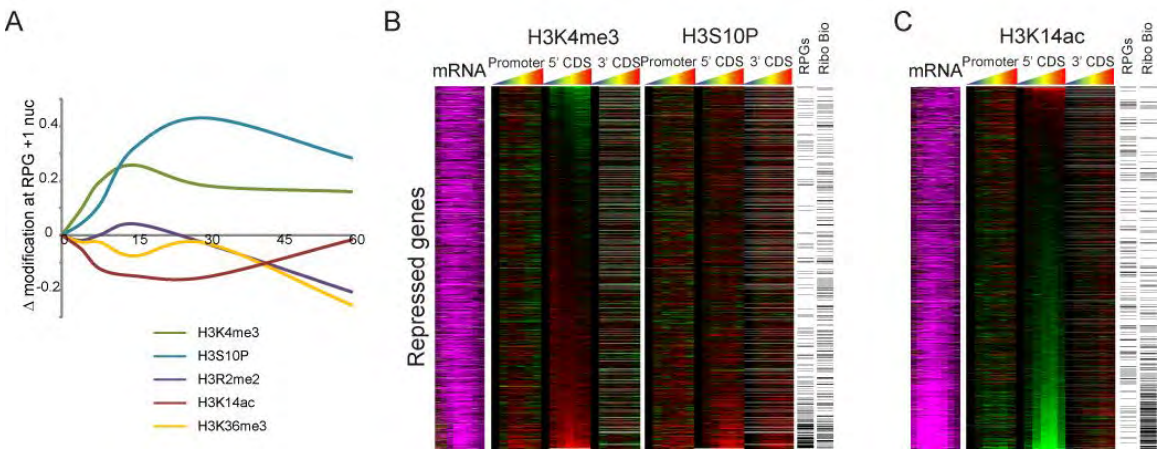

Figure I.S7

Specific chromatin changes associated with RPG and Ribi repression

(A) The majority of diamide-repressed genes that gain H3K4me3 are RPGs. Diamide-repressed genes are sorted by the 5’ change in H3K4me3, with GO annotations shown in the right panel as indicated.

(B) The majority of diamide-repressed genes that lose 5’ H3K14ac are Ribi genes. As in (A), but with genes sorted by 5’ change in H3K14ac.

(Figure I.6A, Tables I.S4 and I.S5). Focusing on the most highly Set1-dependent diamide-repressed genes revealed two clearly distinct clusters based on chromatin changes at the genes' 5' ends (Figure I.6B). Remarkably, we found that ribosomal protein genes (RPGs) were ''paradoxically'' associated with dramatic gains in H3K4me3 at their 5' ends, as well as gains in H3S10P. The changes in H3K4me3 and H3S10P were strongest at the +1 nucleosome but occurred throughout the promoters (Figure I.S7A and analysis not shown). Conversely, non-RPG ribosomal biogenesis (Ribi) genes exhibited similar increases in H3S10P, but modest increases in 5' H3K4me3. Instead, these genes were among the relatively few diamide-repressed genes associated with decreases in H3K14 acetylation. Importantly, these specific modification changes are quite specific for the gene classes in question. RPGs encompass the majority of genes gaining H3K4me3 during diamide repression, whereas Ribi genes provide the majority of cases with H3K14 deacetylation during repression (Figure I.S7B–C).

The distinct chromatin changes observed over RPG and Ribi genes during repression suggested that Set1-dependent repression of these genesets might operate via distinct pathways downstream of H3K4 methylation. We therefore sought to identify additional players in the pathways involved in repression of RPG and Ribi genesets. For each mutant assayed in our nCounter dataset, we compared the effects on diamide repression of RPGs to the effects on Ribi

repression (Figure I.7A). In general, mutants had similar effects on both gene classes, with globally hypo-responsive mutants such as H3K42Q failing to repress both RPGs and Ribi genes to similar extents. Intriguingly, we found a handful of mutants (several are shown in Figure I.7B) with substantially different effects on RPG and Ribi repression: most notably, mutants in the RPD3L complex (e.g., sap30Δ, pho23Δ) exhibit defective repression of Ribi genes, yet have no effect on RPG gene expression during diamide stress. These results are consistent with prior genome-wide studies in yeast which found that repression of Ribi genes in response to heat shock, H2O2, or rapamycin was defective in the absence of RPD3L (Alejandro-Osorio et al., 2009; Humphrey et al., 2004). Together, our results suggest that H3K4me3-dependent recruitment or activation of RPD3L (presumably via the PHD finger in Pho23; (Wang et al., 2011)) is required for Set1-driven repression of Ribi genes, whereas an alternative Set1-dependent pathway, potentially operating via Sir2 (see Discussion), represses RPGs.

Together, these results provide strong evidence for two distinct Set1-dependent gene repression pathways in yeast (Figure I.7C–D). Both sets of genes require intact H3K4 and H3S10 for full repression. However, stress-dependent repression of ribosomal biogenesis genes not only requires H3K4 methylation but also is dependent on the RPD3L repressor complex (which likely is recruited to these genes via the PHD finger in Pho23), and these genes specifically are

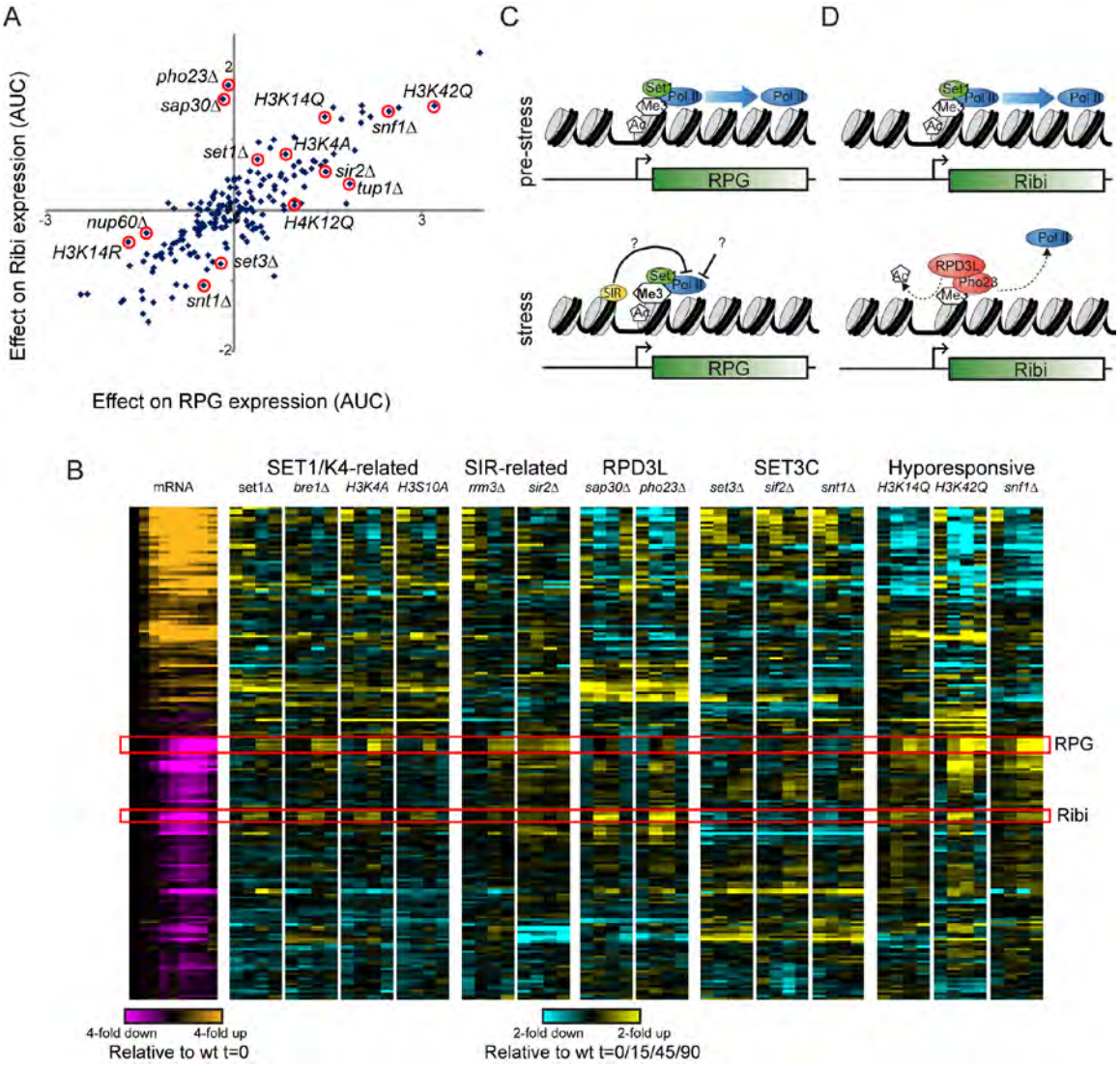
A
Effect on Ribi expression (AUC)
Effect on RPG expression (AUC)
pho23Δ
sap30Δ
H3K14Q
H3K42Q
snf1Δ
set1Δ
H3K4A
sir2Δ
tup1Δ
H4K12Q
nup60Δ
H3K14R
set3Δ
snt1Δ
C
D
pre-stress
stress
RPG
Ribi
Set1
Pol II
Me
Ac
SIR
Me3
RPD3L
Pho23
B
mRNA
SET1/K4-related
SIR-related
RPD3L
SET3C
Hyporesponsive
set1Δ
bre1Δ
H3K4A
H3S10A
rrm3Δ
sir2Δ
sap30Δ
pho23Δ
set3Δ
sif2Δ
snt1Δ
H3K14Q
H3K42Q
snf1Δ
4-fold down
4-fold up
Relative to wt t=0
2-fold down
2-fold up
Relative to wt t=0/15/45/90

Figure I.7

Differential regulation of RPG and Ribi genes by RPD3L.

(A) In silico analysis of mutant effects on RPG and Ribi gene expression. nCounter data were averaged for RPG or Ribi genes, and for each mutant the difference between mutant and wild-type expression is scatterplotted for the two gene classes. Specific mutants of interest are indicated with red circles. In general mutants have highly correlated effects on expression of these genes during diamide stress, with globally hypo-responsive mutants such as H3K42Q exhibiting diminished repression of both gene classes. However, a subset of mutants separate RPG from Ribi gene expression. Most notably, mutants in the RPD3L complex (*sap30*Δ and *pho23*Δ) have no effect on RPG repression, but dramatically affect Ribi repression.

(B) nCounter data for selected mutants with variable effects on RPG/Ribi gene repression. Data are shown as in Figure I.1B,D. Mutants from several complexes of interest are highlighted here.

(C–D) Model for Set1-dependent RPG (C) and Ribi (D) repression. See main text.

deacetylated during stress. In contrast, repression of ribosomal protein genes is delayed relative to Ribi repression, is largely unaffected by loss of the RPD3L complex, and furthermore these genes are associated with increased levels of the ‘‘active mark’’ H3K4me3 during repression.

Set1-Dependent Regulation of Antisense and Intron-Associated Transcripts

Whereas mutants in our dataset that specifically affect Ribi gene repression suggested a clear mechanistic hypothesis regarding Set1's effects on these genes (H3K4me3-dependent recruitment of RPD3L), we observed relatively few mutants that disproportionately dampened RPG repression relative to Ribi repression. How does H3K4 methylation affect RPG expression? Our first hypothesis, that RPGs could be repressed via H3K4me2-dependent recruitment of the repressive Set3C (Kim and Buratowski, 2009), was ruled out by the observation that mutants in Set3C components do not affect RPG repression (Figure I.7A–B).

An emerging concept in Set1 regulation of yeast genes is that Set1 is required for repression of transcription by trans-acting antisense RNAs (Berretta et al., 2008; Camblong et al., 2009; van Dijk et al., 2011). Of the 28 antisense transcripts in our probeset, only a handful were significantly expressed above background during diamide stress. For example, in YPD we find that the *BDH2* sense transcript is expressed at low levels, but its antisense is highly expressed (Figure

I.8A). Upon diamide treatment, the sense transcript is induced and the antisense is concomitantly repressed. We observed a widespread anticorrelation between mutant effects on sense versus antisense transcripts (Figure I.8B). Notably, H3K4 methylation mutants expressed the antisense transcript at lower levels than wild-type in YPD, and conversely hyper-induced the sense transcript during diamide stress. Similar results were observed for the *YTP1* sense/antisense pair (Table I.S1). In contrast, Set1 had little effect on the level of the antisense transcript at the *ARO10* locus, but instead was required for full induction of the *ARO10* sense transcript in diamide (Figure I.8C). Thus, in both cases Set1 primarily affects one transcript in a sense/ antisense pair, with the specific transcript being regulated in each case possibly reflecting the fact that the *ARO10* sense does not overlap the TSS of its antisense (Camblong et al., 2009), whereas for *BDH2* the competing transcripts each overlap each other's TSS.

Many of the mutants that affect sense/antisense ratios also affected RPG expression, raising the question of whether expression of these classes of genes might be linked. However, using strand-specific q-RT-PCR we have been unable to find any evidence for antisense transcription of RPGs under our conditions (unpublished data). Instead, based on the curious observation that antisense-mediated repression of *PHO84* in trans requires that the antisense RNA overlap with the *PHO84* UAS (Camblong et al., 2009), we wondered whether some aspect of RNA structure might affect Set1-dependent repression in yeast.

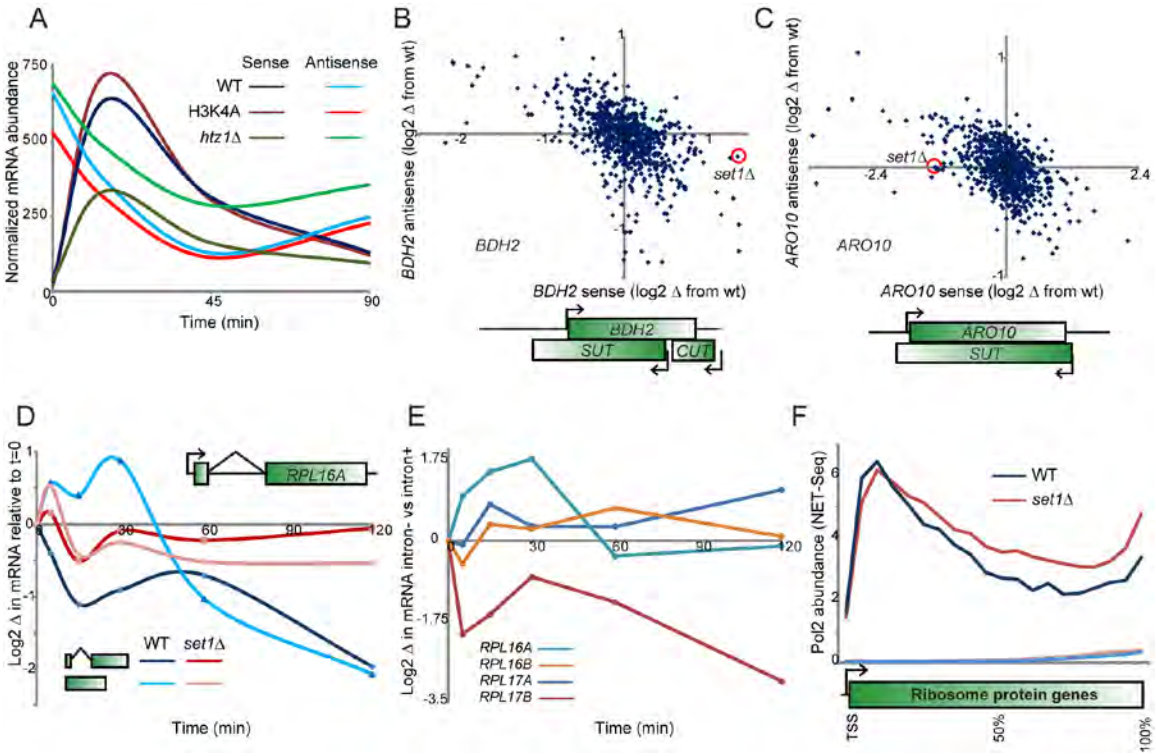
A
Normalized mRNA abundance
750
500
250
0
0
45
90
Time (min)
Sense
Antisense
WT
H3K4A
htz1Δ
B
BDH2 antisense (log2 Δ from wt)
BDH2 sense (log2 Δ from wt)
set1Δ
BDH2
SUT
CUT
C
ARO10 antisense (log2 Δ from wt)
ARO10 sense (log2 Δ from wt)
set1Δ
ARO10
SUT
D
Log2 Δ in mRNA relative to t=0
RPL16A
WT
set1Δ
Time (min)
E
Log2 Δ in mRNA intron- vs intron+
RPL16A
RPL16B
RPL17A
RPL17B
Time (min)
F
Pol2 abundance (NET-Seq)
WT
set1Δ
Ribosome protein genes
TSS
50%
100%

Figure I.8

Set1 effects on antisense and intron-containing genes.

(A) Anticorrelated abundance of sense and antisense transcripts for *BDH2*. nCounter intensity values are plotted for the sense and antisense transcripts at this locus for wild-type and two indicated mutants.

(B–C) Set1 skews sense-antisense ratios. Scatterplot of mutant effects on sense and antisense transcripts for *BDH2* and *ARO10*. Each point in the scatterplot represents the change in expression from wild-type for a given mutant at a specific time point. Here, in both cases, we highlight the effect of *set1*Δ at t=15 min. For both genes the local transcript structure as defined in Xu et al. (Xu et al., 2009) is schematized.

(D) Regulation of *RPL16A* by its intron. Expression of *RPL16A* was measured by q-RT-PCR (normalized relative to *snR13*), for either wild-type *RPL16A* or for yeast carrying an intronless *RPL16A* in its endogenous location. For both versions of this gene, parallel experiments were carried out in *set1*Δ.

(E) Introns contribute to diamide regulation of RPGs. For the four indicated RPGs, the difference in diamide effects on mRNA was calculated for intron-containing versus intronless versions of the gene, as indicated. (F) Set1 plays a role in RPG transcription pausing or termination. Sense strand NET-Seq data from Churchman et al. (Churchman and Weissman, 2011) are shown for all RPGs, for WT and *set1*Δ as indicated. The two lines near the *x*-axis show NET-Seq data on the antisense strand.

Notably, 73% of ribosomal protein genes in yeast carry introns, and these introns are generally much longer than non-RPG introns (Pleiss et al., 2007a, 2007b; Spingola et al., 1999). Moreover, RPG introns tend to have more stable secondary structures, both in absolute predicted DG of folding and in DG per base pair (analysis not shown).

We therefore asked whether RPG introns might contribute to stress-dependent repression of these genes. Figure I.8D shows change in expression of RPL16A, both for the native gene and for a chromosomally integrated intron-lacking version of RPL16A. Notably, diamide repression of this gene was far weaker in the absence of the native intron. We obtained similar results for three of four intronless strains tested, although one intronless gene exhibited hyperrepression in response to diamide stress (Figure I.8E). We next asked whether the intronic contribution to RPL16A repression was in the same pathway at Set1-mediated H3K4 methylation. As expected from Figure I.5, we confirmed that RPL16A repression was dramatically diminished in the absence of Set1. Notably, loss of the native intron had little additional effect on repression beyond that observed in the *set1*Δ mutant (Figure I.8D), suggesting that Set1-dependent repression of RPGs is somehow connected to their long, potentially highly structured introns. Given the recent observation that RPG introns can affect RNA levels not only of their host genes but also of many paralogs (Parenteau et al., 2011), it will be interesting in future studies to determine if such trans-acting gene regulation by

introns is Set1-dependent.

Discussion

We report here a systematic functional genetic analysis of the roles for chromatin regulators and histone mutations in the dynamics of stress response in yeast. We analyzed the effects of 202 chromatin-related mutants on diamide-dependent transcriptional dynamics for 170 RNAs. Importantly, we generalize prior single-gene observations that many chromatin regulators have broader effects on gene induction/repression kinetics than during steady-state growth. Furthermore, we combined these data with whole-genome mapping data for five histone modifications. Together, this dataset provides a rich multidimensional resource for generating hypotheses regarding chromatin biology.

Chromatin Regulation During Transcriptional Reprogramming

A major observation in this study is that chromatin mutants have far greater effects on gene expression during gene induction/repression than they do on steady-state gene expression in midlog growth. These results are consistent with observations using classic model genes such as *PHO5* and *GAL1-10*, and suggest that a great deal of chromatin biology is obscured at steady-state due to homeostatic mechanisms that compensate for deleted chromatin regulators. These results also suggest that chromatin transitions may often be rate-limiting during transcriptional responses to the environment.

By grouping mutants according to their effects on gene expression, we were able to systematically construct chromatin regulation pathways. These analyses complement similar studies in which deletions are grouped by the similarity of their genetic interaction profiles (Collins et al., 2007), or according to their gene expression defects in YPD (Lenstra et al., 2011). Importantly, by analysis of gene expression changes during a stress response, we uncover additional interactions that are not observed in YPD. For example, at t = 0 Rph1 and Rpd3 effects on gene expression are highly correlated (R^2 = 0.51), but during diamide stress they exhibit opposite effects on gene expression (R^2 = -0.38). These correlations may reflect stress-specific interactions between the factors in question, or they may reflect pathways that operate generally under all conditions but whose effects are only observed during dynamic reprogramming of transcription. Furthermore, by jointly analyzing histone point mutants and deletions of chromatin regulators, we correctly assign many histone-modifying enzymes to their known substrates. We uncover a small number of novel connections here (such as that between Nhp6a and H3R8), but did not find clear connections for predicted histone-modifying enzymes such as Set4. We believe the failure to identify a clear substrate for Set4 likely reflects the low levels of this protein in haploid yeast (Ghaemmaghami et al., 2003), although we cannot rule out that this enzyme primarily methylates nonhistone substrates, that it functions redundantly with another factor, or other possibilities.

Joint Analysis of Gene Expression Data and Genome-Wide Mapping Data

As noted in the introduction, the disconnect between global localization of histone marks and their specific, local importance is a key mystery in chromatin at present (Rando, 2012). Here, we carried out genome-wide histone modification mapping to enable comparisons between the functional effects of chromatin mutants with the locations of relevant marks in a dynamic context.

Overall, our modification mapping data were consistent with extensive prior knowledge about the modifications studied. However, we discovered a number of surprising aspects of histone modification changes during stress responses. For example, we found that H3K36 methylation, typically found over coding regions, was highly dynamic over promoters, suggesting a much more widespread role for this mark in regulation of open reading frames by cryptic transcription (Bumgarner et al., 2009) than has been previously appreciated. We are currently following up on the role for promoter-localized H3K36me3 in gene regulation. Similarly, while H3K14ac is correlated with transcription rate of genes during steady-state growth (Figure I.4, Figure I.S5; (Liu et al., 2005; Pokholok et al., 2005)), we found that the majority of genes changing expression in response to diamide stress did not gain or lose H3K14ac in predictable ways. Among repressed genes, deacetylation occurred primarily at genes encoding ribosomal biogenesis factors (Figure I.S7).

Together, these results highlight the difficulty in understanding the function of specific histone modifications. Clearly, not every gene marked with H3K36me3 requires Set2 for expression. Understanding this phenomenon, often termed ‘‘context dependence’’ of histone modifications, is necessary for a deeper understanding of the biological roles for chromatin regulators (Berger, 2007; Rando, 2012).

H3K4 Methylation and Ribosomal Gene Control

Our systematic analyses uncovered several surprising aspects of H3K4 methylation during diamide stress. As noted above, H3K4 methylation is associated with gene transcription at steady-state and thus is considered an ‘‘activating’’ mark, yet in budding yeast most evidence points towards H3K4 methylation as a repressive mark. Loss of Set1 results primarily in derepression of midsporulation and other repressed genes during midlog growth (Carvin and Kladde, 2004; Guillemette et al., 2011; Lenstra et al., 2011; Wang et al., 2011). Set1 appears to broadly play a role in control of sense/antisense ratios (Berretta et al., 2008; van Dijk et al., 2011; Houseley et al., 2008), as perhaps most clearly demonstrated in the case of the antisense transcript for *PHO84* that is capable of repressing sense transcription in trans (Camblong et al., 2009). We extend these results, identifying additional sense/antisense pairs regulated by Set1 (Figure I.8A–C). It remains unclear, however, what distinguishes sense/antisense pairs subject to Set1 regulation from those that are unaffected by Set1, although in

general, transcripts that overlap the promoter of their opposing partner are more likely to regulate the other transcript (Camblong et al., 2009).

Here, we dramatically extend the list of Set1 effects on transcription, finding that during diamide stress Set1 is required for full repression of genes involved in ribosomal biosynthesis. This effect is unlikely to result from nonhistone substrates of Set1, as it is recapitulated in H3K4A mutants. Together with prior observations demonstrating a role for Set1 in rDNA silencing (Briggs et al., 2001; Bryk et al., 2002) during midlog growth in YPD, our results therefore identify Set1 as a general repressor of ribosomal biogenesis, with roles in repressing rRNA, ribosomal protein genes, and ribosomal biogenesis genes. Importantly, *set1*Δ mutants have no effect on RPG and Ribi gene transcription during active growth in YPD (Figure I.5A and (Guillemette et al., 2011; Lenstra et al., 2011)), when ribosomal genes are being extremely highly transcribed, meaning that the identification of Set1 as a broad repressor of ribosomal biogenesis could only be observed under stress conditions as in this study. Conversely, since a subset of rDNA repeats is repressed even during active growth, this enabled the discovery of this aspect of Set1 function in early midlog studies.

Based on chromatin mapping and on functional analysis of all 202 mutants, we find that distinct mechanisms operate in the repression of RPGs and the Ribi regulon. Ribi genes, but not RPGs, are not effectively repressed in mutants

affecting the RPD3L complex. Moreover, Ribi genes are specifically associated with loss of H3K14ac during diamide stress, but exhibit little to no gain in H3K4me3. These results are consistent with a known pathway in which dephosphorylation of the transcriptional repressors Dot6 and Tod6 leads to RDP3L recruitment to Ribi promoters (Alejandro-Osorio et al., 2009; Huber et al., 2011), with binding of RPD3L component Pho23 to H3K4me3 contributing to either RPD3L recruitment or activity (Wang et al., 2011). The molecular details underlying the presumptive ‘‘bivalent’’ recruitment/activation of RPD3L by Dot6/Tod6 and H3K4me3 remain to be elucidated. In striking contrast, we find no role for RPD3L in repression of RPGs (Figure I.7A–B). Consistent with this, published gene expression profiles from *rpd3*Δ mutants in several stress conditions (diamide was not studied) reveal a far greater effect of Rpd3 loss on repression of Ribi genes than RPGs (Alejandro-Osorio et al., 2009). This raises the question of how Set1 contributes to RPG repression.

RPG repression was not accompanied by deacetylation of H3K14, and instead we observed that RPG promoters paradoxically gain H3K4me3 during diamide repression. It is not immediately apparent what aspect of RPGs makes them subject to Set1-regulated repression, but it is well known that RPGs represent roughly half (102 of 250) of all intron-containing genes in budding yeast. Given the emerging picture that Set1 affects gene regulation by antisense RNAs associated with promoters, we speculated that ribosomal introns and promoter-

associated antisenses might share in common some unusual form of locally tethered RNA secondary structure. Ribosomal introns are longer than most other introns in yeast, and generally have much greater predicted RNA secondary structure than other introns. Consistent with the idea that RPG introns might contribute to Set1-dependent repression, we found that in several cases replacement of the native intron-containing RPG with its cDNA (in the native chromosomal context) abrogated repression of the RPG by diamide (Figure I.8D–E), suggesting that either the intronic RNA or the corresponding DNA plays a role in Set1-dependent repression of some RPGs. As for the downstream repressor, we are currently investigating the hypothesis that RPG repression could be mediated by the Sir heterochromatin complex. Genome-wide mapping studies show that Sir3 binds to RPGs (Radman-Livaja et al., 2011; Taddei et al., 2009; Tsankov et al., 2006), and we show here that sir mutants and set1 mutants have similar effects on RPG repression (Figure I.7B). Moreover, in vivo selection studies for RNA-based repressors in yeast found a surprisingly high fraction of tethered RNAs could repress a reporter gene in a Sir-dependent manner (Kehayova and Liu, 2007), suggesting that structured RNAs might recruit the Sir complex in a manner analogous to the role for lincRNAs in repressing metazoan genes by Polycomb recruitment (Rinn et al., 2007; Tsai et al., 2010). In this view, we hypothesize that ribosomal introns might serve in some sense as ‘‘domesticated’’ lincRNAs.

Alternative hypotheses include the possibility that the act of splicing per se could play a role in Set1-dependent repression of RPGs (whose splicing is mechanistically distinct from non-RPG splicing; (Pleiss et al., 2007a, 2007b)) or that Set1 affects RPG expression by regulating Nrd1-dependent transcriptional termination (Terzi et al., 2011). Intriguingly, we observed in published NET-Seq data on RNA Pol2 localization (Churchman and Weissman, 2011) that *set1*Δ mutants exhibit lower 5' peaks of Pol2 over RPGs during midlog growth, with increased Pol2 levels downstream (Figure I.8F). This decrease in 5' Pol2 localization is consistent with the possibility that Set1 regulates RPGs via effects on transcriptional termination. It is also consistent with an alternative mechanism in which Set1 regulates Pol2 pausing at the 5' ends of RPGs and that the delayed Pol2 in wild-type cells either allows intron folding or simply keeps 5' RNA physically tethered near the promoter.

Future studies will be required to determine whether RPGs and antisense-regulated genes do in fact operate via a common mechanism, and to identify whether any specific aspects of RNA or RNA/DNA structures play a role in recruiting repressive complexes.

Conclusion

Taken together, these data show that chromatin regulators have far more effects on changes in gene expression than on steady-state transcription. Our approach

allows systematic linking of chromatin regulators in complexes and of histone-modifying enzymes with their substrates. Finally, we show that joint analysis of functional gene expression data with localization data leads to novel insights even into extensively studied histone modifications such as H3K4me3.

Materials and Methods

Yeast Strains and Growth Conditions

Two collections of yeast mutants were used. Histone point mutants were described in (Dai et al., 2008), and were a kind gift from Jef Boeke. Diploid heterozygous deletion mutants with the SGA reporter developed by (Tong et al., 2004) were sporulated and selected to generate haploid Mata knockouts (Pan et al., 2004). Yeast knockout mutants were grown on selective media (SC–Leu–His–Arg dropout mix+G418 200 mg/L+ L-Canavanine 6 mg/L) for two rounds to select for the deletion and for haploids, then used in the nCounter assays.

For Nanostring nCounter assays, each strain was grown in 80 mL YPD to mid-log phase (OD600 between 0.4 and 0.6) in a shaking 30uC waterbath. At ‘‘time zero’’ cells were treated with 1.5 mM diamide (D3648, Sigma), and 3 mL samples of culture each were taken at t = 0 (immediately prior to diamide addition), 4, 8, 15, 22.5, 30, 45, 60, and 90 min. Samples were immediately fixed with 4.5 mL cold methanol and kept in dry ice-ethanol bath throughout the time course. Cells in each sample were pelleted at 4,000 rpm for 2 min at 4°C, washed with 10 ml nuclease-free water, resuspended in 1 mL RNAlater solution (Ambion), and

stored at -80°C.

For the histone modification mapping time course, six flasks each of 400 mL BY4741 cells were grown in YPD to mid-log phase shaking at 220 rpm at 30°C. Cells were treated with 1.5 mM diamide at time zero. At t=0, 4, 8, 15, 30, and 60 min, cells were fixed by 1% formaldehyde, followed after 15 min by quenching with 125 mM glycine. Cells were then pelleted, washed with water, and subjected to MNase digestion as previously described (Kaplan et al., 2008; Radman-Livaja et al., 2010) and immunoprecipitation (see below).

nCounter Assays (Nanostring Technologies, Seattle, WA)

Approximately $1x10^7$ cells from individual samples were pelleted and resuspended in 600 mL Qiagen RLT buffer. After bead beating for 3 min, the supernatants were collected and 3–5 mL of the cell extracts were used for nCounter assays. The nCounter assays were performed as described (Geiss et al., 2008) with customized probes corresponding to 200 *S. cerevisiae* RNAs.

nCounter Data Normalization

The nCounter dataset reports on the measurement of 200 probes x 202 mutants x 4 time-points. We denote by $M_{i,j}$, the measurement of probe i sample j. To account for differences in hybridization, processing, binding efficiency, and other experimental variables, we used to following normalization procedure:

(1) Each sample was normalized relative to the average of four wild-type replicates taken at the same time point after diamide induction. First, samples were log transformed. Next, we assumed that different samples (WT versus mutant) could be brought on to the same scale by a linear regression (assuming that in the same time point most of the genes do not change their expression level). This was parameterized by two real values b_j and $a_j>0$ corresponding to background subtraction (b_j) and global normalization factor (a_j). Specifically, a_j is a multiplicative factor that is used to control the assay efficiency or to bring the total RNA counts roughly to the same levels, and b_j is an additive factor that corresponds to the average background counts of each sample. We estimated the values of these two normalization parameters for each sample using linear regression and normalized the data using the following equation:

$$\widetilde{M}_{i,j} = b_j + a_j M_{i,j}$$

(2) To overcome the limitation of the log-ratio statistics for weakly expressed genes (increase from 50 to 100 reads is not as significant as the increase from 100,000 to 200,000 reads), we used the variance stabilization method as described in [88]. Briefly, this involves estimating a statistic Dh whose variance is approximately constant along the whole measurement scale. For highly expressed genes, Dh and the log-ratio statistic coincide. We estimated parameters of the statistic Dh as described by Huber et al.,

and represented the data as pseudo-log likelihood to WT at time the matching time point (Figure 1, Table S1).

Correlation Analysis of Expression-Profiles

We computed a correlation matrix (Figure I.3A) by first concatenating the measurements (Dh values) for all probes at the four time points to a single vector for each mutant, and then computing the Pearson correlation between the vectors for each pair of mutants. We clustered the correlation matrix using hierarchical clustering with Euclidian distance metric and unweighted average distance (UPGMA) linkage. Clustering was done using MATLAB 7.10 procedures ‘‘pdist,’’ ‘‘linkage,’’ and ‘‘dendrogram.’’

To identify significant correlations between mutants we used a quantile-quantile plot. For a query mutant, we plotted the quantiles of its correlations vector with all other mutants versus theoretical quantiles from a normal distribution (function ‘‘qqplot,’’ MATLAB 7.10). Values that deviate from the line y = x were considered significant (Figure I.S4).

PCA Analysis

Principal component analysis was applied to the map of 200 probes versus 202 mutants using MATLAB 7.10 procedure ‘‘princomp.’’

Microscopy

To evaluate transcriptional induction in individual cells in a population, we performed time-lapse microscopy of the induction of GFP-tagged protein. Nine deletion strains (*hda2*Δ, *yta7*Δ, *spt8*Δ, *set1*Δ, *rph1*Δ, *snf1*Δ, *cac2*Δ, and *swc3*Δ) were generated using KanMX in the BY4742 background. Four GFP-fusion reporters were selected (GCY1, GRE3, PGM2, and TSA2) from a library (Breker and Schuldiner, personal communication) based on the yeast GFP-tagging library (Huh et al., 2003) with an additional constitutive cytoplasmic mCherry (Genotype: xxx-GFP::HIS3, pTEF2-cherry::URA3, *his3*Δ *leu2*Δ *met15*Δ *ura3*Δ *lyp1*Δ *can1*Δ::pMFA1- LEU2). Knockout strains were mated with GFP reporter strains and sporulated to generate haploid deletions carrying the GFP reporters.

Prior to assay, strains were grown in 96-well plates to mid-log (~0.6 OD 600) in synthetic complete media (SC). We then transferred cells to glass bottom microwell plates (384 format, Matrical Biosciences) pre-treated with concavalin-A (incubation with solution at 0.25 mg/ml for 15 min). Cells were allowed to settle onto the glass surface for 30 min. We then removed the media and replaced with treatment media (SC with 1.5 mM diamide).

Following induction we placed the cell on an automated microscope (Scan^R system, Olympus) and assayed with 406 objective at ~10min intervals, taking transmitted light, mCherry, and GFP images at each time point. Images were analyzed using custom-made software, written in python based on the OpenCV

image analysis package (http://opencv.willowgarage.com/). Briefly, the procedure detects cells by thresholding the mCherry image and finding contours of bright objects. Contours that meet gating criteria for circularity and size were considered cells. The procedure matched detected cells in successive images based on a reciprocal closest hit procedure allowing a maximum of 5 pixel movement. Since cells are adhered to the glass surface, this procedure was effective in following a single cell. If there was a budding event, the closest-hit procedure returns an ambiguous result and the match is not made. Cells that were traced throughout the time course were used in the further analysis steps.

Model

We represented each single cell time-course GFP measurements using a simple kinetic model. We assume that the transcription starts at a certain point following stimuli, termed t_{on}, and stops at t_{off}. Promoter behavior is represented by T(t):

$$T(t) = \begin{cases} 1 & t_{on} \leq t \leq t_{off} \\ 0 & otherwise \end{cases}$$

Only during this time interval is mRNA being transcribed; to simplify the model we assume that transcription occurs with a constant rate of mRNA/min, and we also assume a constant exponential decay rate of mRNA denoted by b. We present the mRNA levels as a function of time using the following differential equation:

$$\frac{d}{dt}R(t) = \alpha T(t) - \beta R(t)$$

Solving this equation we obtained a logistic equation describing mRNA level over time after stress induction at t = 0:

$$R(t) = \begin{cases} 0 & t < t_{on} \\ \frac{\alpha}{\beta}(1 - e^{-\beta(t-t_{on})}) & t_{on} \le t \le t_{off} \\ R(t_{off})\, e^{-\beta(t-t_{off})} & t > t_{off} \end{cases}$$

In the final step we assume that protein is the integration of the mRNA levels (assuming constant translation rate without degradation). We add a final parameter to account for the basal GFP level (prior to stress), solved the integral of R(t), and obtained the following equation:

$$F(t) = \begin{cases} A & t < t_{on} \\ A + \frac{\alpha}{\beta}(t - t_{on} - \frac{1}{\beta} + \frac{1}{\beta} e^{-\beta(t-t_{on})}) & t_{on} \le t \le t_{off} \\ F(t_{off}) + \frac{R(t_{off})}{\beta}\,(1 - e^{-\beta(t-t_{off})}) & t > t_{off} \end{cases}$$

To estimate the parameters for each single cell track, we used MATLAB 7.10 function ‘‘fmincon’’ using the ‘‘active-set’’ optimization algorithm.

Chromatin immunoprecipitation (ChIP)

ChIP assays were carried out as previously described [87]. Antibodies used in the ChIP assays were anti-H3K36me3 (ab9050-100, Lot#412997, Abcam), anit-H3K4me3 (04-745, Lot#NG1643014, Millipore), anti-H3K14ac (07-353, Lot#DAM1548623, Millipore), anti- H3S10p (04-817, Lot#NG1710274, Millipore), and anti- H3R2me2 (07-585, Lot#DAM1731499, Millipore).

Microarray Hybridization of ChIP Material

ChIP material was amplified using the DNA linear amplification method described previously (Liu et al., 2003, 2005). 3 ug of the amplified ChIP products was labeled via the amino-allyl methods as described on http://www.microarrays.org. Labeled probes (a mixture of Cy5-labeled input and Cy3-labeled ChIP-ed material) were hybridized onto an Agilent yeast tiled oligonucleotide microarray (G4495A) at 65°C for 16 h and washed as described on http://www.microarrays.org. The arrays were scanned at 5μ resolution with an Agilent scanner. Image analysis and data normalization were performed using Agilent feature extraction.

CHAPTER II

H3K4 methylation is required for ribosomal protein genes to be adequately repressed in response to a stress.

Abstract

Chapter I showed that H3K4 methylation is required for ribosomal protein genes (RPGs) to be completely repressed during a yeast stress response. However the mechanism, by which a specific histone modification regulates the repression of a specific gene family in response to stress, remains to be elucidated. Set1, H3K4 methylatransferase, has been implicated to regulate antisense-mediated trans-silencing. In the case of RPGs, unlike most other yeast genes, RPGs contain introns. Interestingly, a recent study shows introns within RPGs affect the expression of paralog RPGs. Given the fact that introns within RPGs tend to be longer and highly structured, I hypothesize that introns within RPGs act as non-coding RNAs which regulate the repression of RPGs during stress and are themselves regulated by Set1. While deleting *RPL16A*'s intron decreased the repression of other RPGs, replacing *RPL16A*'s intron with introns from other non-RPG genes has very limited effect on the repression of *RPL16A*. Taken together, this indicates that introns within RPGs regulate the repression of other RPGs during stress and they function independently of sequence.

INTRODUCTION

In Chapter I, I found that Set1-dependent H3K4 methylation is required for adequate repression of ribosomal protein genes during stress. However, the underlying mechanism is still unknown. Set1 was reported to promote the production of *PHO84* antisense RNA which suppresses *PHO84* sense RNA (Camblong et al., 2009), suggesting Set1 plays a role in regulating antisense-mediated trans-silencing. Most RPGs share a feature that is unique among yeast genes – containing introns. Introns within RPGs are usually longer than other introns and tend to be highly structured. Notably, introns within RPGs have recently been shown to regulate the expression of RPGs (Parenteau et al., 2011). More precisely, for duplicated RPGs, deletion of an intron in one gene copy affects the expression of the other. Taken together, I hypothesize that introns within RPGs act as non-coding RNAs regulating the expression of RPGs and the amount of intron is regulated by Set1-dependent H3K4 methylation during stress.

To test the hypothesis, I deleted an intron in one of the RPGs, *RPL16A,* and examined its effect on other genes by genome-wide gene expression microarrays. Surprisingly, I found not only the repression of its paralog, *RPL16B*, was defective during stress but also that of many other RPGs. The results support the hypothesis that introns within RPGs regulate the repression of other RPGs in stress. To further test if introns in RPGs act as non-coding RNAs, I

replaced the intron in *RPL16A* with an intron from another non-RPG yeast genes and checked the repression of intron-swapped *RPL16A* during stress. Previous studies have shown that the sequence of non-coding RNAs is crucial for its function (Tsai et al., 2010). Therefore, should introns within RPGs act as non-coding RNAs their sequences matter. However, three out of the four intron-swapped experiments showed only slight defect in the repression of intron-swapped *RPL16A* during stress. Therefore the repression of RPGs can be achieved by a presence of an intron which does not require specific sequence.

RESULTS

Genes involved in ribosome biogenesis failed to fully repress during stress in intronless *RPL16A* mutant

In order to determine the importance of RPG introns in their regulation, I deleted the intron in *RPL16A* in *S.cerevisiae* genome and measured RNA levels in wild-type and intronless *RPL16A* mutant (*RPL16A*∆i) in a time course after diamide addition (t=0, 15, 45, 90 min), using genome-wide gene expression microarrays. Based on the gene expression data, genes in the yeast genome were clustered into 6 groups (Figure II.1). One of these groups in particular showed a major defect in expression in *RPL16A*∆i mutant; this group showed incomplete repression during diamide stress response. GO analysis showed this group was enriched in genes involved in ribosome biogenesis. Surprisingly, deleting the intron in *RPL16A* affects not only the mRNA abundance of its paralogous gene,

Figure II.1

Genome-wide gene expression analysis of intronless RPL16A effects on diamide stress response.

Genome-wide gene expression data in intronless RPL16A for t=0, 15, 45, 90 min after diamide addition using genome-wide gene expression microarray. For each time course, data are normalized to wild type at the same time point. Genes are clustered by k-mean into 6 groups. GO analysis of one group indicated enrichment in genes involved in ribosome biogenesis.

RPL16B, but also many other genes in the same pathway. More importantly, the defect is consist with the observation from Chapter I where I found *set1*Δ mutant showed the same defect - failing to adequately repress genes involved in ribosome biogenesis. These results showed both *RPL16A*Δi and *set1*Δ share a similar phenotype, supporting the hypothesis that the intron in *RPL16A* plays a role in Set1-dependent *RPL16A* repression during stress.

The repression of RPL16A during stress does not require specific sequence in its intron.

I next sought to test if the repression required a specific sequence in the intron in *RPL16A*. If the *RPL16A* intron behaves in a similar way to long non-coding RNAs, then a specific sequence in long non-coding RNAs would be critical for them to form secondary structure, which is crucial for their function. To test the hypothesis, I decided to replace *RPL16A*'s intron with an intron from other non-RPG genes so that only the sequence is changed, while the splicing remains unaffected. I first replaced *RPL16A*'s intron in the genome with the intron from *ACT1* or *MRK1*, because the introns in *ACT1* and *MRK1* are about the same length as *RPL16A*'s intron, but have different sequence composition. *RPL16A* mRNA abundance in a diamide time course was measure by qPCR (Figure II.2A). While wild-type *RPL16A* was repressed almost 16 fold during stress, *RPL16A*Δi-*ACT1*intron was repressed only 8 fold, which supports the hypothesis. However, in the other case, *RPL16A*Δi-*MRK1*intron was repressed to the same

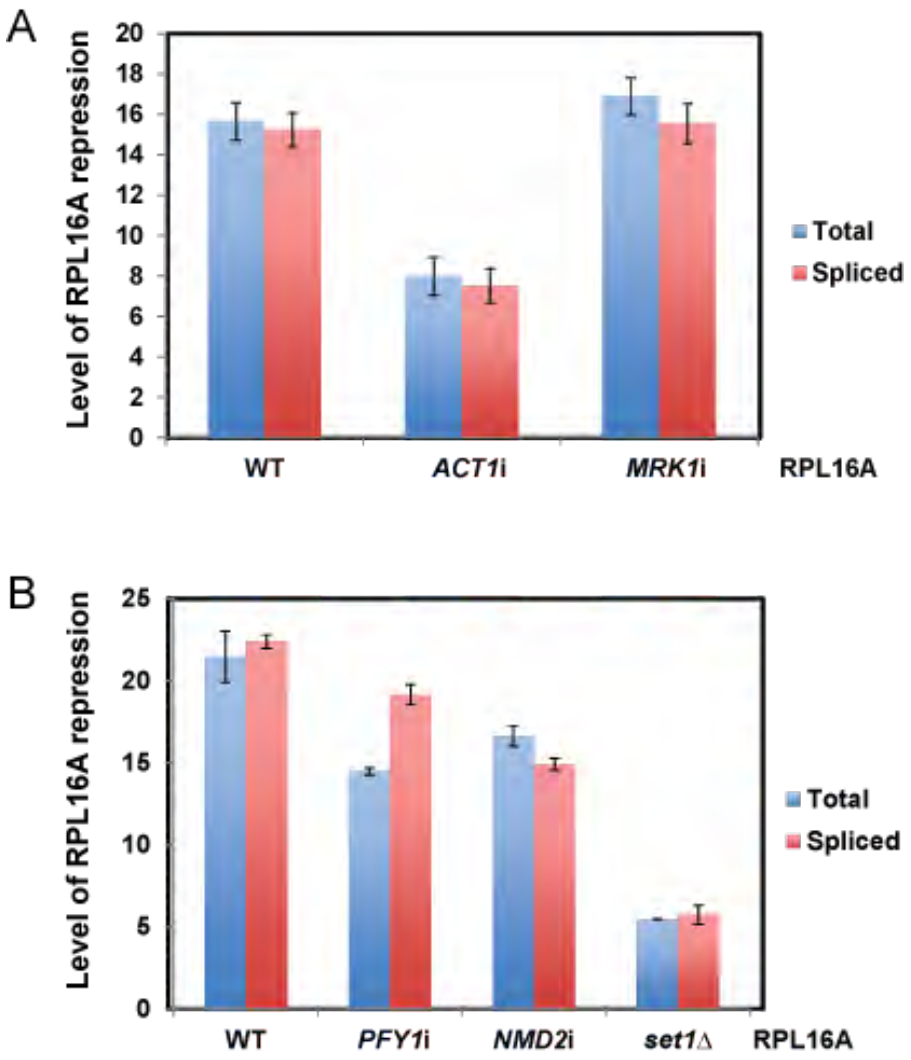

Figure II.2

The effect on *RPL16A* repression of intron-replaced *RPL16A* during stress

(A) The effect of the replacement of *RPL16A* intron with other genes' intron on *RPL16A* repression in diamide stress response. The intron of *RPL16A* was replaced with *ACT1*'s intron or *MRK1*'s intron. WT or mutant *RPL16A* mRNAs was measured before and 45min after diamide addition by qPCR using probes against exon2 for total *RPL16A* mRNAs or exon-exon junction for spliced *RPL16A* mRNAs.

(B) As in (A) but the intron of *RPL16A* was replaced with *PFY1*'s intron or *NMD2*'s intron.

level as wild-type. Due to the contradictory results, I decided to replace the intron in *RPL16A* with the intron in *PFY1* or *NMD2* in order to get a conclusive answer. Both *RPL16A*Δi-*PFY1*intron and *RPL16A*Δi-*NMD2*intron showed 15-17 fold repression, which was only slightly defective comparing to 22 fold repression in wild-type (Figure II.2B). In conclusion, three out of the four intron-replacement experiments showed almost wild-type level repression, suggesting the repression of *RPL16A* mRNA requires an intron regardless of the sequence of the intron.

DISCUSSION

I report here that deletion of the intron in one RPG attenuates the repression of many genes in the same pathway during stress. The effect could either be a direct result from the absence of the intron or a secondary effect resulted from the misregulated level of *RPL16A* mRNA caused by the absence of intron. To distinguish between the two possibilities, one could overexpress intronless *RPL16A* and check the repression during stress. If the level of repression were decreased to the same extent as intronless *RPL16A* driven by its own promoter, the result would suggest the defective repression of other RPGs is a direct response from the absence of intron in *RPL16A*. On the other hand, if the RPGs were less repressed than in the original intronless *RPL16A*, the effect on other RPGs is more likely due to the level of *RPL16A* mRNA instead of its intron.

Parenteau *et al*. showed that deletion of the intron in one RPG affects the

expression of its paralogous RPG. This is also true for most RPGs they tested. Surprisingly, I found that deletion of *RPL16A*'s intron affects many more genes involved in ribosome biogenesis. It would be interesting to test if this is a general phenomenon for most RPGs. Also, if this phenomenon is unique to introns within RPGs, comparing introns within RPGs to other non-RPG introns should shed light on the function of RPG's introns.

The finding that the presence of an intron is required for *RPL16A* repression during stress but not its sequence disagrees with the hypothesis. This is supported by three intron replacement experiments; interestingly this did not extend to the replacement with *ACT1* intron. What differs between the *ACT1* intron and the other introns? One study showed the ACT1 intron contains a promoter for an antisense RNA. Therefore, it is possible that the antisense RNA interferes with the repression of *RPL16A* whose intron was replace with *ACT1* intron.

MATERIALS AND METHODS

Yeast Strains and Growth conditions

The intronless and intron-replaced *RPL16A* strains were constructed as follows: *RPL16A* consists of two exons and one intron. DNA sequence of *RPL16A's* exon1 and exon2 were PCR amplified and cloned into a yeast vector pRS415 using a T4 DNA polymerase dependent ligation. The ligation product of *RPL16A*

exon1 and exon2 was PCR amplified and transformed into BY4741. The endogenous *RPL16A* were deleted by homologous recombination using DNA fragments encoded *URA3* gene. The *URA3* gene in *RPL16A* locus was subsequently replaced with intronless *RPL16A* DNA fragments by homologous recombination. For the intron-replaced RPL16A strains, introns from non-RPG genes, such as *ACT1*, was PCR amplified from BY4741 genomic DNA and inserted in between *RPL16A* exon1 and exon2 on yeast pRS415 vector. Intron-replaced *RPL16A* was amplified by PCR. The *URA3* gene in *RPL16A* locus in *RPL16A* deletion strain was replaced with intron-replaced *RPL16A* DNA fragments by homologous recombination.

Each strain was grown in 50 mL YPD to mid-log phase (OD600 between 0.4 and 0.6) in a shaking 30°C waterbath. At "time zero" cells were treated with 1.5 mM diamide (D3648, Sigma), and cells were collected at time 0, 15, 45, and 90 min. Total RNAs were extracted from yeast cells using bead beating and TRIzol following manufacture's instructions.

Gene expression microarray

20ug DNase I-treated total RNAs was used for cDNA synthesis with amino-allyl UTP and superscript II. Amino-allyl incorporated cDNAs of WT and mutant were incubated with Cy5 and Cy3 dyes respectively in the dark for 1 hour. Labeled probes (a mixture of Cy5-labeled WT and Cy3-labeled mutant cDNAs) were

hybridized onto an Agilent yeast gene expression microarrays at 65°C for 16 h and washed as described on http://www.microarrays.org. The arrays were scanned at 5 μ resolution with an Agilent scanner. Image analysis and data normalization were performed using Agilent feature extraction.

RT-qPCR

5ug total RNAs were reverse transcribed into cDNA using random hexamers and superscript III. qPCR was carried out using KAPA SYBR Fast reaction mix and according to the manufacture's instructions. Each sample was run in triplicate in three independent experiments. Two housekeeping genes were used as internal controls to normalize the variation in expression levels.

CHAPTER III

Set1 and Xrn1 antagonistically regulate total mRNA levels in *S. cerevisiae*.

Abstract

Histone H3K4 methylation is one of the most studied histone modifications, and yet its function in gene expression still remains largely unknown. An interesting connection between Set1, the H3K4 methyltransferase, and Xrn1, 5'-3' exonuclease, has been reported in several studies. Set1 is found to be required for trans-silencing mediated by antisense RNAs, which are degraded by Xrn1. In addition to the relatively well-known effects of Xrn1 on non-coding transcripts, Xrn1 was also recently reported to globally up-regulate total mRNA abundance. Given that H3K4 methylation is a global histone modification that marks active-transcribing genes in the genome, I decided to test if loss of *SET1* would suppress the up-regulated mRNAs in *xrn1*Δ. Interestingly, I found that the large-cell phenotype of *xrn1*Δ cells was partially suppressed in set*1*Δ*xrn1*Δ double mutant. In addition, genome-wide analysis of mRNA abundance revealed that the global increase in total mRNA abundance in *xrn1*Δ mutants was suppressed in the *set1*Δ*xrn1*Δ double mutant. To further understand how loss of *SET1* leads to suppression of mRNA levels in double mutant, I assayed global mRNA levels in mutants including those affecting the nuclear exosome or Rat1, finding that neither of these factors was involved in the same pathway. Finally, I focused on

an unusual phenotype *xrn1*Δ has – accumulation of uncapped RNAs. Surprisingly, I found that capped mRNA abundance was maintained in both *xrn1*Δ and *set1*Δ*xrn1*Δ, indicating that the global gain in mRNA abundance in *xrn1*Δ that was suppressed in *set1*Δ*xrn1*Δ double mutants resulted from changes in the levels of uncapped mRNAs. In conclusion, the results suggest Set1 plays a role in regulating synthesis or stability of uncapped mRNAs that are only revealed in the absence of the 5' exonuclease Xrn1.

INTRODUCTION

Histone H3K4 methylation is a widespread histone modification that has been the subject of thousands of studies, yet its function in gene expression still remains to be elucidated. H3K4 methylation is highly conserved from yeast to human, and is deposited on nucleosomal histones by one or several multi-subunit complexes in different organisms. In *S.cerevisiae*, the COMPASS complex is the only H3K4 methyltransferase, and the catalytic activity is carried out by the Set1 subunit. Previous studies have shown the loss of Set1 resulted in complete loss of histone H3K4 methylation (Briggs et al., 2001; Krogan et al., 2002). The most well-known feature about this mark is that it specifically marks the 5' end of actively-transcribed genes in the genome (Boa et al., 2003; Santos-Rosa et al., 2002), and levels of H3K4 trimethylation correlated with the expression level of the gene in question (Pokholok et al., 2005). Nonetheless, Set1 deletion has very limited effect on steady-state total mRNA abundance, which is inconsistent with

the widespread description of H3K4 methylation as playing a widespread role in activating gene transcription.

Synthetic genetic studies in yeast have provided some insights into potential functions of Set1. Specifically, Set1 and Xrn1 have been reported to antagonistically regulate antisense-mediated gene silencing (Berretta et al., 2008; van Dijk et al., 2011). Xrn1 is 5'-3' exonuclease which functions in cytoplasmic mRNA decay, and loss of Xrn1 activity reveals a novel class of noncoding antisense RNAs known as XUTs (Xrn1-sensitive antisense ncRNAs). Interestingly, Set1 is required for silencing of genes with XUTs (van Dijk et al., 2011). In another study, trans-silencing of *Ty1* retrotransposon was disrupted after deleting *SET1* in *xrn1*Δ background. Notably, *Ty1* antisense RNA expression in *xrn1*Δ was partially suppressed in *set1*Δ*xrn1*Δ (Berretta et al., 2008). More recently, Sun et al. reported a global increase in total mRNA abundance was found in *xrn1*Δ (Sun et al., 2013). This raises the question of whether this global up-regulation of mRNAs might be suppressed in *set1*Δ*xrn1*Δ.

Here, I generated *set1*Δ*xrn1*Δ double knockout mutants in *S.cerevisiae*. By examining their morphology under microscope, I found while *xrn1*Δ cells were usually large, some *set1*Δ*xrn1*Δ cells were much smaller than *xrn1*Δ cells. More importantly, *set1*Δ*xrn1*Δ cells grew much slower than WT or any single mutant. I performed RNAseq to profile gene expression genome-wide. Interestingly, I

found up-regulated mRNAs in *xrn1*Δ were suppressed in *set1*Δ*xrn1*Δ. The suppression in total mRNAs did not involve nuclear exonucleases, such as nuclear exosome or Rat1. Most importantly, after comparing the abundance of capped mRNAs to that of total mRNAs, the results showed comparable levels of capped RNAs in both *xrn1*Δ and *set1*Δ*xrn1*Δ, indicating the suppression was derived from the huge decrease in uncapped mRNAs after deleting *SET1* in *xrn1*Δ background. Together, these data suggests the high level of uncapped mRNAs in *xrn1*Δ was maintained by Set1 and greatly reduced once Set1 was deleted in *xrn1*Δ.

RESULTS

Large-cell phenotype of *xrn1*Δ cells was partially suppressed in *set1*Δ*xrn1*Δ cells.

I generated *set1*Δ*xrn1*Δ double mutant yeast strain by mating *set1*Δ with *xrn1*Δ haploid cells and s porulating the diploid cells to get spores with correct genetic background. Mutant (*set1*Δ, *xrn1*Δ*, set1*Δ *xrn1*Δ) and wild-type (WT) yeast cells were grown in YPD to mid-log phase and cell morphology was examined under microscope. As previously reported (Jorgensen et al., 2002), *xrn1*Δ cells were large, sometime mal-shaped (Figure III.1C, D). In contrast, consistent with prior studies we find only minor cell size and shape alterations in *set1*Δ cells (Figure III.1B). Interestingly, unlike *xrn1*Δ cells, *set1*Δ*xrn1*Δ cells were

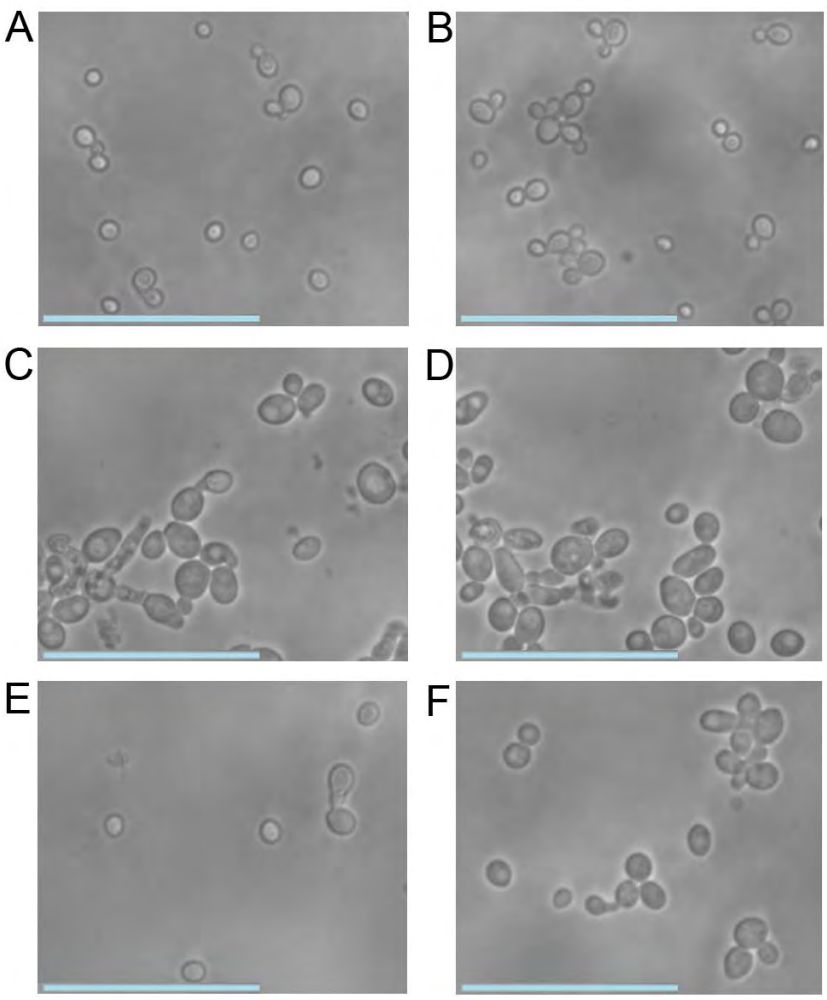

Figure III.1

Cell morphology analysis of wild-type and mutant yeast strains.

Yeast cells were grown in rich media to mid-log phase and taken pictures under microscope.

(A) Wild-type cells

(B) *set1*Δ cells

(C) and (D) *xrn1*Δ cells

(E) and (F) *set1*Δ*xrn1*Δ cells. The scale bar indicates 50 μm.

variable in sizes (Figure III.1E, F). Some double mutant cells were much smaller and WT-shaped comparing to *xrn1*Δ cells. The observation suggests the morphological defects in *xrn1*Δ cells were partially suppressed in *set1*Δ*xrn1*Δ cells.

_set1_Δ_xrn1_Δ cells show additional growth defects than _xrn1_Δ cells.

As *xrn1*Δmutants exhibit slow growth, I next asked if this slow growth phenotype was also suppressed in *set1*Δ*xrn1*Δ cells. I grew overnight cultures of WT and mutant yeast cells and diluted the cultures to OD600=0.1. The diluted cultures started to grow at 30°C and the growth was measured by recording the absorption of the yeast cultures at OD600 every hour. The results showed *xrn1*Δ cells grew slower than WT while *set1*Δ cells grew similarly to WT cells (Figure III.2A). Surprisingly, *set1*Δ*xrn1*Δ cells grew much slower than WT or any single mutant. By calculating the doubling time of each strain, I found the doubling time of *set1*Δ*xrn1*Δ cells was ~160 minutes, which is much longer than any single mutant or WT (108 min) (Figure III.2B). Clearly the deletion of *SET1* in *xrn1*Δ cells impaired cell growth, which suggests the mutant effect of *SET1* deletion on cell growth has long been masked in WT background and i s uncovered when cells lack Xrn1.

A

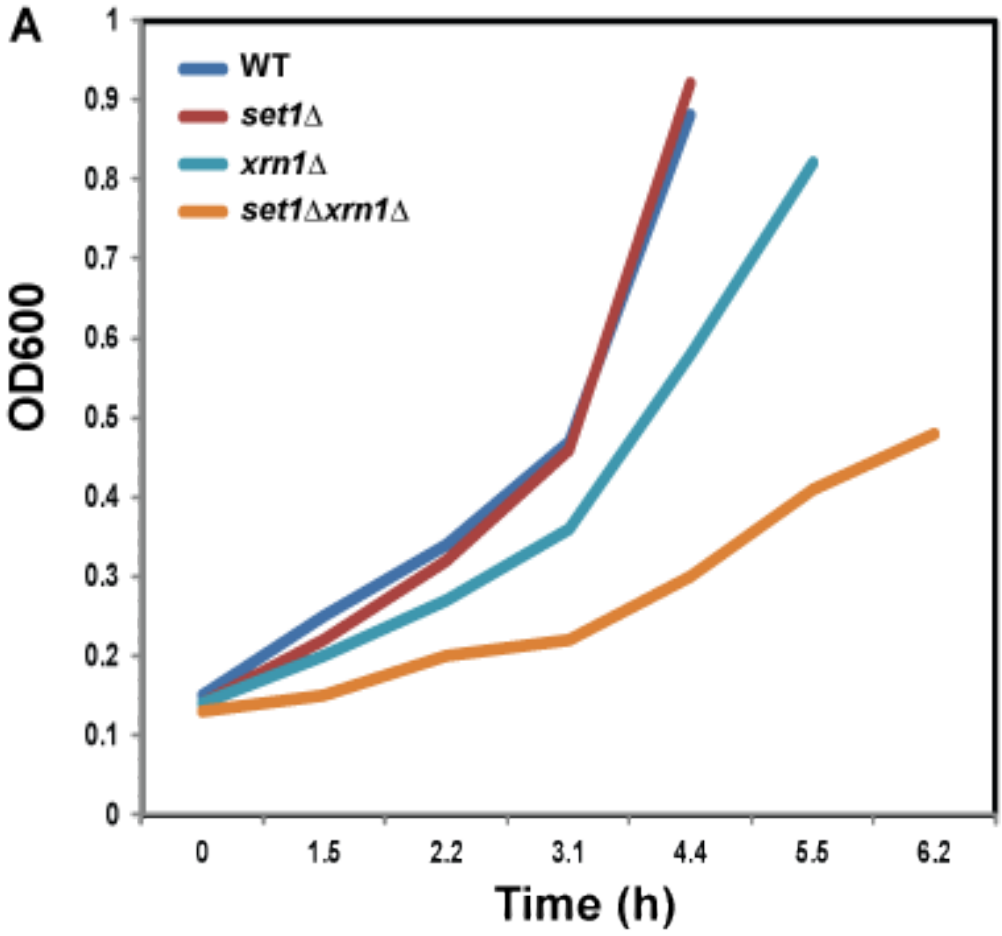

B

Strain	WT	*set1*Δ	*xrn1*Δ	*set1*Δ*xrn1*Δ
Doubling time (min)	108	97	119	161

Figure III.2

Growth analysis of wild-type and mutant yeast strains.

(A) Growth curves of wild-type and mutant yeast strains were measured by recording optical density of yeast cultures in YPD at 600 nm.

(B) Doubling time in minutes of wild-type and mutant yeast strains were calculated based on growth curves.

The general increase in mRNAs in *xrn1*Δ cells was suppressed in *set1*Δ*xrn1*Δ cells.

Histone H3K4 trimethylation has been shown to mark at the 5'end of active-transcribing genes, and yet the removal of H3K4 methylation by deleting *SET1* results in very limited effects on gene expression. Given the genetic interactions between Set1 and Xrn1 in cell morphology and growth rate, I next sought to identify whether Set1 and Xrn1 affect similar target genes. A recent study discovered that there is a global 3 fold increase in total mRNA abundance in *xrn1*Δ when total mRNAs were normalized to cell number by using an internal *Schizosaccharomyces pombe* (*S.pombe*) spike-in control (Sun et al., 2013). Taking a similar approach to enable global RNA abundance changes to be quantified, I freeze yeast cells after they were in mid-log phase growth. Before isolating polyA-RNAs, I mixed $1x10^8$ *S.cerevisiae* cells with $7x10^5$ *S.pombe* cells. RNA-seq libraries were prepared using isolated polyA-RNAs and deep sequenced to allow for genome-wide gene expression analysis. Consistent with prior studies, we find that *xrn1*Δ □□□□□□□showed a global increase in total mRNAs while, *set1*Δ exhibited far more subtle effects on a subset of specific mRNAs (Figure III.3). Interestingly, the global increase in total mRNAs present in *xrn1*Δ was suppressed in *set1*Δ*xrn1*Δ. The boxplot representing the distribution of fold changes to WT indicates that an average 2 fold increase in total mRNAs in *xrn1*Δ was decreased to an average WT level in *set1*Δ*xrn1*Δ (Figure III.3D). This observation suggests Set1 plays a role in maintaining the high level total mRNAs

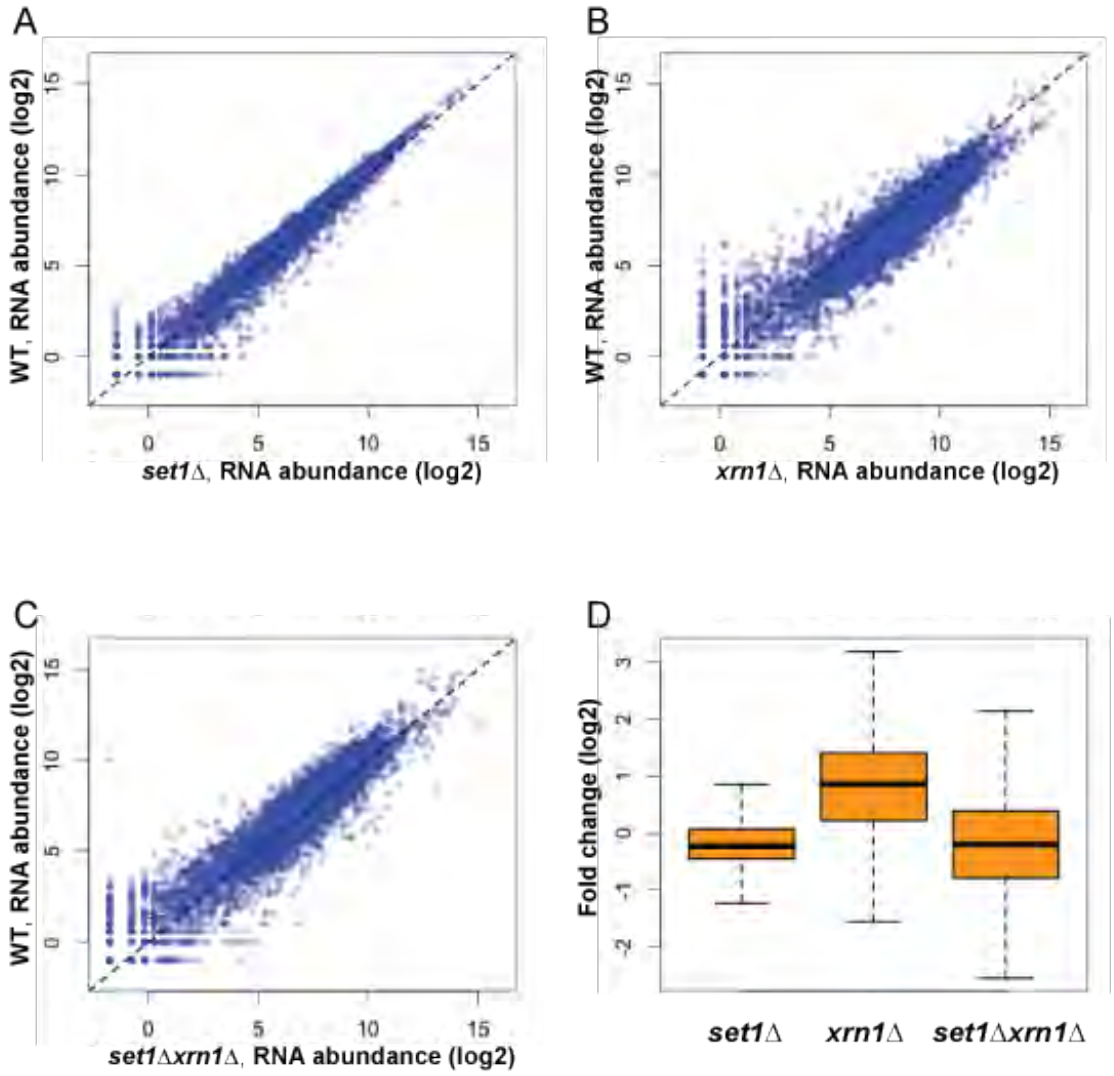
A
WT, RNA abundance (log2)
set1Δ, RNA abundance (log2)
B
WT, RNA abundance (log2)
xrn1Δ, RNA abundance (log2)
C
WT, RNA abundance (log2)
set1Δxrn1Δ, RNA abundance (log2)
D
Fold change (log2)
set1Δ
xrn1Δ
set1Δxrn1Δ

Figure III.3

The mutant effect on genome-wide gene expression

Genome-wide polyA-RNA abundance of wild-type and mutant yeast strains was measured by RNA-seq. The abundance for each gene was normalized by an internal *S.pombe* RNA control.

(A) Scatter plot of RPKM in log2 scale for whole genome in WT vs *set1*Δ cells.

(B) Scatter plot of RPKM in log2 scale for whole genome in WT vs *xrn1*Δ cells.

(C) Scatter plot of RPKM in log2 scale for whole genome in WT vs *set1*Δ*xrn1*Δ cells.

(D) Boxplot of fold-change of polyA-RNA abundance in log2 scale for *set1*Δ, *xrn1*Δ, and *set1*Δ*xrn1*Δ cells.

in *xrn1*Δ. The observation that Set1 could suppress overexpression of total mRNAs in *xrn1*Δ is consistent with two potential classes of mechanism. First, it is possible that Set1 could protect excess mRNAs from RNA nucleases other than Xrn1 in *xrn1*Δ cells. Without Set1, these excess mRNAs would then degraded by other RNA nucleases in double mutant. Alternatively, Set1 could be responsible for a global overproduction of mRNAs which are normally degraded by Xrn1. The two possibilities were tested in the following experiments.

Nuclear exosome complex does not degrade excess mRNAs in *set1*Δ*xrn1*Δ.

In addition to the 5' to 3' exonuclease Xrn1, budding yeast also encode additional RNA degradation pathways. One of the primary RNA nucleases in many organisms including budding yeast is the nuclear exosome, which degrades RNAs from 3' to 5' end. I decided to test if Set1 function somehow antagonizes exosome function by deleting the core enzyme – Rrp6 – in *set1*Δ*xrn1*Δ cells. The same approach which uses *S.pombe* internal control and RNA-seq was used to examine the effect of *RRP6* deletion on total mRNAs in triple mutant *set1*Δ*xrn1*Δrrp6Δ. The fold change of total mRNAs in 7 different mutants (single, double, and t riple mutants) is presented in a heatmap (Figure III.4A). Surprisingly, *set1*Δ*rrp6*Δ showed very limited changes in total mRNA abundance. Also, total mRNAs which increased globally in *xrn1*Δ were modestly suppressed in *xrn1*Δ*rrp6*Δ, instead of being further up-regulated. Most importantly, the triple

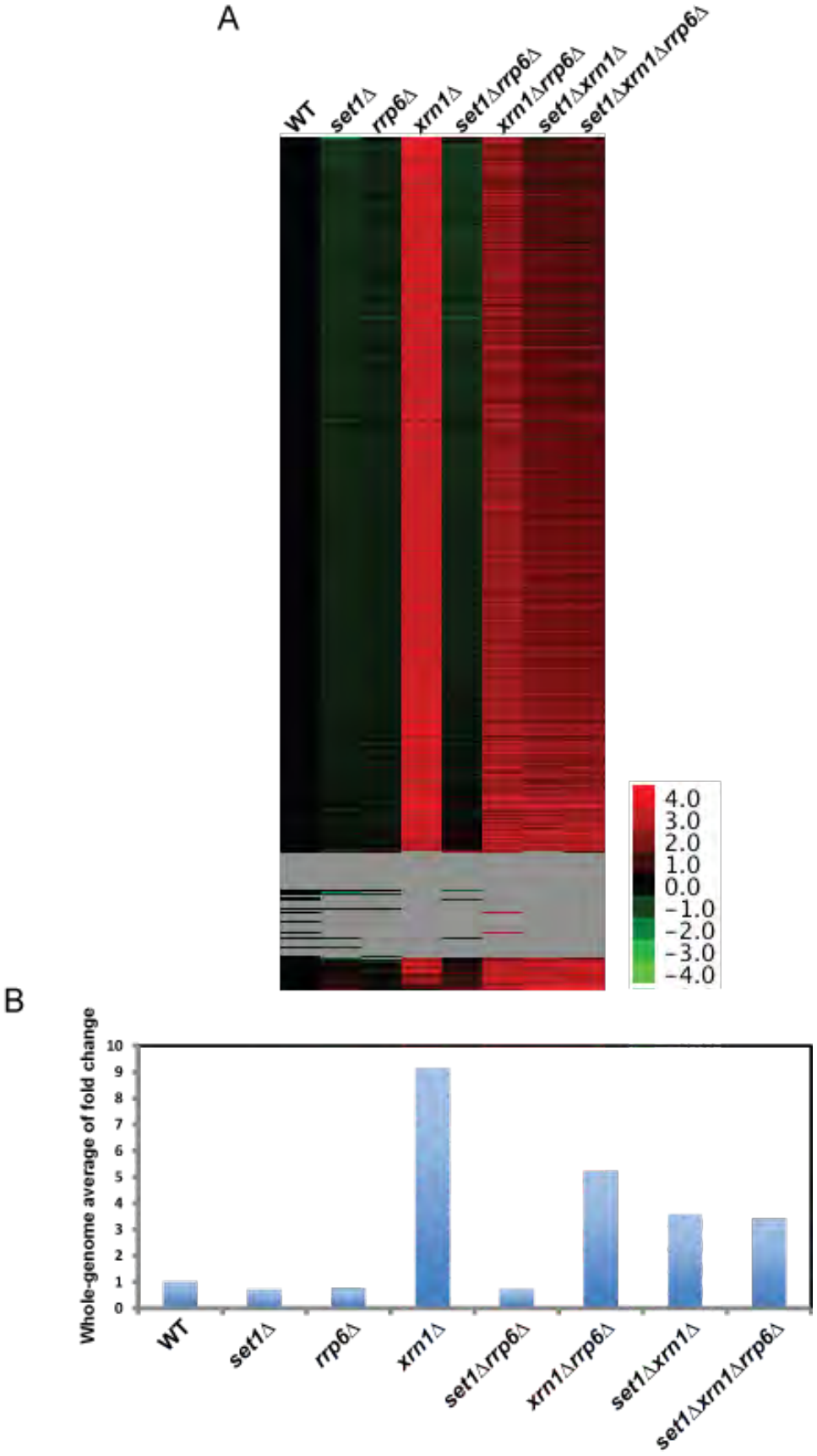
A
WT
set1Δ
rrp6Δ
xrn1Δ
set1Δrrp6Δ
xrn1Δrrp6Δ
set1Δxrn1Δ
set1Δxrn1Δrrp6Δ
4.0
3.0
2.0
1.0
0.0
−1.0
−2.0
−3.0
−4.0
B
Whole-genome average of fold change
0
1
2
3
4
5
6
7
8
9
10
WT
set1Δ
rrp6Δ
xrn1Δ
set1Δrrp6Δ
xrn1Δrrp6Δ
set1Δxrn1Δ
set1Δxrn1Δrrp6Δ

Figure III.4

The effect of the deletion of *RRP6* on *set1*Δ*xrn1*Δ suppression

(A) Genome-wide mRNA abundance of wild-type and mutant yeast strains was measured by RNA-seq. The abundance for each gene was normalized by an internal *S.pombe* RNA control. The fold changes of mRNA levels in log2 scale of mutant to wild-type shown as a heatmap.

(B) Bar graph representing the whole-genome average of fold changes of mRNA abundance for mutant yeast strains while comparing to WT.

mutant, *set1*Δ*xrn1*Δrrp6Δ, still showed suppression of excess mRNA production which was comparable to the suppression in *set1*Δ*xrn1*Δ. These results show that the nuclear exosome does not play a role in Set1-dependent degradation of excess RNAs. Overall, the results suggest if the total mRNA suppression in *set1*Δ*xrn1*Δ was carried out by a RNA nuclease, nuclear exosome is not the RNA nuclease.

Rat1, nuclear paralog of Xrn1, was not the RNA nuclease that cause the suppression in *set1*Δ*xrn1*Δ.

Since nuclear exosome was not the RNA nuclease responsible for the suppression, the next candidate is Rat1/Xrn2. Rat1 is homologous to Xrn1 and acts as a 5' to 3' exonuclease, but is typically localized to the nucleus rather than the cytoplasm, and its function can be complemented by directing Xrn1 into the nucleus (Johnson, 1997). Given that the lack of Xrn1 resulted in excess mRNAs, it makes Rat1 a potential candidate which can replace Xrn1 and degrade those mRNAs in *set1*Δ*xrn1*Δ mutant. A similar approach was taken to test if Rat1 is the nuclease with some alteration. Rat1 is an essential protein, which means making a triple deletion mutant is impossible. Fortunately a temperature-sensitive (ts) allele of Rat1, *rat1-1*, was available, so I made a triple *set1*Δ*xrn1*Δ*rat1-1* mutant along with set1Δ*rat1-1* and *xrn1*Δ*rat1-1* and collect RNA samples 2 hours after shifting to 37°C to remove functional Rat1. I also included *S.pombe* internal control and carried out RNA-seq to check RNA abundance in a genome-wide

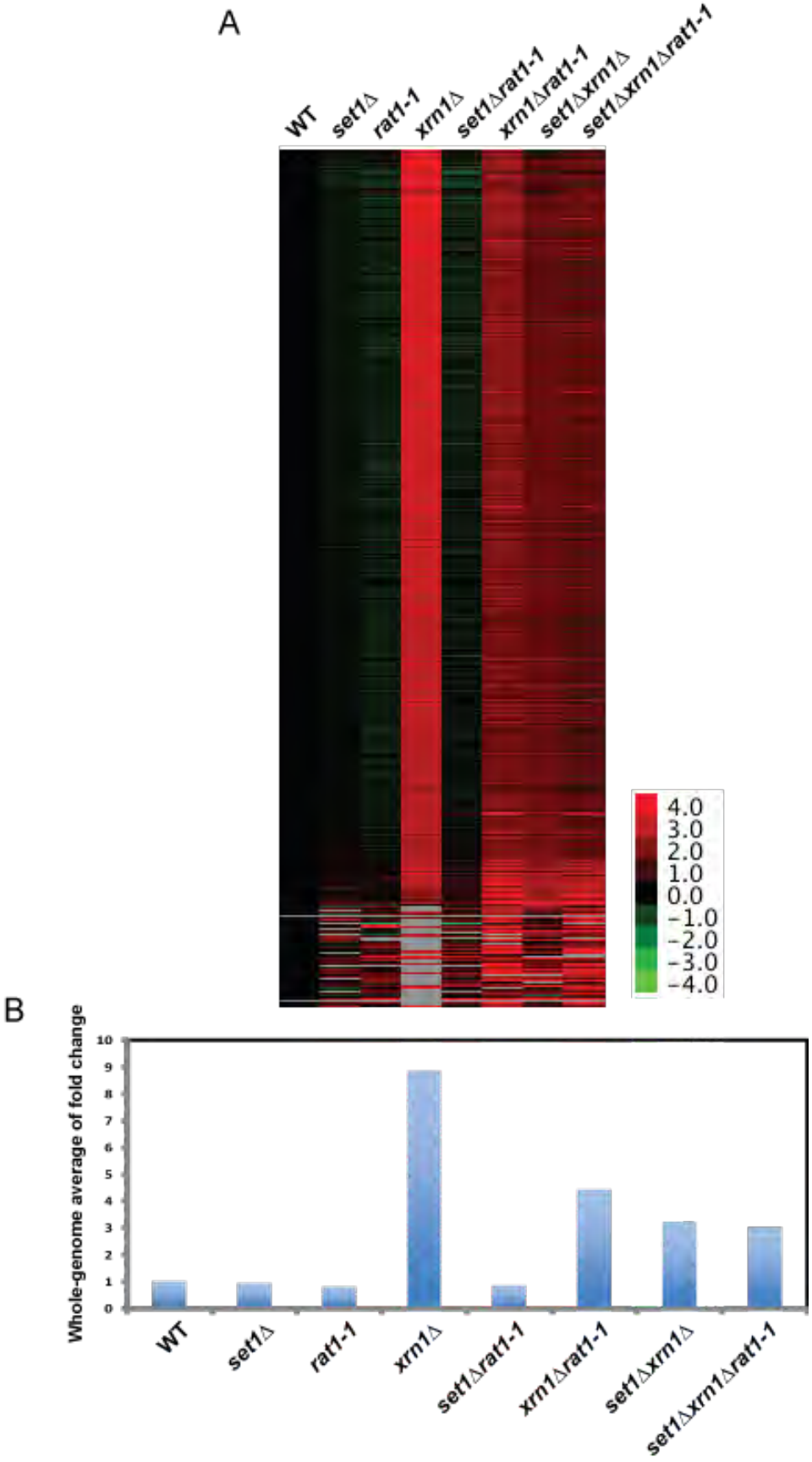
A
WT
set1Δ
rat1-1
xrn1Δ
set1Δrat1-1
xrn1Δrat1-1
set1Δxrn1Δ
set1Δxrn1Δrat1-1
4.0
3.0
2.0
1.0
0.0
-1.0
-2.0
-3.0
-4.0
B
Whole-genome average of fold change
0
1
2
3
4
5
6
7
8
9
10
WT
set1Δ
rat1-1
xrn1Δ
set1Δrat1-1
xrn1Δrat1-1
set1Δxrn1Δ
set1Δxrn1Δrat1-1

Figure III.5

The effect of the removal of Rat1 on *set1*Δ*xrn1*Δ suppression

(A) RNA samples of wild-type and mutant yeast cells was collected two hours after shifting the cultures to 37°C. Genome-wide mRNA abundance of wild-type and mutant yeast strains was measured by RNA-seq. The abundance for each gene was normalized by an internal *S.pombe* RNA control. The fold changes of mRNA levels in log2 scale of mutant to wild-type shown as a heatmap.

(B) Bar graph representing the genome-wide average of fold changes of mRNA abundance for mutant yeast strains while comparing to WT.

scale. The result was presented in a heatmap showing the fold changes in total mRNA abundance for every gene in all mutants and a genome-wide average of fold-changes was shown in a bar graph (Figure III.5). Given that rat1-1 is a ts mutant, although 2 hour incubation at 37°C would likely remove most functional Rat1, total RNAs was already suppressed before shifting to 37°C, so the suppression could only be relieved if the suppression was not resulted from decreased RNA synthesis in *set1*Δ*xrn1*Δ. With an average 9 fold increase in total mRNA abundance in *xrn1*Δ, total RNAs in *xrn1*Δrat1-1 and *set1*Δ*xrn1*Δrat1-1 were still both suppressed 5 or 6 fold comparing to *xrn1*Δ. The results showed the removal of Rat1 did not affect the suppression in *set1*Δ*xrn1*Δ so Rat1 is not the RNA nuclease. In fact, the experiments which tested if Rrp6 or Rat1 is the RNA nuclease argue against the hypothesis that the suppression in *set1*Δ*xrn1*Δ involves an RNA nuclease. The negative results support another hypothesis that Set1 regulates transcription in *xrn1*Δ and after deleting *SET1* transcription was affected in *set1*Δ*xrn1*Δ , which causes the suppression in total RNAs.

Capped mRNA abundance changes in *xrn1*Δ are not suppressed in *set1*Δ*xrn1*Δ double mutants

Our triple mutant analyses argue against the hypothesis that transcripts revealed by loss of Xrn1 are lost in set1 mutants because Set1 is required to protect these transcripts from degradation. Although not definitive, the data instead suggest

that Set1 plays a positive role in transcription of excess transcripts that are typically degraded by Xrn1. In order to investigate the role for Set1 in production of excess transcripts, we focus on an unusual phenotype of *xrn1*Δ yeast – the accumulation of excess uncapped mRNAs. Does Set1 specifically affect the abundance of capped or uncapped mRNAs? I modified a method that was developed by Ni T *et al*. (Ni et al., 2010) that utilizes Tobacco acid pyrophosphatase (TAP) in order to map only capped transcripts genome-wide. Most reads from these libraries mapped to the 5' end of genes, as indicated for *HSP150* and *CCW12* (Figure III.6A), confirming that this method works for mapping capped RNAs. Interestingly, both *xrn1*Δ and *set1*Δ*xrn1*Δ showed up-regulated capped RNAs (Figure III.6B). For *HSP150*, total RNAs increased 5 fold in *xrn1*Δ and decreased to 1.5 fold in *set1*Δ*xrn1*Δ, while capped RNAs only increased slightly in *xrn1*Δ and increased almost 2 fold in *set1*Δ*xrn1*Δ. *CCW12* behaved in a similar pattern as *HSP150* but to an even greater extent. Previous studies have shown that most mRNAs in cells were capped (He and Jacobson, 2001), which means for most genes, the abundance of total mRNAs is comparable to that of capped mRNAs. This equivalency is disrupted in the *xrn1*Δ mutant and partially (*CCW12)* or mostly (*HSP150*) restored in the *set1*Δ*xrn1*Δ double mutant. Comparing fold changes in total RNAs and capped RNAs indicates that the increased mRNAs in *xrn1*Δ were mostly uncapped, which is consistent with the literature. Surprisingly, the *set1*Δ*xrn1*Δ mutant showed an

A

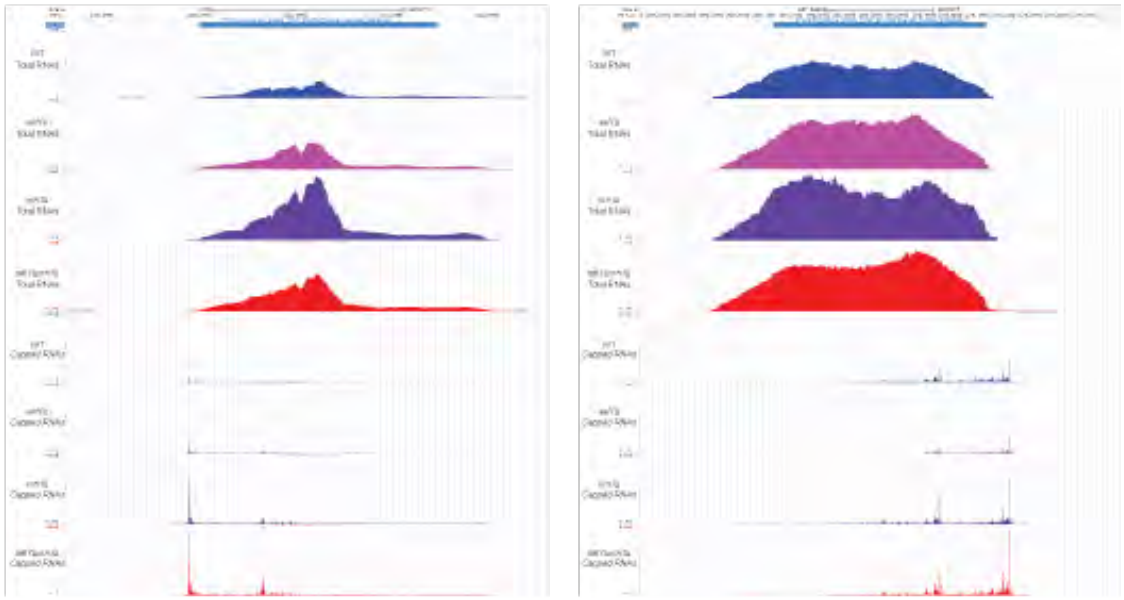

B

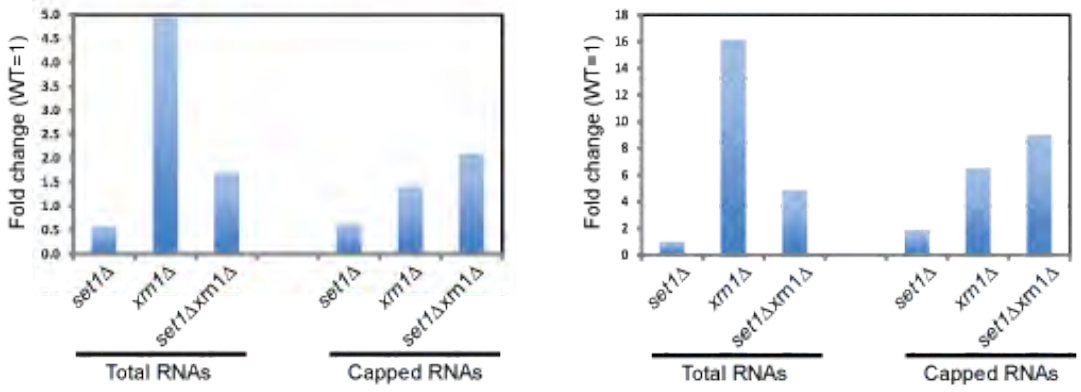
Fold change (WT=1)
5.0
4.5
4.0
3.5
3.0
2.5
2.0
1.5
1.0
0.5
0.0
set1Δ
xm1Δ
set1Δxm1Δ
set1Δ
xm1Δ
set1Δxm1Δ
Total RNAs
Capped RNAs
Fold change (WT=1)
18
16
14
12
10
8
6
4
2
0
set1Δ
xm1Δ
set1Δxm1Δ
set1Δ
xm1Δ
set1Δxm1Δ
Total RNAs
Capped RNAs

Figure III.6

Single-gene analysis of *set1*Δ*xrn1*Δ mutant effect on total and capped mRNAs.

(A) The screenshot shows genome browser tracks for total RNAs (top 4 tracks) and capped RNAs (bottom 4 tracks) for two genes, *HSP150* and *CCW12.* Four different yeast strains were shown in different color: wild-type in blue, *set1*Δ in magenta, *xrn1*Δ in purple, *set1*Δ*xrn1*Δ in red. The level of total RNAs and capped RNAs was measured by RNA-seq and normalized by an internal *S.pombe* RNA control. The abundance of capped RNAs was presented by the sum of all capped RNAs within 250 bps upstream of ATG.

(B) Bar graph representing the fold changes of mutant to WT in total RNAs and capped RNAs for *HSP150* (left) and *CCW12* (right).

increase in capped RNAs while the increase in total RNAs was greatly suppressed compared to *xrn1*Δ. In other words, the suppression of mRNA abundance seen in the double mutant is due to Set1 deletion preventing accumulation of massively upregulated uncapped RNAs in *xrn1*Δ mutants.

The observation is true for most genes, when I compared total and capped mRNA abundance between WT and mutants genome-wide. Capped RNAs were globally increased in *xrn1*Δ and *set1*Δ*xrn1*Δ (Figure III.7A, B, C). The increase in abundance of capped mRNAs for all genes in *xrn1*Δ and *set1*Δ*xrn1*Δ mutants are highly correlated (R square=0.96) (Figure III.7D). As in the single gene analysis, deletion of Xrn1 primarily affects uncapped RNA abundance, as most genes whose total expression is upregulated show only modest increases in the amount of capped RNA in this mutant (Figure III.7E). On the contrary, the fold changes in total RNAs and capped RNAs in *set1*Δ*xrn1*Δ are more comparable (Figure III.7F&G). While total RNAs increase 9 fold on average in the *xrn1*Δ mutant, the capped RNAs increase only about 3 fold. As most mRNA in wild type cells has been shown to be capped, this indicates a massive increase in uncapped RNAs to account for an additional 6 fold increase in the total RNA abundance. Most importantly, these excess uncapped RNAs were specifically suppressed after deleting *SET1* in *xrn1*Δ as *set1*Δ*xrn1*Δ showed similar distribution in fold changes in total and capped RNA abundance.

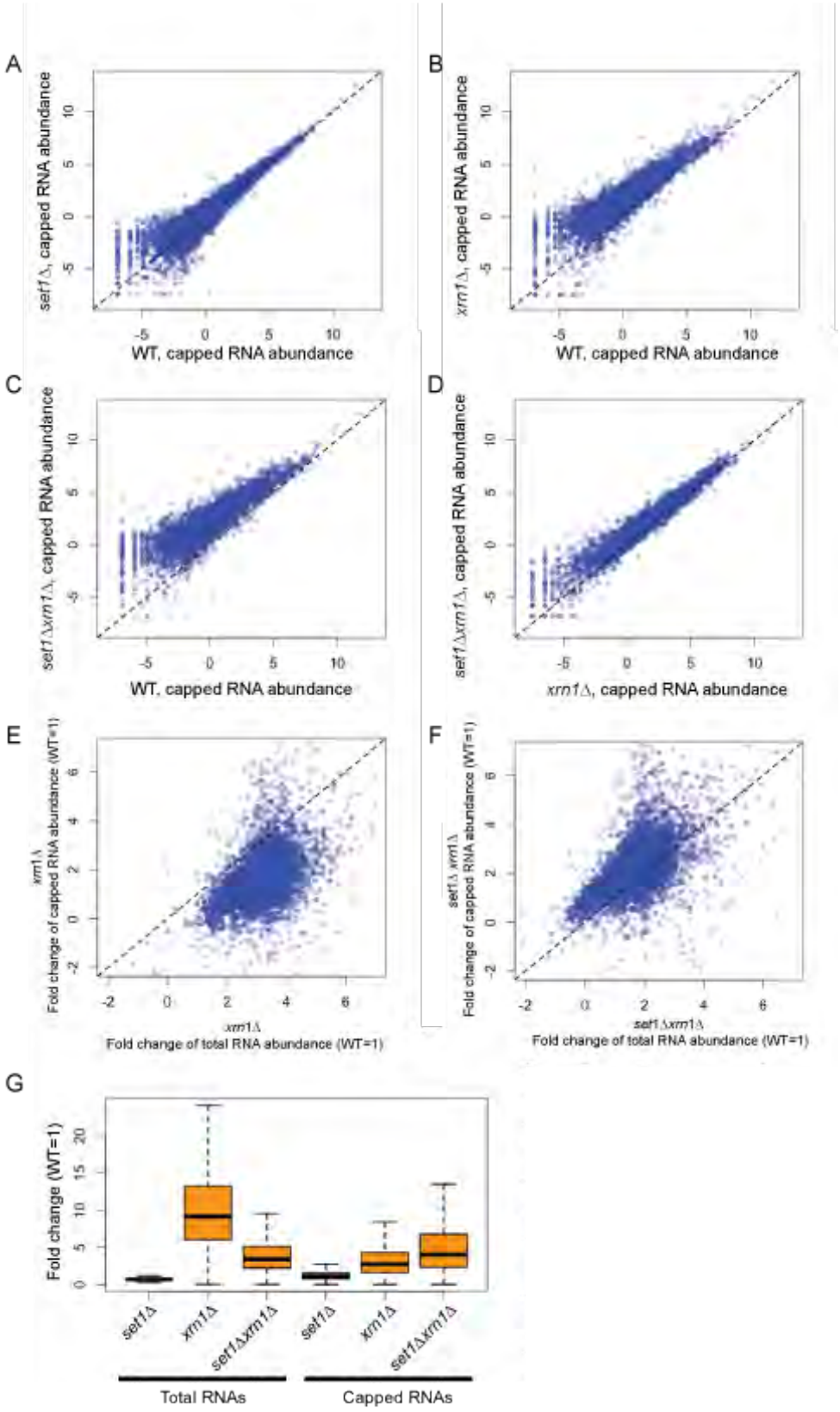
A
set1Δ, capped RNA abundance
WT, capped RNA abundance
B
xrn1Δ, capped RNA abundance
WT, capped RNA abundance
C
set1Δxrn1Δ, capped RNA abundance
WT, capped RNA abundance
D
set1Δxrn1Δ, capped RNA abundance
xrn1Δ, capped RNA abundance
E
xrn1Δ
Fold change of capped RNA abundance (WT=1)
xrn1Δ
Fold change of total RNA abundance (WT=1)
F
set1Δ xrn1Δ
Fold change of capped RNA abundance (WT=1)
set1Δxrn1Δ
Fold change of total RNA abundance (WT=1)
G
Fold change (WT=1)
set1Δ
xrn1Δ
set1Δxrn1Δ
set1Δ
xrn1Δ
set1Δxrn1Δ
Total RNAs
Capped RNAs

Figure III.7

Genome-wide analysis of *set1*Δ*xrn1*Δ mutant effect on total and capped mRNA abundance.

The level of total and capped RNAs were measured by RNA-seq and normalized by an internal *S.pombe* RNA control. The capped RNA abundance for each gene was presented by the sum of all capped RNAs within 250 bps upstream of ATG.

(A) Scatter plot of capped RNA abundance in log2 for whole genome in WT vs *set1*Δ cells.

(B) Scatter plot of capped RNA abundance in log2 for whole genome in WT vs *xrn1*Δ cells.

(C) Scatter plot of capped RNA abundance in log2 for whole genome in WT vs *set1*Δ*xrn1*Δ cells.

(D) Scatter plot of capped RNA abundance in log2 for whole genome in *xrn1*Δ vs *set1*Δ*xrn1*Δ cells.

(E) Scatter plot of fold change in log2 in total RNAs vs capped RNAs in *xrn1*Δ cells.

(F) Scatter plot of fold change in log2 in total RNAs vs capped RNAs in *set1*Δ*xrn1*Δ cells.

(G) Boxplot representing the fold changes in total RNAs (left three boxes) and capped RNAs (right three boxes) for three mutants, *set1*Δ, *xrn1*Δ, and *set1*Δ*xrn1*Δ.

DISCUSSION

I report here that deletion of *SET1* in *xrn1*Δ background suppressed both the morphological and m RNA up-regulation phenotypes of *xrn1*Δ, yet the *set1*Δ*xrn1*Δ double mutant showed additional growth defect than *xrn1*Δ. Suppression of the massive increase in total mRNA levels was due to a role for Set1 in protecting the increase in uncapped RNAs due to Xrn1 deletion. This does not appear to be due to Set1 preventing degradation by other known RNA nuclease. However, in order to conclusively establish whether Set1's role in uncapped mRNA accumulation is due to increased production of these RNAs or protection from degradation, it would be necessary to measure synthesis and decay rates of these uncapped mRNAs.

Set1 plays a role in maintaining the level of uncapped mRNAs in cells.

Previous studies report Set1 deletion has little effect on total mRNA abundance. Surprisingly, here I found Set1 deletion in *xrn1*Δ background decreased the amount of total mRNAs while the level of capped mRNAs was maintained, suggesting uncapped mRNAs were suppressed in the double mutant. This may be the reason why the *set1*Δ mutant effect is hidden in an otherwise wild type background. Only when uncapped RNAs would be accumulated, in *xrn1*Δ background, is the decrease in uncapped mRNAs after deleting *SET1* distinguishable. Recent studies have identified uncapped transcripts in

Arabidopsis and human cells (Gregory et al., 2008; Jiao et al., 2008; Karginov et al., 2010; Mercer et al., 2010). It is still not clear whether these uncapped transcripts were capable of being recapped and translated into proteins or if they are intermediates in the decay process. Nonetheless, It would be interesting to characterize the uncapped transcripts in yeast cells and test if Set1 were required for their existence.

Uncapped mRNAs might be functional.

It should be noted that while total mRNAs were suppressed in *set1*Δ*xrn1*Δ, presumably due to decrease in uncapped mRNAs, the double mutant actually showed additional growth defects and had significantly longer doubling time than *xrn1*Δ cells. The observation suggests the additional growth defect may result from decrease in uncapped mRNAs. If the uncapped mRNAs were intermediate product in the decay process, why would reduction in nonfunctional, intermediate product make cells sicker? Recent research has identified a new pathway – cytoplasmic recapping, in which some uncapped mRNAs were re-capped in the cytoplasm and translated into proteins (Schoenberg and Maquat, 2009). Although it is unclear whether uncapped mRNAs in *xrn1*Δ can be re-capped and translated, it is possible that the uncapped mRNAs in *xrn1*Δ contribute to cell growth. Hence, the loss of the uncapped mRNAs in *set1*Δ*xrn1*Δ result in defective cell growth.

MATERIALS AND METHODS

Yeast strains and growth conditions

*set1*Δ*xrn1*Δ double mutant was generated by mating haploid strain *set1*Δ with *xrn1*Δ. The sporulation was carried out for the diploid yeast cells for 4 days at room temperature. The spores were dissected and assayed for the genetic background.

S.cerevisiae strains were grown in YPD and *S.pombe* cells were grown in YES. When yeast cells grew to mid-log phase (OD600 between 0.4 and 0.6) at 30°C, yeast cultures were centrifuged for 1 minute and the media was removed. Yeast cells were quickly resuspend in 1ml RNAlater, frozen in liquid nitrogen and stored at -80 °C.

RNA-seq

Cell number of *S.cerevisiae* and *S.pombe* cells was calculated manually using hemocytometer. $1x10^8$ S.cerevisiae cells were mixed with $7x10^5$ *S.pombe* cells. Total RNAs from the mixed yeast cells were extracted from yeast cells using bead beating and TRIzol following manufacture's instructions. 100 ng DNase I-treated total RNAs were used for RNA-seq. RNA-seq was performed according to the dUTP 2nd strand protocol described in Levin et al., 2010 (Levin et al., 2010).

Capped RNA-seq

Capped RNA-seq was carried out following the method developed by Ni T et al., 2010 (Ni et al., 2010) with some modifications. rRNAs from 5ug DNase I-treated total RNAs from the mixed yeast cells were depleted using Ribo-Zero magnetic gold kit (MRZY1324). 100ng rRNA-depleted total RNAs were treated with CIP enzyme to remove 5' phosphates and treated with TAP (Epicentre) to remove the cap from mRNAs, which left 5' phosphate at the 5' end of mRNAs. A 5' linker was ligated to TAP-treated total RNAs and reversed transcribed with random hexamers carrying an adapt or sequence. The cDNAs with 5' linker and 3' adaptor were amplified using Illumina pair-end primers. The libraries were sequenced by NextSeq desktop sequencer.

CHAPTER IV

CONCLUSIONS AND PERSPECTIVES

Chromatin regulators play critical roles in regulating the kinetics of gene induction and repression. Out of the 202 mutants in the screen presented in Chapter I, most chromatin regulator mutants exhibit defects in gene induction and/or repression during stress. This observation generalizes the role of chromatin regulators in dynamic gene expression. Based on their responsiveness to stress, the mutants group into hyper- and hypo-responsive mutant clusters. The induction and repression of genes are delayed in hypo-responsive mutants. To the contrary, hyper-responsive mutants activate and repress genes too quickly or too much. Notably, genes whose induction was severely affected in hyper-responsive mutants tend to have highly nucleosome-occupied promoters, suggesting their response to stress may result from their mutant effect on nucleosome stability in the promoters.

The correlation matrix for the histone mutants and gene deletion mutants provides invaluable information for novel chromatin pathways. We compute correlation matrices depending on the similarity between mutant effects on dynamic gene expression in a stress response. Because the matrix successfully validates known substrate-enzyme and protein complex relationships, one can use it to predict new interactions between histone modifications and chromatin

regulators. For example, H3K18R is highly correlated with H3K4A and H3S10A, suggesting H3K18 acetylation, H3K4 methylation, and H3S10 phosphorylation may function in the same pathway. Genome-wide mapping of H3K18 acetylation in yeast and human cells reveals its enrichment at 5' end of active-transcribing genes (Wang et al., 2008; Weiner et al., 2015), which overlaps with H3K4 trimethylation. These three mutants share the failure to fully repress genes involved in ribosome biogenesis during stress. Interestingly, a recent study showed that H3K18 deacetylation down-regulated the small ribosomal protein gene, *RPS7,* in human cancer cells (Pandey and Kumar, 2015). This finding suggests the regulation of ribosomal protein genes (RPGs) by H3K18 acetylation and H3K4 trimethylation is conserved in yeast and human. The key question here is to determine if the three modifications crosstalk to one another to regulate RPGs.

Other interesting interactions found in the correlation matrix await further characterization. For instance, H3K27Q is highly correlated with H3S28A (R^2=0.66), while H3K9Q does not correlated with H3S10A. Notably, the functional difference between the two pairs has also been reported in literature. H3K9 modifications were selectively maintained by H3S10 phosphorylation in mitotic cells, as H3K27-S28 did not show the same pattern (Jeong et al., 2010). Both observations indicate there are more than one type of interactions between lysine-serine pairs on the histones.

Set1 may play a role in regulating synthesis or stability of uncapped mRNAs

Total mRNA abundance in *xrn1* null mutant was recently found to be globally up-regulated. Interestingly, genome-wide analysis of mRNA abundance revealed loss of Set1 in *xrn1* null mutant suppressed the increase in total mRNA abundance. Further analysis excluded the possibility that neither nuclear exosome nor Rat1 was involved in the same pathway. To my surprise, by assaying capped mRNA levels in *xrn1Δ* and double mutant, I found capped mRNAs abundance was correlated in both mutants. The observation indicates the gain in total mRNA abundance in *xrn1Δ* that was suppressed in double mutant was due to changes in the level of uncapped mRNAs. To conclude, the results suggest Set1 may function in maintaining the level of uncapped mRNAs by regulating the synthesis or stability of uncapped mRNAs.

Direct evidence is required to show Set1 affects the level of uncapped mRNAs. This would require selectively isolating and sequencing these uncapped RNAs. Alternatively, the level of uncapped RNAs can be determined after depleting capped mRNAs by an antibody specifically recognized cap. Another critical question is whether the regulation of uncapped RNAs by Set1 is H3K4 methylation-dependent. One would need to mutate H3K4 in *xrn1*Δ background in order to answer the question.

If uncapped RNAs were actively maintained in WT cells, this would imply that they have a function. Studies have shown some uncapped transcripts can be re-capped in the cytosol and translated into proteins (Schoenberg and Maquat, 2009). Therefore it would be enlightening to determine the protein levels in *xrn1*Δ and *set1*Δ*xrn1*Δ. Since both mutants have similar level of capped mRNAs, the difference in protein level would indicate if uncapped RNA were capable of being translated. Ribosome footprinting for isolated uncapped RNAs can also be used to test the same idea. Set1 may affect the synthesis or stability of uncapped RNAs. To distinguish between the two possibilities, metabolic labeling of uncapped transcripts can measure their synthesis and decay rates at the same time. The above experiments could all be used to establish a role for Set1 in regulating uncapped mRNAs.

Genome wide analysis of dynamic gene regulation is a powerful tool for discovering new interactions and roles for chromatin regulators. It opens up several avenues for further investigation, such as the link between Chd1 and H3K36 methylation. While pursuing the role of Set1 in RPG regulation, I observed that Set1 may be involved in maintaining the level of uncapped RNAs. Whether this is due to a role in synthesis or decay has not been conclusively establish, although I was able to rule out a role for the most likely candidates in a degradation pathway. It is also unclear whether Set1 maintains uncapped mRNA level via its methyltransferase activity. This work shows a general role for

chromatin regulators in dynamic gene regulation that could be achieved through many mechanisms.

BIBLIOGRAPHY

Ahmad, K., and Henikoff, S. (2002). The histone variant H3.3 marks active chromatin by replication-independent nucleosome assembly. Mol. Cell *9*, 1191–1200.

Albert, I., Mavrich, T.N., Tomsho, L.P., Qi, J., Zanton, S.J., Schuster, S.C., and Pugh, B.F. (2007). Translational and rotational settings of H2A.Z nucleosomes across the Saccharomyces cerevisiae genome. Nature *446*, 572–576.

Alejandro-Osorio, A.L., Huebert, D.J., Porcaro, D.T., Sonntag, M.E., Nillasithanukroh, S., Will, J.L., and Gasch, A.P. (2009). The histone deacetylase Rpd3p is required for transient changes in genomic expression in response to stress. Genome Biol. *10*, R57.

Allfrey, V.G. (1966). Structural modifications of histones and their possible role in the regulation of ribonucleic acid synthesis. Proc. Can. Cancer Conf. *6*, 313–335.

Allfrey, V.G., Faulkner, R., and Mirsky, A.E. (1964). Acetylation and methylation of histones and their possible role in the regulation of RNA synthesis. Proc. Natl. Acad. Sci. U. S. A. *51*, 786–794.

Barbaric, S. (2001). Increasing the rate of chromatin remodeling and gene activation--a novel role for the histone acetyltransferase Gcn5. EMBO J. *20*, 4944–4951.

Barth, T.K., and Imhof, A. (2010). Fast signals and slow marks: the dynamics of histone modifications. Trends Biochem. Sci. *35*, 618–626.

Berger, S.L. (2007). The complex language of chromatin regulation during transcription. Nature *447*, 407–412.

Bernstein, B.E., and Schreiber, S.L. (2002). Global approaches to chromatin. Chem. Biol. *9*, 1167–1173.

Berretta, J., Pinskaya, M., and Morillon, A. (2008). A cryptic unstable transcript mediates transcriptional trans-silencing of the Ty1 retrotransposon in S. cerevisiae. Genes Dev. *22*, 615–626.

Boa, S., Coert, C., and Patterton, H.-G. (2003). Saccharomyces cerevisiae Set1p is a methyltransferase specific for lysine 4 of histone H3 and is required for efficient gene expression. Yeast Chichester Engl. *20*, 827–835.

Borde, V., Robine, N., Lin, W., Bonfils, S., Géli, V., and Nicolas, A. (2009). Histone H3 lysine 4 trimethylation marks meiotic recombination initiation sites. EMBO J. *28*, 99–111.

Briggs, S.D., Bryk, M., Strahl, B.D., Cheung, W.L., Davie, J.K., Dent, S.Y., Winston, F., and Allis, C.D. (2001). Histone H3 lysine 4 methylation is mediated by Set1 and required for cell growth and rDNA silencing in Saccharomyces cerevisiae. Genes Dev. *15*, 3286–3295.

Bryant, G.O., Prabhu, V., Floer, M., Wang, X., Spagna, D., Schreiber, D., and Ptashne, M. (2008). Activator Control of Nucleosome Occupancy in Activation and Repression of Transcription. PLoS Biol *6*, e317.

Bryk, M., Briggs, S.D., Strahl, B.D., Curcio, M.J., Allis, C.D., and Winston, F. (2002). Evidence that Set1, a Factor Required for Methylation of Histone H3, Regulates rDNA Silencing in S. cerevisiae by a Sir2-Independent Mechanism. Curr. Biol. *12*, 165–170.

Bumgarner, S.L., Dowell, R.D., Grisafi, P., Gifford, D.K., and Fink, G.R. (2009). Toggle involving cis-interfering noncoding RNAs controls variegated gene expression in yeast. Proc. Natl. Acad. Sci. U. S. A. *106*, 18321–18326.

Camblong, J., Iglesias, N., Fickentscher, C., Dieppois, G., and Stutz, F. (2007). Antisense RNA stabilization induces transcriptional gene silencing via histone deacetylation in S. cerevisiae. Cell *131*, 706–717.

Camblong, J., Beyrouthy, N., Guffanti, E., Schlaepfer, G., Steinmetz, L.M., and Stutz, F. (2009). Trans-acting antisense RNAs mediate transcriptional gene cosuppression in S. cerevisiae. Genes Dev. *23*, 1534–1545.

Carr, A.M., Dorrington, S.M., Hindley, J., Phear, G.A., Aves, S.J., and Nurse, P. (1994). Analysis of a histone H2A variant from fission yeast: evidence for a role in chromosome stability. Mol. Gen. Genet. MGG *245*, 628–635.

Carrozza, M.J., Li, B., Florens, L., Suganuma, T., Swanson, S.K., Lee, K.K., Shia, W.-J., Anderson, S., Yates, J., Washburn, M.P., et al. (2005). Histone H3 methylation by Set2 directs deacetylation of coding regions by Rpd3s to suppress spurious intragenic transcription. Cell *123*, 581–592.

Carvin, C.D., and Kladde, M.P. (2004). Effectors of lysine 4 methylation of histone H3 in Saccharomyces cerevisiae are negative regulators of PHO5 and GAL1-10. J. Biol. Chem. *279*, 33057–33062.

Celona, B., Weiner, A., Di Felice, F., Mancuso, F.M., Cesarini, E., Rossi, R.L., Gregory, L., Baban, D., Rossetti, G., Grianti, P., et al. (2011). Substantial histone

reduction modulates genomewide nucleosomal occupancy and global transcriptional output. PLoS Biol. *9*, e1001086.

Cheng, H., He, X., and Moore, C. (2004). The essential WD repeat protein Swd2 has dual functions in RNA polymerase II transcription termination and lysine 4 methylation of histone H3. Mol. Cell. Biol. *24*, 2932–2943.

Chestier, A., and Yaniv, M. (1979). Rapid turnover of acetyl groups in the four core histones of simian virus 40 minichromosomes. Proc. Natl. Acad. Sci. U. S. A. *76*, 46–50.

Churchman, L.S., and Weissman, J.S. (2011). Nascent transcript sequencing visualizes transcription at nucleotide resolution. Nature *469*, 368–373.

Clapier, C.R., and Cairns, B.R. (2009). The biology of chromatin remodeling complexes. Annu. Rev. Biochem. *78*, 273–304.

Collins, S.R., Miller, K.M., Maas, N.L., Roguev, A., Fillingham, J., Chu, C.S., Schuldiner, M., Gebbia, M., Recht, J., Shales, M., et al. (2007). Functional dissection of protein complexes involved in yeast chromosome biology using a genetic interaction map. Nature *446*, 806–810.

Crosio, C., Cermakian, N., Allis, C.D., and Sassone-Corsi, P. (2000). Light induces chromatin modification in cells of the mammalian circadian clock. Nat. Neurosci. *3*, 1241–1247.

Crosio, C., Fimia, G.M., Loury, R., Kimura, M., Okano, Y., Zhou, H., Sen, S., Allis, C.D., and Sassone-Corsi, P. (2002). Mitotic phosphorylation of histone H3: spatio-temporal regulation by mammalian Aurora kinases. Mol. Cell. Biol. *22*, 874–885.

van Daal, A., and Elgin, S.C. (1992). A histone variant, H2AvD, is essential in Drosophila melanogaster. Mol. Biol. Cell *3*, 593–602.

Dai, J., Hyland, E.M., Yuan, D.S., Huang, H., Bader, J.S., and Boeke, J.D. (2008). Probing nucleosome function: a highly versatile library of synthetic Histone H3 and H4 mutants. Cell *134*, 1066–1078.

Dehé, P.-M., Dichtl, B., Schaft, D., Roguev, A., Pamblanco, M., Lebrun, R., Rodríguez-Gil, A., Mkandawire, M., Landsberg, K., Shevchenko, A., et al. (2006). Protein Interactions within the Set1 Complex and Their Roles in the Regulation of Histone 3 Lysine 4 Methylation. J. Biol. Chem. *281*, 35404–35412.

Dichtl, B., Aasland, R., and Keller, W. (2004). Functions for S. cerevisiae Swd2p in 3' end formation of specific mRNAs and snoRNAs and global histone 3 lysine 4 methylation. RNA N. Y. N *10*, 965–977.

van Dijk, E.L., Chen, C.L., d'Aubenton-Carafa, Y., Gourvennec, S., Kwapisz, M., Roche, V., Bertrand, C., Silvain, M., Legoix-Né, P., Loeillet, S., et al. (2011). XUTs are a class of Xrn1-sensitive antisense regulatory non-coding RNA in yeast. Nature *475*, 114–117.

Dion, M.F., Altschuler, S.J., Wu, L.F., and Rando, O.J. (2005). Genomic characterization reveals a simple histone H4 acetylation code. Proc. Natl. Acad. Sci. U. S. A. *102*, 5501–5506.

Dion, M.F., Kaplan, T., Kim, M., Buratowski, S., Friedman, N., and Rando, O.J. (2007). Dynamics of replication-independent histone turnover in budding yeast. Science *315*, 1405–1408.

Dixon, S.J., Costanzo, M., Baryshnikova, A., Andrews, B., and Boone, C. (2009). Systematic mapping of genetic interaction networks. Annu. Rev. Genet. *43*, 601–625.

Dowell, N.L., Sperling, A.S., Mason, M.J., and Johnson, R.C. (2010). Chromatin-dependent binding of the S. cerevisiae HMGB protein Nhp6A affects nucleosome dynamics and transcription. Genes Dev. *24*, 2031–2042.

Eisen, M.B., Spellman, P.T., Brown, P.O., and Botstein, D. (1998). Cluster analysis and display of genome-wide expression patterns. Proc. Natl. Acad. Sci. U. S. A. *95*, 14863–14868.

Faast, R., Thonglairoam, V., Schulz, T.C., Beall, J., Wells, J.R., Taylor, H., Matthaei, K., Rathjen, P.D., Tremethick, D.J., and Lyons, I. (2001). Histone variant H2A.Z is required for early mammalian development. Curr. Biol. CB *11*, 1183–1187.

Field, Y., Kaplan, N., Fondufe-Mittendorf, Y., Moore, I.K., Sharon, E., Lubling, Y., Widom, J., and Segal, E. (2008). Distinct modes of regulation by chromatin encoded through nucleosome positioning signals. PLoS Comput. Biol. *4*, e1000216.

Fillingham, J., Recht, J., Silva, A.C., Suter, B., Emili, A., Stagljar, I., Krogan, N.J., Allis, C.D., Keogh, M.-C., and Greenblatt, J.F. (2008). Chaperone control of the activity and specificity of the histone H3 acetyltransferase Rtt109. Mol. Cell. Biol. *28*, 4342–4353.

Fillingham, J., Kainth, P., Lambert, J.-P., van Bakel, H., Tsui, K., Peña-Castillo, L., Nislow, C., Figeys, D., Hughes, T.R., Greenblatt, J., et al. (2009). Two-color cell array screen reveals interdependent roles for histone chaperones and a chromatin boundary regulator in histone gene repression. Mol. Cell *35*, 340–351.

Fingerman, I.M., Wu, C.-L., Wilson, B.D., and Briggs, S.D. (2005). Global Loss of Set1-mediated H3 Lys4 Trimethylation Is Associated with Silencing Defects in Saccharomyces cerevisiae. J. Biol. Chem. *280*, 28761–28765.

Fischle, W., Tseng, B.S., Dormann, H.L., Ueberheide, B.M., Garcia, B.A., Shabanowitz, J., Hunt, D.F., Funabiki, H., and Allis, C.D. (2005). Regulation of HP1–chromatin binding by histone H3 methylation and phosphorylation. Nature *438*, 1116–1122.

Gasch, A.P., Spellman, P.T., Kao, C.M., Carmel-Harel, O., Eisen, M.B., Storz, G., Botstein, D., and Brown, P.O. (2000). Genomic Expression Programs in the Response of Yeast Cells to Environmental Changes. Mol. Biol. Cell *11*, 4241–4257.

Gavin, A.-C., Aloy, P., Grandi, P., Krause, R., Boesche, M., Marzioch, M., Rau, C., Jensen, L.J., Bastuck, S., Dümpelfeld, B., et al. (2006). Proteome survey reveals modularity of the yeast cell machinery. Nature *440*, 631–636.

Geiss, G.K., Bumgarner, R.E., Birditt, B., Dahl, T., Dowidar, N., Dunaway, D.L., Fell, H.P., Ferree, S., George, R.D., Grogan, T., et al. (2008). Direct multiplexed measurement of gene expression with color-coded probe pairs. Nat Biotech *26*, 317–325.

Ghaemmaghami, S., Huh, W.-K., Bower, K., Howson, R.W., Belle, A., Dephoure, N., O'Shea, E.K., and Weissman, J.S. (2003). Global analysis of protein expression in yeast. Nature *425*, 737–741.

Gregory, B.D., O'Malley, R.C., Lister, R., Urich, M.A., Tonti-Filippini, J., Chen, H., Millar, A.H., and Ecker, J.R. (2008). A link between RNA metabolism and silencing affecting Arabidopsis development. Dev. Cell *14*, 854–866.

Guillemette, B., Drogaris, P., Lin, H.-H.S., Armstrong, H., Hiragami-Hamada, K., Imhof, A., Bonneil, É., Thibault, P., Verreault, A., and Festenstein, R.J. (2011). H3 lysine 4 is acetylated at active gene promoters and is regulated by H3 lysine 4 methylation. PLoS Genet *7*, e1001354.

Halbach, A., Zhang, H., Wengi, A., Jablonska, Z., Gruber, I.M.L., Halbeisen, R.E., Dehé, P.-M., Kemmeren, P., Holstege, F., Géli, V., et al. (2009). Cotranslational assembly of the yeast SET1C histone methyltransferase complex. EMBO J. *28*, 2959–2970.

Han, M., and Grunstein, M. (1988). Nucleosome loss activates yeast downstream promoters in vivo. Cell *55*, 1137–1145.

Hardwick, J.S., Kuruvilla, F.G., Tong, J.K., Shamji, A.F., and Schreiber, S.L. (1999). Rapamycin-modulated transcription defines the subset of nutrient-sensitive signaling pathways directly controlled by the Tor proteins. Proc. Natl. Acad. Sci. U. S. A. *96*, 14866–14870.

Hartzog, G.A., and Tamkun, J.W. (2007). A new role for histone tail modifications in transcription elongation. Genes Dev. *21*, 3209–3213.

Hassan, A.H., Prochasson, P., Neely, K.E., Galasinski, S.C., Chandy, M., Carrozza, M.J., and Workman, J.L. (2002). Function and Selectivity of Bromodomains in Anchoring Chromatin-Modifying Complexes to Promoter Nucleosomes. Cell *111*, 369–379.

He, F., and Jacobson, A. (2001). Upf1p, Nmd2p, and Upf3p Regulate the Decapping and Exonucleolytic Degradation of both Nonsense-Containing mRNAs and Wild-Type mRNAs. Mol. Cell. Biol. *21*, 1515–1530.

Houseley, J., Rubbi, L., Grunstein, M., Tollervey, D., and Vogelauer, M. (2008). A ncRNA Modulates Histone Modification and mRNA Induction in the Yeast GAL Gene Cluster. Mol. Cell *32*, 685–695.

Huber, A., French, S.L., Tekotte, H., Yerlikaya, S., Stahl, M., Perepelkina, M.P., Tyers, M., Rougemont, J., Beyer, A.L., and Loewith, R. (2011). Sch9 regulates ribosome biogenesis via Stb3, Dot6 and Tod6 and the histone deacetylase complex RPD3L. EMBO J. *30*, 3052–3064.

Huh, W.-K., Falvo, J.V., Gerke, L.C., Carroll, A.S., Howson, R.W., Weissman, J.S., and O'Shea, E.K. (2003). Global analysis of protein localization in budding yeast. Nature *425*, 686–691.

Huisinga, K.L., and Pugh, B.F. (2004). A genome-wide housekeeping role for TFIID and a highly regulated stress-related role for SAGA in Saccharomyces cerevisiae. Mol. Cell *13*, 573–585.

Humphrey, E.L., Shamji, A.F., Bernstein, B.E., and Schreiber, S.L. (2004). Rpd3p relocation mediates a transcriptional response to rapamycin in yeast. Chem. Biol. *11*, 295–299.

Hwang, W.W., Venkatasubrahmanyam, S., Ianculescu, A.G., Tong, A., Boone, C., and Madhani, H.D. (2003). A conserved RING finger protein required for histone H2B monoubiquitination and cell size control. Mol. Cell *11*, 261–266.

Hyland, E.M., Molina, H., Poorey, K., Jie, C., Xie, Z., Dai, J., Qian, J., Bekiranov, S., Auble, D.T., Pandey, A., et al. (2011). An evolutionarily “young” lysine residue in histone H3 attenuates transcriptional output in Saccharomyces cerevisiae. Genes Dev. *25*, 1306–1319.

Ihmels, J., Bergmann, S., and Barkai, N. (2004). Defining transcription modules using large-scale gene expression data. Bioinforma. Oxf. Engl. *20*, 1993–2003.

Imbeault, D., Gamar, L., Rufiange, A., Paquet, E., and Nourani, A. (2008). The Rtt106 histone chaperone is functionally linked to transcription elongation and is involved in the regulation of spurious transcription from cryptic promoters in yeast. J. Biol. Chem. *283*, 27350–27354.

Jackson, J.D., and Gorovsky, M.A. (2000). Histone H2A.Z has a conserved function that is distinct from that of the major H2A sequence variants. Nucleic Acids Res. *28*, 3811–3816.

Jackson, V., Shires, A., Chalkley, R., and Granner, D.K. (1975). Studies on highly metabolically active acetylation and phosphorylation of histones. J. Biol. Chem. *250*, 4856–4863.

Jeong, Y.S., Cho, S., Park, J.S., Ko, Y., and Kang, Y.-K. (2010). Phosphorylation of serine-10 of histone H3 shields modified lysine-9 selectively during mitosis. Genes Cells *15*, 181–192.

Jiao, Y., Riechmann, J.L., and Meyerowitz, E.M. (2008). Transcriptome-wide analysis of uncapped mRNAs in Arabidopsis reveals regulation of mRNA degradation. Plant Cell *20*, 2571–2585.

Johnson, A.W. (1997). Rat1p and Xrn1p are functionally interchangeable exoribonucleases that are restricted to and required in the nucleus and cytoplasm, respectively. Mol. Cell. Biol. *17*, 6122–6130.

Jorgensen, P., Nishikawa, J.L., Breitkreutz, B.-J., and Tyers, M. (2002). Systematic identification of pathways that couple cell growth and division in yeast. Science *297*, 395–400.

Joshi, A.A., and Struhl, K. (2005). Eaf3 chromodomain interaction with methylated H3-K36 links histone deacetylation to Pol II elongation. Mol. Cell *20*, 971–978.

Kaplan, T., Liu, C.L., Erkmann, J.A., Holik, J., Grunstein, M., Kaufman, P.D., Friedman, N., and Rando, O.J. (2008). Cell cycle- and chaperone-mediated regulation of H3K56ac incorporation in yeast. PLoS Genet. *4*, e1000270.

Karginov, F.V., Cheloufi, S., Chong, M.M.W., Stark, A., Smith, A.D., and Hannon, G.J. (2010). Diverse endonucleolytic cleavage sites in the mammalian transcriptome depend upon microRNAs, Drosha, and additional nucleases. Mol. Cell *38*, 781–788.

Katan-Khaykovich, Y., and Struhl, K. (2005). Heterochromatin formation involves changes in histone modifications over multiple cell generations. EMBO J. *24*, 2138–2149.

Kehayova, P.D., and Liu, D.R. (2007). In Vivo Evolution of an RNA-Based Transcriptional Silencing Domain in S. cerevisiae. Chem. Biol. *14*, 65–74.

Keogh, M.-C., Kurdistani, S.K., Morris, S.A., Ahn, S.H., Podolny, V., Collins, S.R., Schuldiner, M., Chin, K., Punna, T., Thompson, N.J., et al. (2005). Cotranscriptional set2 methylation of histone H3 lysine 36 recruits a repressive Rpd3 complex. Cell *123*, 593–605.

Kim, T., and Buratowski, S. (2009). Dimethylation of H3K4 by Set1 recruits the Set3 histone deacetylase complex to 5' transcribed regions. Cell *137*, 259–272.

Kim, T.S., Liu, C.L., Yassour, M., Holik, J., Friedman, N., Buratowski, S., and Rando, O.J. (2010). RNA polymerase mapping during stress responses reveals widespread nonproductive transcription in yeast. Genome Biol. *11*, R75.

Kizer, K.O., Phatnani, H.P., Shibata, Y., Hall, H., Greenleaf, A.L., and Strahl, B.D. (2005). A novel domain in Set2 mediates RNA polymerase II interaction and couples Histone H3 k36 methylation with transcript elongation. Mol Cell Biol *25*, 3305–3316.

Kobor, M.S., Venkatasubrahmanyam, S., Meneghini, M.D., Gin, J.W., Jennings, J.L., Link, A.J., Madhani, H.D., and Rine, J. (2004). A Protein Complex Containing the Conserved Swi2/Snf2-Related ATPase Swr1p Deposits Histone Variant H2A.Z into Euchromatin. PLoS Biol *2*, e131.

Korber, P., Barbaric, S., Luckenbach, T., Schmid, A., Schermer, U.J., Blaschke, D., and Hörz, W. (2006). The histone chaperone asf1 increases the rate of histone eviction at the yeast pho5 and pho8 promoters. J. Biol. Chem. *281*, 5539–5545.

Kornberg, R.D., and Lorch, Y. (1999). Twenty-five years of the nucleosome, fundamental particle of the eukaryote chromosome. Cell *98*, 285–294.

Kouzarides, T. (2007). Chromatin modifications and their function. Cell *128*, 693–705.

Krogan, N.J., Dover, J., Khorrami, S., Greenblatt, J.F., Schneider, J., Johnston, M., and Shilatifard, A. (2002). COMPASS, a Histone H3 (Lysine 4) Methyltransferase Required for Telomeric Silencing of Gene Expression. J. Biol. Chem. *277*, 10753–10755.

Krogan, N.J., Keogh, M.-C., Datta, N., Sawa, C., Ryan, O.W., Ding, H., Haw, R.A., Pootoolal, J., Tong, A., Canadien, V., et al. (2003). A Snf2 family ATPase complex required for recruitment of the histone H2A variant Htz1. Mol. Cell *12*, 1565–1576.

Krogan, N.J., Baetz, K., Keogh, M.-C., Datta, N., Sawa, C., Kwok, T.C.Y., Thompson, N.J., Davey, M.G., Pootoolal, J., Hughes, T.R., et al. (2004). Regulation of chromosome stability by the histone H2A variant Htz1, the Swr1 chromatin remodeling complex, and the histone acetyltransferase NuA4. Proc. Natl. Acad. Sci. U. S. A. *101*, 13513–13518.

Krogan, N.J., Cagney, G., Yu, H., Zhong, G., Guo, X., Ignatchenko, A., Li, J., Pu, S., Datta, N., Tikuisis, A.P., et al. (2006). Global landscape of protein complexes in the yeast Saccharomyces cerevisiae. Nature *440*, 637–643.

Lee, D.Y., Hayes, J.J., Pruss, D., and Wolffe, A.P. (1993). A positive role for histone acetylation in transcription factor access to nucleosomal DNA. Cell *72*, 73–84.

Lee, J.-S., Smith, E., and Shilatifard, A. (2010). The language of histone crosstalk. Cell *142*, 682–685.

van Leeuwen, F., Gafken, P.R., and Gottschling, D.E. (2002). Dot1p modulates silencing in yeast by methylation of the nucleosome core. Cell *109*, 745–756.

Lenstra, T.L., Benschop, J.J., Kim, T., Schulze, J.M., Brabers, N.A.C.H., Margaritis, T., van de Pasch, L.A.L., van Heesch, S.A.A.C., Brok, M.O., Groot Koerkamp, M.J.A., et al. (2011). The specificity and topology of chromatin interaction pathways in yeast. Mol. Cell *42*, 536–549.

Levin, J.Z., Yassour, M., Adiconis, X., Nusbaum, C., Thompson, D.A., Friedman, N., Gnirke, A., and Regev, A. (2010). Comprehensive comparative analysis of strand-specific RNA sequencing methods. Nat. Methods *7*, 709–715.

Li, B., Carey, M., and Workman, J.L. (2007). The role of chromatin during transcription. Cell *128*, 707–719.

Liu, C.L., Schreiber, S.L., and Bernstein, B.E. (2003). Development and validation of a T7 based linear amplification for genomic DNA. BMC Genomics *4*, 19.

Liu, C.L., Kaplan, T., Kim, M., Buratowski, S., Schreiber, S.L., Friedman, N., and Rando, O.J. (2005). Single-nucleosome mapping of histone modifications in S. cerevisiae. PLoS Biol *3*, e328.

Liu, X., Bowen, J., and Gorovsky, M.A. (1996). Either of the major H2A genes but not an evolutionarily conserved H2A.F/Z variant of Tetrahymena thermophila can function as the sole H2A gene in the yeast Saccharomyces cerevisiae. Mol. Cell. Biol. *16*, 2878–2887.

Lombardi, L.M., Ellahi, A., and Rine, J. (2011). Direct regulation of nucleosome density by the conserved AAA-ATPase Yta7. Proc. Natl. Acad. Sci. U. S. A. *108*, E1302–E1311.

Lopes da Rosa, J., Holik, J., Green, E.M., Rando, O.J., and Kaufman, P.D. (2011). Overlapping regulation of CenH3 localization and histone H3 turnover by CAF-1 and HIR proteins in Saccharomyces cerevisiae. Genetics *187*, 9–19.

Lorch, Y., LaPointe, J.W., and Kornberg, R.D. (1987). Nucleosomes inhibit the initiation of transcription but allow chain elongation with the displacement of histones. Cell *49*, 203–210.

Luger, K., Mäder, A.W., Richmond, R.K., Sargent, D.F., and Richmond, T.J. (1997). Crystal structure of the nucleosome core particle at 2.8 A resolution. Nature *389*, 251–260.

Luk, E., Ranjan, A., Fitzgerald, P.C., Mizuguchi, G., Huang, Y., Wei, D., and Wu, C. (2010). Stepwise histone replacement by SWR1 requires dual activation with histone H2A.Z and canonical nucleosome. Cell *143*, 725–736.

Malik, H.S., and Henikoff, S. (2003). Phylogenomics of the nucleosome. Nat. Struct. Biol. *10*, 882–891.

Margueron, R., and Reinberg, D. (2010). Chromatin structure and the inheritance of epigenetic information. Nat. Rev. Genet. *11*, 285–296.

Meneghini, M.D., Wu, M., and Madhani, H.D. (2003). Conserved histone variant H2A.Z protects euchromatin from the ectopic spread of silent heterochromatin. Cell *112*, 725–736.

Mercer, T.R., Dinger, M.E., Bracken, C.P., Kolle, G., Szubert, J.M., Korbie, D.J., Askarian-Amiri, M.E., Gardiner, B.B., Goodall, G.J., Grimmond, S.M., et al. (2010). Regulated post-transcriptional RNA cleavage diversifies the eukaryotic transcriptome. Genome Res. *20*, 1639–1650.

Miller, T., Krogan, N.J., Dover, J., Erdjument-Bromage, H., Tempst, P., Johnston, M., Greenblatt, J.F., and Shilatifard, A. (2001). COMPASS: A complex of proteins associated with a trithorax-related SET domain protein. Proc. Natl. Acad. Sci. *98*, 12902–12907.

Mizuguchi, G., Shen, X., Landry, J., Wu, W.-H., Sen, S., and Wu, C. (2004). ATP-driven exchange of histone H2AZ variant catalyzed by SWR1 chromatin remodeling complex. Science *303*, 343–348.

Nagai, K., Oubridge, C., Ito, N., Avis, J., and Evans, P. (1995). The RNP domain: a sequence-specific RNA-binding domain involved in processing and transport of RNA. Trends Biochem. Sci. *20*, 235–240.

Nagy, P.L., Griesenbeck, J., Kornberg, R.D., and Cleary, M.L. (2002). A trithorax-group complex purified from Saccharomyces cerevisiae is required for methylation of histone H3. Proc. Natl. Acad. Sci. *99*, 90–94.

Nekrasov, M., Amrichova, J., Parker, B.J., Soboleva, T.A., Jack, C., Williams, R., Huttley, G.A., and Tremethick, D.J. (2012). Histone H2A.Z inheritance during the cell cycle and its impact on promoter organization and dynamics. Nat. Struct. Mol. Biol. *19*, 1076–1083.

Ng, H.H., Robert, F., Young, R.A., and Struhl, K. (2003). Targeted Recruitment of Set1 Histone Methylase by Elongating Pol II Provides a Localized Mark and Memory of Recent Transcriptional Activity. Mol. Cell *11*, 709–719.

Ni, T., Corcoran, D.L., Rach, E.A., Song, S., Spana, E.P., Gao, Y., Ohler, U., and Zhu, J. (2010). A paired-end sequencing strategy to map the complex landscape of transcription initiation. Nat Meth *7*, 521–527.

Nightingale, K.P., Wellinger, R.E., Sogo, J.M., and Becker, P.B. (1998). Histone acetylation facilitates RNA polymerase II transcription of the Drosophila hsp26 gene in chromatin. EMBO J. *17*, 2865–2876.

Nislow, C., Ray, E., and Pillus, L. (1997). SET1, A Yeast Member of the Trithorax Family, Functions in Transcriptional Silencing and Diverse Cellular Processes. Mol Biol Cell *8*, 2421–2436.

Pan, X., Yuan, D.S., Xiang, D., Wang, X., Sookhai-Mahadeo, S., Bader, J.S., Hieter, P., Spencer, F., and Boeke, J.D. (2004). A robust toolkit for functional profiling of the yeast genome. Mol. Cell *16*, 487–496.

Pandey, V., and Kumar, V. (2015). Stabilization of SIRT7 deacetylase by viral oncoprotein HBx leads to inhibition of growth restrictive RPS7 gene and facilitates cellular transformation. Sci. Rep. *5*, 14806.

Papamichos-Chronakis, M., Watanabe, S., Rando, O.J., and Peterson, C.L. (2011). Global regulation of H2A.Z localization by the INO80 chromatin-remodeling enzyme is essential for genome integrity. Cell *144*, 200–213.

Parenteau, J., Durand, M., Morin, G., Gagnon, J., Lucier, J.-F., Wellinger, R.J., Chabot, B., and Abou Elela, S. (2011). Introns within Ribosomal Protein Genes Regulate the Production and Function of Yeast Ribosomes. Cell *147*, 320–331.

Pleiss, J.A., Whitworth, G.B., Bergkessel, M., and Guthrie, C. (2007a). Rapid, transcript-specific changes in splicing in response to environmental stress. Mol. Cell *27*, 928–937.

Pleiss, J.A., Whitworth, G.B., Bergkessel, M., and Guthrie, C. (2007b). Transcript Specificity in Yeast Pre-mRNA Splicing Revealed by Mutations in Core Spliceosomal Components. PLoS Biol *5*, e90.

Pokholok, D.K., Harbison, C.T., Levine, S., Cole, M., Hannett, N.M., Lee, T.I., Bell, G.W., Walker, K., Rolfe, P.A., Herbolsheimer, E., et al. (2005). Genome-wide map of nucleosome acetylation and methylation in yeast. Cell *122*, 517–527.

Quan, T.K., and Hartzog, G.A. (2010). Histone H3K4 and K36 methylation, Chd1 and Rpd3S oppose the functions of Saccharomyces cerevisiae Spt4-Spt5 in transcription. Genetics *184*, 321–334.

Radman-Livaja, M., Liu, C.L., Friedman, N., Schreiber, S.L., and Rando, O.J. (2010). Replication and Active Demethylation Represent Partially Overlapping Mechanisms for Erasure of H3K4me3 in Budding Yeast. PLoS Genet *6*, e1000837.

Radman-Livaja, M., Verzijlbergen, K.F., Weiner, A., van Welsem, T., Friedman, N., Rando, O.J., and van Leeuwen, F. (2011). Patterns and mechanisms of ancestral histone protein inheritance in budding yeast. PLoS Biol. *9*, e1001075.

Raisner, R.M., Hartley, P.D., Meneghini, M.D., Bao, M.Z., Liu, C.L., Schreiber, S.L., Rando, O.J., and Madhani, H.D. (2005). Histone variant H2A.Z marks the 5' ends of both active and inactive genes in euchromatin. Cell *123*, 233–248.

Rando, O.J. (2012). Combinatorial complexity in chromatin structure and function: revisiting the histone code. Curr. Opin. Genet. Dev. *22*, 148–155.

Rando, O.J., and Chang, H.Y. (2009). Genome-wide views of chromatin structure. Annu. Rev. Biochem. *78*, 245–271.

Rinn, J.L., Kertesz, M., Wang, J.K., Squazzo, S.L., Xu, X., Brugmann, S.A., Goodnough, L.H., Helms, J.A., Farnham, P.J., Segal, E., et al. (2007). Functional demarcation of active and silent chromatin domains in human HOX loci by noncoding RNAs. Cell *129*, 1311–1323.

Roguev, A. (2001). The Saccharomyces cerevisiae Set1 complex includes an Ash2 homologue and methylates histone 3 lysine 4. EMBO J. *20*, 7137–7148.

Rufiange, A., Jacques, P.-E., Bhat, W., Robert, F., and Nourani, A. (2007). Genome-wide replication-independent histone H3 exchange occurs predominantly at promoters and implicates H3 K56 acetylation and Asf1. Mol. Cell *27*, 393–405.

Rusche, L.N., Kirchmaier, A.L., and Rine, J. (2003). The establishment, inheritance, and function of silenced chromatin in Saccharomyces cerevisiae. Annu. Rev. Biochem. *72*, 481–516.

Sadakierska-Chudy, A., and Filip, M. (2014). A Comprehensive View of the Epigenetic Landscape. Part II: Histone Post-translational Modification, Nucleosome Level, and Chromatin Regulation by ncRNAs. Neurotox. Res. *27*, 172–197.

Santos-Rosa, H., Schneider, R., Bannister, A.J., Sherriff, J., Bernstein, B.E., Emre, N.C.T., Schreiber, S.L., Mellor, J., and Kouzarides, T. (2002). Active genes are tri-methylated at K4 of histone H3. Nature *419*, 407–411.

Schlichter, A., and Cairns, B.R. (2005). Histone trimethylation by Set1 is coordinated by the RRM, autoinhibitory, and catalytic domains. EMBO J *24*, 1222–1231.

Schneider, J., Wood, A., Lee, J.-S., Schuster, R., Dueker, J., Maguire, C., Swanson, S.K., Florens, L., Washburn, M.P., and Shilatifard, A. (2005). Molecular regulation of histone H3 trimethylation by COMPASS and the regulation of gene expression. Mol. Cell *19*, 849–856.

Schoenberg, D.R., and Maquat, L.E. (2009). Re-capping the message. Trends Biochem. Sci. *34*, 435–442.

Shi, Y.G., and Tsukada, Y. (2013). The Discovery of Histone Demethylases. Cold Spring Harb. Perspect. Biol. *5*.

Shi, Y., Lan, F., Matson, C., Mulligan, P., Whetstine, J.R., Cole, P.A., Casero, R.A., and Shi, Y. (2004). Histone Demethylation Mediated by the Nuclear Amine Oxidase Homolog LSD1. Cell *119*, 941–953.

Shogren-Knaak, M., Ishii, H., Sun, J.-M., Pazin, M.J., Davie, J.R., and Peterson, C.L. (2006). Histone H4-K16 Acetylation Controls Chromatin Structure and Protein Interactions. Science *311*, 844–847.

Sommermeyer, V., Béneut, C., Chaplais, E., Serrentino, M.E., and Borde, V. (2013). Spp1, a Member of the Set1 Complex, Promotes Meiotic DSB Formation in Promoters by Tethering Histone H3K4 Methylation Sites to Chromosome Axes. Mol. Cell *49*, 43–54.

Spingola, M., Grate, L., Haussler, D., and Ares, M. (1999). Genome-wide bioinformatic and molecular analysis of introns in Saccharomyces cerevisiae. RNA N. Y. N *5*, 221–234.

Stassen, M.J., Bailey, D., Nelson, S., Chinwalla, V., and Harte, P.J. (1995). The Drosophila trithorax proteins contain a novel variant of the nuclear receptor type DNA binding domain and an ancient conserved motif found in other chromosomal proteins. Mech. Dev. *52*, 209–223.

Steger, D.J., Lefterova, M.I., Ying, L., Stonestrom, A.J., Schupp, M., Zhuo, D., Vakoc, A.L., Kim, J.-E., Chen, J., Lazar, M.A., et al. (2008). DOT1L/KMT4 recruitment and H3K79 methylation are ubiquitously coupled with gene transcription in mammalian cells. Mol. Cell. Biol. *28*, 2825–2839.

Strahl, B.D., and Allis, C.D. (2000). The language of covalent histone modifications. Nature *403*, 41–45.

Suganuma, T., and Workman, J.L. (2008). Crosstalk among Histone Modifications. Cell *135*, 604–607.

Sun, M., Schwalb, B., Pirkl, N., Maier, K.C., Schenk, A., Failmezger, H., Tresch, A., and Cramer, P. (2013). Global Analysis of Eukaryotic mRNA Degradation Reveals Xrn1-Dependent Buffering of Transcript Levels. Mol. Cell *52*, 52–62.

Suto, R.K., Clarkson, M.J., Tremethick, D.J., and Luger, K. (2000). Crystal structure of a nucleosome core particle containing the variant histone H2A.Z. Nat. Struct. Biol. *7*, 1121–1124.

Taddei, A., Van Houwe, G., Nagai, S., Erb, I., van Nimwegen, E., and Gasser, S.M. (2009). The functional importance of telomere clustering: global changes in gene expression result from SIR factor dispersion. Genome Res. *19*, 611–625.

Talbert, P.B., and Henikoff, S. (2010). Histone variants: Ancient wrap artists of the epigenome. Nat Rev Mol Cell Biol *11*, 264–275.

Terzi, N., Churchman, L.S., Vasiljeva, L., Weissman, J., and Buratowski, S. (2011). H3K4 Trimethylation by Set1 Promotes Efficient Termination by the Nrd1-Nab3-Sen1 Pathway. Mol. Cell. Biol. *31*, 3569–3583.

Tessarz, P., and Kouzarides, T. (2014). Histone core modifications regulating nucleosome structure and dynamics. Nat. Rev. Mol. Cell Biol. *15*, 703–708.

Tirosh, I., and Barkai, N. (2008). Two strategies for gene regulation by promoter nucleosomes. Genome Res. *18*, 1084–1091.

Tong, A.H.Y., Lesage, G., Bader, G.D., Ding, H., Xu, H., Xin, X., Young, J., Berriz, G.F., Brost, R.L., Chang, M., et al. (2004). Global mapping of the yeast genetic interaction network. Science *303*, 808–813.

Trésaugues, L., Dehé, P.-M., Guérois, R., Rodriguez-Gil, A., Varlet, I., Salah, P., Pamblanco, M., Luciano, P., Quevillon-Cheruel, S., Sollier, J., et al. (2006). Structural Characterization of Set1 RNA Recognition Motifs and their Role in Histone H3 Lysine 4 Methylation. J. Mol. Biol. *359*, 1170–1181.

Tsai, M.-C., Manor, O., Wan, Y., Mosammaparast, N., Wang, J.K., Lan, F., Shi, Y., Segal, E., and Chang, H.Y. (2010). Long noncoding RNA as modular scaffold of histone modification complexes. Science *329*, 689–693.

Tsankov, A.M., Brown, C.R., Yu, M.C., Win, M.Z., Silver, P.A., and Casolari, J.M. (2006). Communication between levels of transcriptional control improves robustness and adaptivity. Mol. Syst. Biol. *2*, 65.

Tschiersch, B., Hofmann, A., Krauss, V., Dorn, R., Korge, G., and Reuter, G. (1994). The protein encoded by the Drosophila position-effect variegation suppressor gene Su(var)3-9 combines domains of antagonistic regulators of homeotic gene complexes. EMBO J. *13*, 3822–3831.

Verzijlbergen, K.F., van Welsem, T., Sie, D., Lenstra, T.L., Turner, D.J., Holstege, F.C.P., Kerkhoven, R.M., and van Leeuwen, F. (2011). A barcode screen for epigenetic regulators reveals a role for the NuB4/HAT-B histone acetyltransferase complex in histone turnover. PLoS Genet. *7*, e1002284.

Vettese-Dadey, M., Grant, P.A., Hebbes, T.R., Crane- Robinson, C., Allis, C.D., and Workman, J.L. (1996). Acetylation of histone H4 plays a primary role in enhancing transcription factor binding to nucleosomal DNA in vitro. EMBO J. *15*, 2508–2518.

Wang, S.-S., Zhou, B.O., and Zhou, J.-Q. (2011). Histone H3 lysine 4 hypermethylation prevents aberrant nucleosome remodeling at the PHO5 promoter. Mol. Cell. Biol. *31*, 3171–3181.

Wang, Z., Zang, C., Rosenfeld, J.A., Schones, D.E., Barski, A., Cuddapah, S., Cui, K., Roh, T.-Y., Peng, W., Zhang, M.Q., et al. (2008). Combinatorial patterns of histone acetylations and methylations in the human genome. Nat Genet *40*, 897–903.

Wapinski, I., Pfeffer, A., Friedman, N., and Regev, A. (2007). Natural history and evolutionary principles of gene duplication in fungi. Nature *449*, 54–61.

Weake, V.M., and Workman, J.L. (2008). Histone ubiquitination: triggering gene activity. Mol. Cell *29*, 653–663.

Weiner, A., Hughes, A., Yassour, M., Rando, O.J., and Friedman, N. (2010). High-resolution nucleosome mapping reveals transcription-dependent promoter packaging. Genome Res. *20*, 90–100.

Weiner, A., Hsieh, T.-H.S., Appleboim, A., Chen, H.V., Rahat, A., Amit, I., Rando, O.J., and Friedman, N. (2015). High-resolution chromatin dynamics during a yeast stress response. Mol. Cell *58*, 371–386.

Welsem, T. van, Frederiks, F., Verzijlbergen, K.F., Faber, A.W., Nelson, Z.W., Egan, D.A., Gottschling, D.E., and Leeuwen, F. van (2008). Synthetic Lethal Screens Identify Gene Silencing Processes in Yeast and Implicate the Acetylated Amino Terminus of Sir3 in Recognition of the Nucleosome Core. Mol. Cell. Biol. *28*, 3861–3872.

West, M.H.P., and Bonner, W.M. (1980). Histone 2A, a heteromorphous family of eight protein species. Biochemistry (Mosc.) *19*, 3238–3245.

Williams, S.K., Truong, D., and Tyler, J.K. (2008). Acetylation in the globular core of histone H3 on lysine-56 promotes chromatin disassembly during transcriptional activation. Proc. Natl. Acad. Sci. U. S. A. *105*, 9000–9005.

Wyce, A., Xiao, T., Whelan, K.A., Kosman, C., Walter, W., Eick, D., Hughes, T.R., Krogan, N.J., Strahl, B.D., and Berger, S.L. (2007). H2B ubiquitylation acts as a barrier to Ctk1 nucleosomal recruitment prior to removal by Ubp8 within a SAGA-related complex. Mol. Cell *27*, 275–288.

Xu, F., Zhang, K., and Grunstein, M. (2005). Acetylation in Histone H3 globular domain regulates gene expression in yeast. Cell *121*, 375–385.

Xu, Z., Wei, W., Gagneur, J., Perocchi, F., Clauder-Munster, S., Camblong, J., Guffanti, E., Stutz, F., Huber, W., and Steinmetz, L.M. (2009). Bidirectional promoters generate pervasive transcription in yeast. Nature *457*, 1033–1037.

Ye, J., Ai, X., Eugeni, E.E., Zhang, L., Carpenter, L.R., Jelinek, M.A., Freitas, M.A., and Parthun, M.R. (2005). Histone H4 lysine 91 acetylation: a core domain modification associated with chromatin assembly. Mol. Cell *18*, 123–130.

Zee, B.M., Levin, R.S., Dimaggio, P.A., and Garcia, B.A. (2010). Global turnover of histone post-translational modifications and variants in human cells. Epigenetics Chromatin *3*, 22.

Zhang, K., Lin, W., Latham, J.A., Riefler, G.M., Schumacher, J.M., Chan, C., Tatchell, K., Hawke, D.H., Kobayashi, R., and Dent, S.Y.R. (2005). The Set1 Methyltransferase Opposes Ipl1 Aurora Kinase Functions in Chromosome Segregation. Cell *122*, 723–734.